EFFECT OF ATLANTIC MERIDIONAL OVERTURNING CIRCULATION CHANGES ON TROPICAL COUPLED OCEAN-ATMOSPHERE SYSTEM

A Dissertation

by

XIUQUAN WAN

Submitted to the Office of Graduate Studies of
Texas A&M University
in partial fulfillment of the requirements for the degree of

DOCTOR OF PHILOSOPHY

August 2009

Major Subject: Oceanography

EFFECT OF ATLANTIC MERIDIONAL OVERTURNING CIRCULATION CHANGES ON TROPICAL COUPLED OCEAN-ATMOSPHERE SYSTEM

A Dissertation

by

XIUQUAN WAN

Submitted to the Office of Graduate Studies of
Texas A&M University
in partial fulfillment of the requirements for the degree of

DOCTOR OF PHILOSOPHY

Approved by:

Chair of Committee,	Ping Chang
Committee Members,	Benjamin Giese
	Gerald North
	Matthew W. Schmidt
	Achim Stössel
Head of Department,	Piers Chapman

August 2009

Major Subject: Oceanography

ABSTRACT

Effect of Atlantic Meridional Overturning Circulation Changes on Tropical Coupled Ocean-Atmosphere System. (August 2009)

Xiuquan Wan, B.S., Ocean University of China;

M.S., Ocean University of China

Chair of Advisory Committee: Dr. Ping Chang

The objective of this study is to investigate the effect of Atlantic meridional overturning circulation (AMOC) changes on tropical coupled ocean-atmosphere system via oceanic and atmospheric processes. A suite of numerical simulations have been conducted and the results show that both oceanic and atmospheric circulation changes induced by AMOC changes can have a profound impact on tropical sea surface temperature (SST) and sea surface salinity (SSS) conditions, but their dominance varies in different parts of the tropical oceans. The oceanic process has a dominant control on SST and SSS response to AMOC changes in the South Tropical Atlantic, while the atmospheric teleconnection is mainly responsible for SST and SSS changes over the North Tropical Atlantic and Pacific Oceans during the period of reduced AMOC.

The finding has significant implication for the interpretation of the paleo-temperature reconstructions over the southern Caribbean and the western Tropical Atlantic regions during the Younger Dryas. It suggests that the strong spatial inhomogeneity of the SST change revealed by the proxy records in these regions may be attributed to the competing oceanic and atmospheric processes that dominate the SST response. Similar mechanisms may also explain the reconstructed paleo-salinity change in the tropical Atlantic, which shows a basin-wide increase in SSS during the Younger Dryas, according to recent paleo climate studies.

Finally, we show that atmospheric teleconnection induced by the surface cooling of the North Atlantic and the North Pacific in response to a weakened AMOC, is a leading physical mechanism that dictates the behavior of El Niño/Southern Oscillation（ENSO）

response to AMOC changes. However, depending on its origin, the atmospheric teleconnection can affect ENSO variability in different ways. The atmospheric process associated with the North Atlantic cooling tends to enhance El Niño occurrence with a deepened mean thermocline depth in the eastern Pacific, whereas the atmospheric process associated with the North Pacific cooling tends to produce more La Niña events with a reduced mean thermocline depth in the eastern Pacific. Preliminary analysis suggests that the change in ENSO characteristics is associated with the change in internal atmospheric variability caused by the surface cooling in the North Atlantic and North Pacific. Complex nature of the underlying dynamics concerning the effect of the AMOC on ENSO calls for further investigation into this problem.

ACKNOWLEDGEMENTS

A great many thanks go first and foremost to Dr. Ping Chang, the chair of my committee, for his expert guidance, patience and generosity throughout the course of my Ph.D. Study. He has walked me through all the stages of the writing of this dissertation. Without his consistent and illuminating instruction, this dissertation could not have reached its present form. His passion and curiosity about the science, and his responsible attitude towards scientific research have inspired me and benefited my research not only today but also tomorrow and beyond.

I would like to thank my other committee members: Dr. Benjamin Giese, Dr. Gerald North and Dr. Achim Stössel for their warm encouragement and useful suggestions. Many thanks especially to Dr. Matthew W. Schmidt for serving on my committee during the later period of my study as a paleoceanography expert.

I would also like to thank Dr. R. Saravanan for his inspiring discussions and mathematical skills, Dr. Link Ji for her help with computer programming, and Dr. Hank Seidel for his technical support. I also want to extend my gratitude to my friends and the department faculty and staff for making my time at Texas A&M University a great experience.

Last and foremost, I am greatly indebted to my family and my family-in-law for their infinite encouragement and unconditional support from the other side of the Pacific Ocean during this six-year-long journey called Ph.D. Most important, I'd like to express particular thanks to my wife, Hui Wu, and my son, who love me so much that would support me studying far away from home, though not without a desire of my coming back one day. Without their support, patience and love, I feel that there would have been no way for me to finish this work on time.

TABLE OF CONTENTS

CHAPTER Page

LIST OF FIGURES

Page

Page

Page

Page

Page

Page

Page

Page

LIST OF TABLES

CHAPTER I
INTRODUCTION

A. Motivation

Tropical oceans are key regions that directly and/or indirectly affect global climate variations through dynamical and thermodynamical interactions with the atmosphere on various time scales. In the tropical Pacific Ocean, the El Niño/Southern Oscillation (ENSO) is the earth's dominant climate phenomenon on interannual time scales and is the best-known example of coupled ocean-atmosphere modes. In the tropical Atlantic Ocean, the strength and the location of the Intertropical Convergence Zone (ITCZ) is affected by the Atlantic meridional and zonal mode, seasonal manifestations of coupled ocean-atmosphere variability in the Atlantic sector. In the tropical Indian Ocean, the Asian monsoon system and the Indian Ocean Dipole (IOD), an east-west internal mode of variability locked to the seasons, own their existence to regional ocean-atmosphere interactions. Because of their tremendous influence on global climate, the earth's ecosystems, human living conditions and the global economy, climate research community has focused more attention on understanding the role of tropical oceans in climate variability and change [see special issue of the *Journal of Geophysical Research* (JGR, 1998,vol.103, No.7); review of Chang et al., 2006].

Although, considerable progress has been made in our understanding of tropical climate variability over the past decades, there are still many fundamental issues that are not well understood. For example, the amplitude of ENSO varies on decadal-

---

This dissertation follows the style and the format of the *Journal of Climate.*

multidecadal time scales. Even though this variation is believed to be related to interdecadal changes in mean states of the tropical Pacific, it is still an open question as to whether the changes in Atlantic sea surface temperature (SST) could play a role in this ENSO amplitude modulation. This means the causes of low-frequency ENSO modulation remain largely undetermined and need to be further investigated. Furthermore, the Atlantic Multidecadal Oscillation (AMO) is thought to be related to multidecadal fluctuations of the Atlantic thermohaline circulation, whose influence on the mean climate of the tropical Pacific appears to be transmitted through both atmospheric processes and oceanic processes. However, the nature of these physical processes also remains unclear. In addition, reducing large biases and maintaining good agreement with the observations in the tropical oceans of coupled climate models has also been a challenge. The ultimate goal of climate studies is to improve our ability to predict future climate variations and changes. To achieve this goal, we must first have a solid understanding of how different components of the climate system work together at various time scales.

While studies on tropical ocean dynamics and its interactions with the atmosphere have been a focused area of climate research in past decades, considerable recent research has expanded beyond the tropical upper oceans to explore the influence of high latitude regions, deep ocean circulations and interactions among different ocean basins in the global climate system. As a whole, large-scale ocean circulation acts as a global conveyor belt, transporting large amounts of heat and water through wind-driven upper ocean circulation and deep ocean thermohaline circulation. Analysis of ocean observations and model simulations suggests that there have been possible changes in the thermohaline circulation during the last century, which may have had profound implication for climate variability and change in the tropics. Using hydrographic data of a transatlantic section along latitude 25°N, Bryden et al. (2005) argued that the Atlantic

meridional overturning circulation (AMOC) slowed down by about 30 percent between 1957 and 2004. Using observations over the past 50 years, McPhaden and Zhang (2002) found that the meridional overturning circulation (MOC) in the upper Pacific Ocean has been slowing down since the 1970s which results in a decrease in upwelling of about 25% in the equatorial region and an increase in equatorial sea surface temperature of about 0.8°C. However, new measurements from the Rapid Climate Change (RAPID) mooring array along 26.5°N indicate that there are surprisingly large variations in the North Atlantic thermohaline circulation (Church, 2007). From 1 year of measurements, Kanzow et al. (2007) and Cunningham et al. (2007) showed that the AMOC varies by 5.7 sverdrups (Sv) at 26.5°N. Many coupled general circulation models used for climate change studies exhibit multi-decadal oscillations in the AMOC (Delworth et al., 1993; Dai et al., 2005; Jungclaus et al., 2005). Therefore, it is also important to understand driving mechanisms for AMOC variability.

The changes in global ocean circulation may have a major impact on the ocean-atmosphere coupled system at decadal or longer time scales. However, due to the lack of long-term ocean observations, the effect of global ocean circulation changes on climate is, at present, investigated theoretically or through numerical model experiments. This dissertation investigates the role of global ocean circulation changes on tropical coupled ocean-atmosphere system using numerical model experiments.

B. Background

The world's oceans are connected through a circulation driven by both atmospheric wind stress and buoyancy forcing. The subtropical cells (STCs) are shallow meridional overturning circulation features in the upper ocean that link subduction in subtropics to the equatorial thermocline (McCreary and Lu, 1994). It is shown that in this system, the

subtropical surface water is first subducted into the thermocline as described in the ventilated thermocline theory (Luyten et al., 1983). At depths of about 100-400m, the subducted water flows equatorward to the tropics and partially feeds the equatorial undercurrent systems in the equatorial Pacific and Atlantic, then upwells to the surface in the eastern equatorial oceans and finally flows poleward back to the subtropical surface oceans (Gu and Philander, 1997). Many observational and modeling results support the finding that the source of the waters of the equatorial undercurrent and the equatorial cold tongue is the subtropical or extratropical region (Pedlosky, 1987; Liu et al., 1994; Lu et al., 1998; Rothstein et al., 1998; Huang and Liu, 1999; Johnson and McPhaden, 1999; Harper, 2000; Malanotte-Rizzoli et al., 2000; Wu et al., 2003; Fukumori et al., 2004).

Because the STC circulation connects the subtropics with the equatorial regions, questions are being raised as to whether and how tropical variability may respond to a significant change of temperature or circulation in the subtropical ocean. Our understanding on this subject is still very incomplete. Some modeling studies suggest that small changes in the subtropical ocean could propagate from midlatitudes to the equator and give rise to changes in the tropical thermocline and thereby influence the tropical climate variability. For example, Sun et al. (2004) showed that an enhanced subtropical cooling over the Pacific Ocean leads to stronger ENSO activity. Gu and Philander (1997) used a simple ocean box model to show that the extratropical-tropical exchange could result in interdecadal oscillations. Kleeman et al. (1999) showed that the changes in STC strength generate a decadal SST variation in the tropics by varying the amount of the cold water that is transported into the tropics. Recent observations show that the STCs in the tropical Pacific have indeed experienced a decadal variation since the 1970s, which may lead to changes in the tropical Pacific SST (McPhaden and Zhang, 2002). If these findings are proven to be robust, they imply that the variability in the

tropical-extratropical exchange via STCs plays an important role in ENSO at decadal and longer time scales. However, these studies did not take into consideration of the role of atmospheric processes in the tropical-extratropical teleconnection.

Although the majority of studies on tropical coupled climate variability focus on the wind-driven STCs, it has been recognized that the thermohaline circulation may also play an important role on the order of decadal and longer timescales. These two components of ocean circulation are often combined and simply referred to as the Meridional Overturning Circulation (MOC). In the real ocean these two forms of circulation not only co-exist, but also interact with each other. Due to its complexity, interactions between STCs and the thermohaline circulation are often studied using only comprehensive general circulation models (GCMs). Recent modeling studies with coupled climate models suggest that major changes in the AMOC significantly affect the atmospheric and oceanic circulation on a global scale. Yang (1999) proposes that the low frequency variability of the cross-equatorial SST gradient is correlated with changes in Labrador Sea water thickness in the subpolar North Atlantic. Dong and Sutton (2002) show that a sudden weakening of the thermohaline circulation leads to a cooler SST within 4-6 years and an El-Niño event at year 7 of their simulation after a high-latitude disturbance was introduced. Zhang and Delworth (2005) show that a steady freshwater forcing in the North Atlantic results in a weakening of the AMOC, a southward shift of the intertropical convergence zone over the Atlantic and Pacific, and an El-Niño-like pattern in the southeastern tropical Pacific. It is noteworthy that the tropical response to the change in the high latitudes can occur within a relatively short time. With a recent intercomparison of 14 models, Stouffer et al. (2006) further confirmed the robustness of certain aspects of the response resulting from a slowdown of the AMOC, like the dipole response in Atlantic SST and the southward shift of ITCZ. These results appear to be corroborated by paleo-records (Stott et al., 2002; Peterson et al., 2000).

Paleo-temperature reconstructions from the Atlantic basin listed in Table 1.1 clearly show that the SST cooled over the north Atlantic and warmed over tropical and south Atlantic during the Younger Dryas event (12.8 and 11.5 cal. Kyr BP), although significant differences exist with respect to the timing and magnitude of the SST changes. Pollen evidence from Europe also suggests a Younger Dryas cooling over the continent (Walker et al., 1994; Ammann et al., 1994; deBeaulieu et al., 1994). A tropical ice-core record from Huascaran, Peru, also suggests a cooling during the Younger Dryas (Thompson et al., 1995). Several studies, however, document a warming of tropical Atlantic SSTs during the Younger Dryas. These studies include sites off the coast of Grenada (~ 1°C, Rühlemann et al., 1999), off the coast of northeast Brazil (Arz et al, 1999; Jaeschke et al., 2007; Weldeab et al., 2006), over western African margin (Mulitza and Rühlemann, 2000), at equatorial Atlantic (Weijers et al., 2007) and from southwestern Caribbean (Schmidt et al., 2004). For a more comprehensive map of the Atlantic responses during the Younger Dryas event, refer to Dahl et al. (2005).

In addition, Herbert and Schuffert (2000) also estimated a $U^{k'}_{37}$-SST warming up to 1.5°C based on alkenone unsaturation measurements in the Cariaco basin core ODP 1002C (10°42.73'N, 65°10.18'W), while there is widespread agreement in the paleo-data community that this basin underwent substantial cooling during the Younger Dryas. For example, the cooling is thought to be unequivocal in the Mg/Ca record of Lea et al (2003) and supported by the reflectivity data of Peterson et al. (2000). The Ti and Fe data of Haug et al. (2001) indicates stronger winds, more southerly ITCZ, and increased upwelling/productivity. There is still no satisfactory explanation about the opposite temperature signs between the Lea et al. (2003) Mg/Ca-SST and the Herbert and Schuffert (2000) $U^{k'}_{37}$ proxy records of temperature change in the Cariaco Basin during the Younger Dryas. However, the age model used in Herbert and Schuffert (2000) was preliminary. Therefore, we used the published age model in Peterson et al. (2000) for

their $U^{k'}_{37}$ record for ODP 1002C (Figure 1.1, personal communication). Based on the updated age model, the $U^{k'}_{37}$ temperatures show no temperature change at the initiation of the Younger Dryas event, remain constant through the Younger Dryas, and indicate a SST increase by 1°C at the termination of the Younger Dryas. The Mg/Ca-SSTs and the $U^{k'}_{37}$-SSTs no longer show opposite trends during the Younger Dryas. Instead, both the Mg/Ca- and the $U^{k'}_{37}$-SSTs suggest SSTs in the range of 24-24.5°C from 11.5-13.0 kyr. Nevertheless, the Mg/Ca-SST record indicates a large warming at the start of the Bølling-Allerød, while the $U^{k'}_{37}$-SSTs suggest this was the coldest interval over the last 25 kyr. Also, the $U^{k'}_{37}$-SSTs are significantly cooler than the Mg/Ca-SSTs over the last 11.5 kyr. These offsets could result from a seasonal bias between the proxy records. Tedesco and Thunell (2003) showed that the flux of *G. ruber* in the Cariaco Basin is highest from spring through late summer, suggesting the Mg/Ca-SST record may be biased toward warmer seasons, at least for the recent part of the record.

Generally, thorough and to-the-point review of the paleo-SST reconstruction tell a complex divergent SST histories, especially over the Caribbean Ocean during the Younger Dryas event, which might be due to seasonality or depth habitats of the organisms responsible for the proxy signal, for instance; or perhaps diagenesis, poor age control, lateral advection, etc. But this still provides a strong basis for the comparison of paleoclimate data to the model simulations and it also challenges us to better understand the physical dynamics and unravel the degree to which it constitutes an oceanic response due to the AMOC change, or an atmospheric response due to high-latitude cooling.

Table 1.1 Summary of the Younger Dryas SST anomalies from paleo records over the Atlantic Ocean

#	Location	SSTA	Type of Data	Leg/Core	Reference
1	Barra Fan (56º43'N, 09º19'W)	-4 ~ -6 °C	Corral $\delta^{13}C$	Core 56/-10/36	Kroon et al. (1997)
2	Iberian margin (37°46N, 10°11W)	-3 ~ -4 °C	Alkenone	SU8118	Bard et al. (2000)
3	Northwest African margin (19ºN, 20º10´W; 20º45´N, 18º35´W)	-2 ~ -4 °C	Alkenone	Core 31k; ODP658C	Zhao et al. (1995)
4	Barbados (13ºN, 59º30´W)	-4.5 °C	Coral $\delta^{18}O$	N/A	Guilderson et al.(2001)
5	Cariaco Basin (10º42´N, 64º56´W)	-3 ~ -4 °C	Foraminifera	PL07-39PC	Lea et al. (2003)
6	West African margin (6º23´S,10º57´E)	+1.5 °C	Alkenone	GeoB1007-4	Mulitza and Rühlemann (2000)
7	Northeast Brazil slope (4º11´S, 37º8´W; 7ºS, 34º26´W)	+1 ~ 3 °C	Planktonic $\delta^{18}O$	GeoB3117-1; GeoB3176-1;	Arz et al. (1999)
8	Grenada (12° 05' N, 61°15'W)	+1.2 °C	Alkenone	M35003-4	Rühlemann et al. (1999)
9	Tobago Basin (12° 05' N, 61°15'W)	+2 °C	Foraminiferal census	M35003-4	Hüls and Zahn (2000)
10	Northeast Brazil (4°14.7′S, 36°20.7′W)	+ 0.5 °C	Alkenone	GeoB3910-2	Jaeschke et al. (2007)
11	Northeast Brazil (4°36.8′S, 36°38.2′W)	+1.7 °C	Mg/Ca SST	GeoB3129/3911	Weldeab et al. (2006)
12	Southwestern Caribbean (11°34′N, 78°25′W)	+1.2 °C	Mg/Ca SST	VM28-122	Schmidt et al. (2004)
13	Equatorial Atlantic (5°35.3'S, 11°13.3'E)	+4 °C	Alkenone	GeoB6518-1	Weijers et al. (2007)
14	Cariaco Basin (10°42.73'N, 65°10.18'W)	+1.5 °C (??)	Alkenone	ODP 1002C	Herbert and Schuffert (2000)

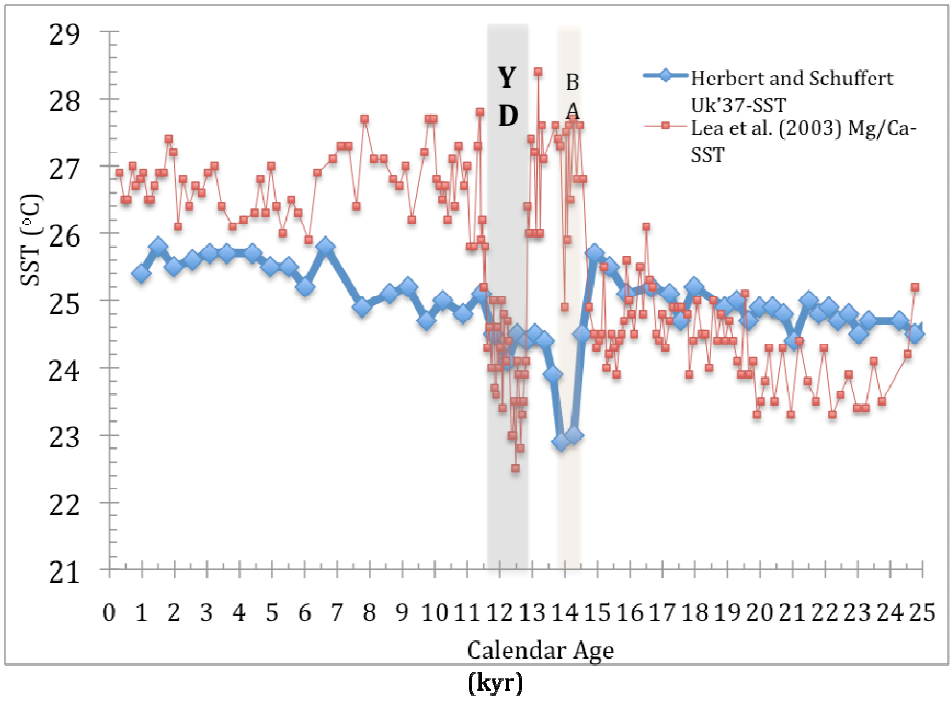

Figure 1.1 Temperature records between the Lea et al. (2003) Mg/Ca-SST and the Herbert and Schuffert (2000) $U^{k'}_{37}$-SST proxy records in the Cariaco Basin using the published age model in Peterson et al. (2000) (Courtesy of Dr. Matthew W. Schmidt).

As paleoceanographic evidences indicate during the Younger Dryas event, the Atlantic thermohaline circulation weakens substantially (Boyle, 2000; Mcmanus et al., 2004), causing wide-spread surface cooling in the north Atlantic and warming in tropical south Atlantic. A growing number of studies also indicate that the effect of a weakening of the thermohaline circulation is not just limited to the Atlantic Ocean (Dong and Sutton, 2002; Zhang and Delworth, 2005). Historically, the failure to simulate large changes

outside of high-latitude Atlantic regions in models during the Younger Dryas event has led some to suggest that the tropics drive the global climate changes on long time scales, which may deny the role of high latitude regions (Dahl et al., 2005). Until recently, the so-called “hosing experiment”, in which an additional freshwater flux is applied to the northern North Atlantic Ocean to mimic one of the possible consequences of future global warming in high latitudes, provides a means for testing and comparing those global influences with paleo-record. However, it must be noted that the present day boundary conditions used in these experiments are likely to be very different from the Younger Dryas boundary conditions. Nevertheless, these experiments have shown some responses that are consistent with paleo-climate data and may provide some clues on future climate change (Stouffer et al, 2006).

Several possible mechanisms have also been recently proposed to explain the recognized robust responses of a slowdown in the AMOC, including the pronounced southward displacement of the tropical Atlantic ITCZ and the associated meridional SST gradient change. One of the proposed mechanisms is the advection mechanism that reduces the northward Atlantic heat transport to cause the extreme cooling in high-latitudes (Haarsma et al., 2008) and then directly brings anomalous temperature at northern North Atlantic into the low-latitude region by upper ocean gyres. Chiang et al. (2008) proposed another mechanism involving Wind-Evaporation-SST (WES) feedback and atmospheric boundary processes through which initial high latitude cooling can reach the deep tropics within a decade. The third mechanism is related to oceanic Kelvin/Rossby wave adjustment process that results in a weak equatorial south Atlantic warming accompanied with the cooling in the northern hemisphere (Knutti et al., 2004).

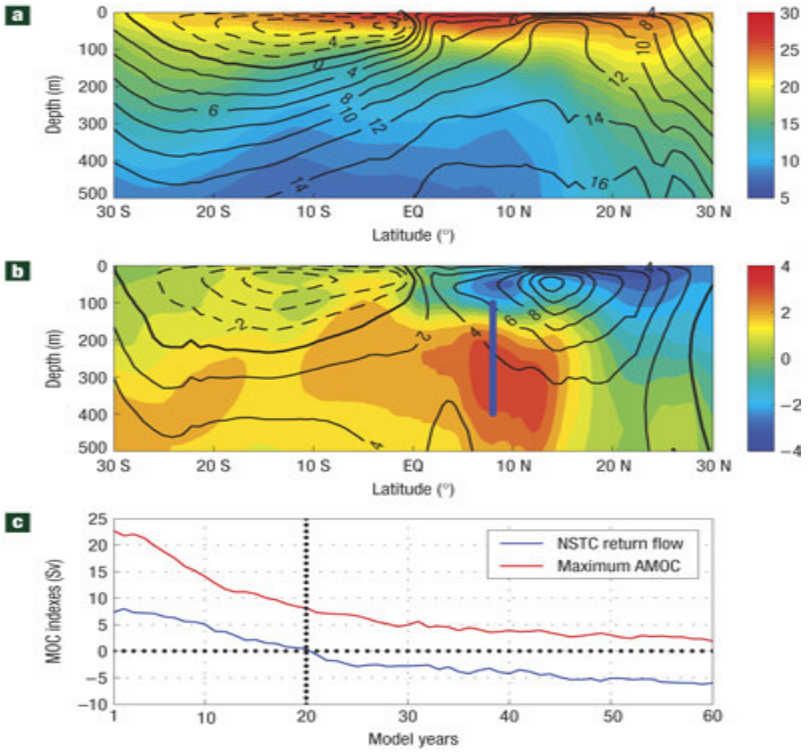

Figure 1.2 Changes in AMOC, the return branch of northern STC (NSTC) and temperature (Chang et al., 2008). a, AMOC streamfunction (contour) that shows the ocean circulation in the meridional plane and zonally averaged temperature (color) in the upper tropical Atlantic ocean from 30° S to 30° N and 0–500 m averaged over 100 year of the control simulation. b, AMOC streamfunction (contour) and zonally averaged temperature change (color) in reference to the control simulation averaged over the last 40 years of the water-hosing simulation. In a,b, the contour interval is 2 Sv and temperature is in °C. c, The maximum AMOC streamfunction as a function of time and the mass transport in the low branch of the NSTC averaged across the basin along 8° N from 100 to 400 m indicated by the blue vertical line in b. The latter is dominated by the North Brazil Current along the western boundary and it reverses direction at year 20 as indicated by the vertical dotted line in c. The transport is measured in Sv, where 1 Sv=10^6 m^3 s^{-1}. Reprinted with permission of the Nature Publishing Group from Chang et al. (2008).

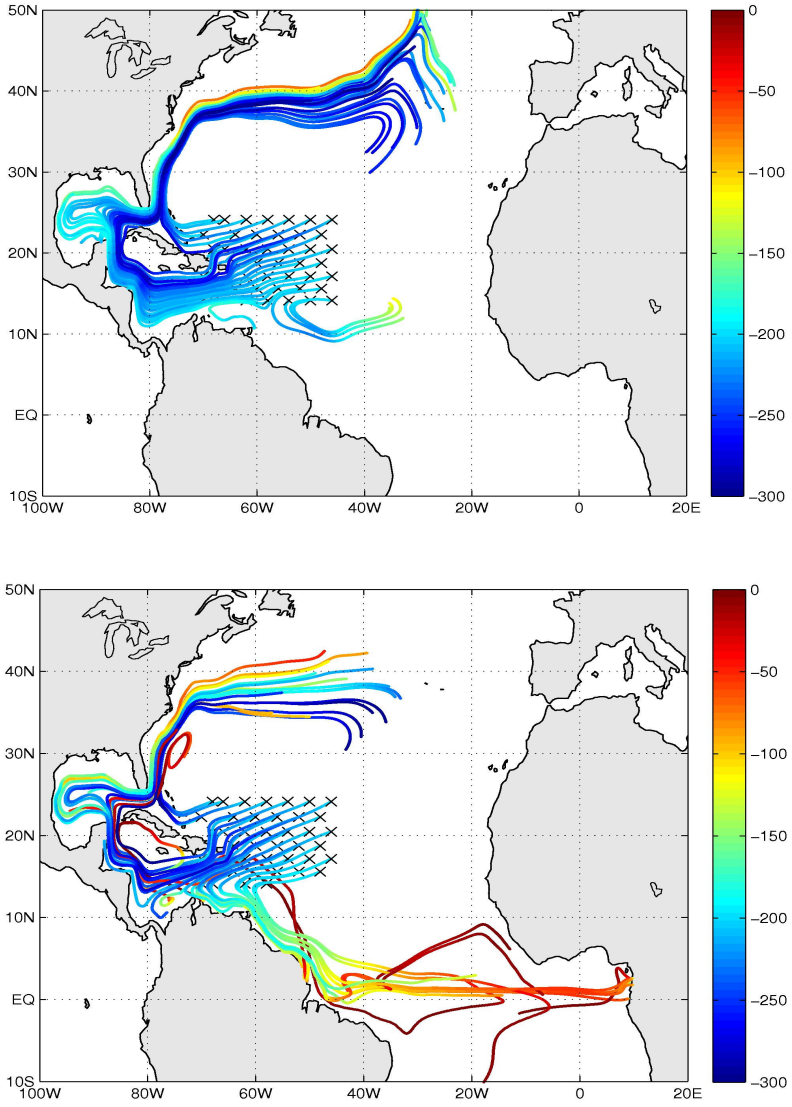

Figure 1.3 Trajectories of water parcels over a period of 2 years after being released over the western tropical Atlantic region (indicated by x) using the model data of Chang et al. (2008). The parcels in the top (bottom) panel were released at the beginning of year 1 (40) as shown in Figure 1.2c. The colors indicate the depth of parcels in meter. It is evident that more parcels move from the subtropical gyre into the equatorial thermocline after the NBC reverses its direction and then rise to the surface in the eastern equatorial Atlantic.

A more recent oceanic mechanism proposed by Chang et al. (2008) draws the attention to the effect of thermohaline circulation change on the pathway of the northern Atlantic STC. Chang et al. (2008) show that a substantially weakened thermohaline circulation can cause the reversal of the North Brazil Current (NBC) below the surface (Figure 1.2), which then advects the warm and salty subtropical gyre water into the tropics, causing warming in south equatorial Atlantic (Figure 1.3). This mechanism competes with the mechanism proposed by Haarsma et al. (2008) in that the warming is mainly due to a reduction in vertical entrainment of cooler water into the mixed layer, caused by a reduced ventilation of water originating from the South Atlantic. Barreiro et al. (2008) argue that the most important processes associated with a major change in the AMOC are oceanic processes, whose impacts are amplified by the atmosphere through various feedbacks.

A substantial weakening of the AMOC can have significant impacts on the seasonal cycle and the interannual variability of the atmosphere-ocean coupled system. Haarsma et al. (2008) argue that the equatorial SST warming reduces Atlantic Niño variability and the SST cooling in the northern hemisphere causes the southward shift of the Atlantic ITCZ. Chang et al. (2008) show that major changes in the AMOC during the past abrupt climate events, such as the Younger Dryas, can contribute to abrupt regime shifts in West African Monsoon. The changes in Atlantic Ocean also transmit their influences to the tropical Pacific climate and variability. Timmermann et al. (2005) suggested that a weakened AMOC leads to a weakening of ENSO variability while Dong et al. (2006) showed that an enhanced thermohaline circulation leads to a reduced ENSO variability in a coupled GCM experiment. More controversially, Dong et al. (2007) showed that a weakened thermohaline circulation not only leads to a stronger ENSO variability, but also leads to a stronger asymmetry between El Niño and La Niña events. These results are completely opposite to what is shown by Timmermann et al (2005). However,

Timmermann et al. (2005) focused on the role of oceanic teleconnections between the North Atlantic and tropical Pacific, whereas Dong et al. (2006, 2007) focused on the role of atmospheric teleconnections. The timescales associated with these teleconnections are very different. The results of Timmermann et al. (2005) suggest that the oceanic teleconnection has a typical timescale of many decades or longer, whereas an atmospheric influence can propagate from the tropical Atlantic into the tropical Pacific in a matter of days or weeks. Understanding possible interactions between these two mechanisms is an important area of climate research.

It has long been noted by Manabe et al. (1991) and others that global warming may lead to a substantial weakening of the MOC due to the polar amplification of climate change associated with a gradual increase of atmospheric CO_2. In many climate change simulations, the strength of the AMOC substantially weakens due to the addition of freshwater in the northern North Atlantic (Zhang and Delworth, 2005; Stouffer et al., 2006) or changes in wind stress south of 30°S (Toggweiler and Samuels, 1995; Brix and Gerdes, 2003). It is shown that a freshwater flux exceeding 0.3 Sv into the North Atlantic between 50°N and 70°N is necessary to cause a significant AMOC change and abrupt climate changes (Barreiro et al., 2008). After a combined analysis of ocean hydrographic data and model results, Latif et al. (2006) proposed that the expected anthropogenic weakening of the AMOC will continue during the next several decades. Therefore, a full understanding of the impact of AMOC change on climate system and its underlying dynamics is of great importance for improving our ability to assess and project future climate change.

C. Objective

This dissertation focuses on the investigation of tropical coupled ocean-atmosphere

system's response to changes in global ocean circulation caused by freshwater input in the northern North Atlantic. Some of the specific questions we intend to address are: Whether and how ocean circulation changes or surface cooling in the North Atlantic can cause changes in tropical Atlantic SST that are consistent with the spatially heterogeneous pattern observed during the Younger Dryas event? How sensitive are the tropical SST changes to changes in ocean circulation? Can AMOC changes be a significant driver for low-frequency climate variability, such as decadal modulation of ENSO? Are oceanic or atmospheric teleconnections individually or collectively responsible for Pacific Ocean response to AMOC changes? How do these teleconnection mechanisms work?

Our knowledge of these issues is still in early stage of development. The primary goal of this dissertation is to improve our current understanding of these issues by means of numerical modeling studies. The main objectives of this study are 1) development of a set of modeling tools for exploring oceanic and atmospheric pathway linking high latitude changes to the tropics; 2) assessing the influence of the AMOC changes on tropical coupled ocean-atmosphere system, especially the modulation of ENSO amplitude and gain insight into the physics of AMOC-induced tropical coupled system response; 3) using the numerical simulation results for the interpretation of the tropical Atlantic paleo-temperature and paleo-salinity reconstructions during the Younger Dryas event.

D. Hypotheses and Approach

As mentioned previously, changes in the AMOC are expected to play a crucial role in altering the variability of tropical climate system. What is lacking in our current understanding is how pathways between changes in the high latitudes and the tropics are

established and how these changes might lead to changes in climate patterns. The research outlined here aims at testing three specific hypotheses regarding the consequences of AMOC changes:

1) Western boundary current changes associated with AMOC changes provide a major oceanic teleconnection linking high latitude changes to the tropics. Moreover, the SST change induced by the oceanic teleconnection is mainly confined to the equatorial south Atlantic region.

2) Opposing and competing influences of oceanic and atmospheric teleconnections in response to a weakening in the AMOC may provide a physical explanation for the paleo SST and SSS reconstruction in the tropical Atlantic for the Younger Dryas event.

3) A major change in the AMOC can trigger a detectable coupled ocean-atmosphere response in tropical Pacific sector and alter tropical air-sea interactions in this region.

To test these hypotheses, we develop a new regional coupled ocean-atmosphere model that combines an atmospheric general circulation model (AGCM) with a tropical oceanic general circulation model (OGCM). In this modeling framework, internal tropical variability is self-determined by the coupled model and the change of global ocean circulation can be imposed through lateral oceanic open boundaries. A large number of 100-year coupled integrations are conducted and used to examine the behavior of the model response to AMOC changes, as well as AMOC-induced changes in the global ocean circulation. Detailed analyses are performed to examine the underlying physical mechanisms that determine the relative importance of oceanic versus atmospheric teleconnections.

E. Overview

This dissertation presents results of numerical simulations designed to explore the

mechanisms by which the tropical atmosphere-ocean system can be impacted by AMOC changes, and how various linkages between the tropical region and the high latitudes are established. The organization of this dissertation is as follows: Chapter II describes the numerical model and experiments designed to test the above-described hypotheses. It also validates the results from model simulations against observations. Chapter III examines oceanic processes associated with AMOC changes and their effects on tropical ocean condition. It also discusses a multi-decadal AMOC oscillation generated by freshwater forcing in the northern North Atlantic. Chapter IV is a discussion on coupled model simulations with an attempt to separate atmospheric influences from oceanic influences. Using these simulation results, we then present a physical explanation reconciling the tropical Atlantic paleo-temperature and paleo-salinity reconstructions during the Younger Dryas event. We further discuss results concerning the effect of AMOC changes on ENSO. Finally, Chapter V summarizes the major conclusions and discusses future work.

CHAPTER II
EXPERIMENTAL DESIGN AND MODEL VALIDATION

A. Model Description

Many of the earlier studies that attempt to address the questions mentioned previously have relied on models that contain simplified physics in either the oceans or the atmosphere, or both. In order to further elucidate the dynamical processes, we use a coupled ocean-atmosphere general circulation model (GCM) that includes a comprehensive representation of atmospheric and oceanic processes, and is capable of simulating not only tropical climate variability, but also the impact of the AMOC changes in the tropical region.

Specifically, we have developed a novel tropical coupled GCM with oceanic open boundaries where MOC-induced ocean circulation changes can be imposed. The ocean component is based on a global version of Geophysical Fluid Dynamics Laboratory's Modular Ocean Model (GFDL MOM3.0). More details about the model are documented in the MOM3.0 manual (Pacanowski and Griffies, 1999). The ocean model domain is a global tropical channel between 30°S and 30°N including the Pacific, the Atlantic and the Indian oceans. Open boundary conditions are employed at the northern and southern boundaries. The strength of the MOC can be regulated by specifying the lateral open boundary conditions. The coastline and bottom topography are realistic except that the ocean bottom shallower than 150 m is set to 150 m and the maximum depth is set to 5000m. The zonal resolution is 1.5°. The meridional grid spacing is 0.5° between 10°S and 10°N, gradually increasing to 1.5° at 30°S and 30°N. There are 25 levels in the vertical with 17 levels in the upper 450m. The vertical mixing scheme is the nonlocal K-profile parameterization （KPP） of Large et al.（1994）. The horizontal mixing of

tracers and momentum is Laplacian. The momentum mixing uses the space-time-dependent scheme of Smagorinsky (1963) and the tracer mixing uses Redi (1982) diffusion along with Gent and McWilliams (1990) quasi-adiabatic stirring.

The atmospheric component is the National Center for Atmosphere Research (NCAR) Community Climate Model version 3.6.6 (CCM3) AGCM. The horizontal resolution of the CCM3 model used is T42 global spectral horizontal resolution, which translates to roughly 2.8×2.8 degrees grid size in longitude and latitude. And it has 18 levels in the vertical. The details of the model are described in Kiehl et al. (1998).

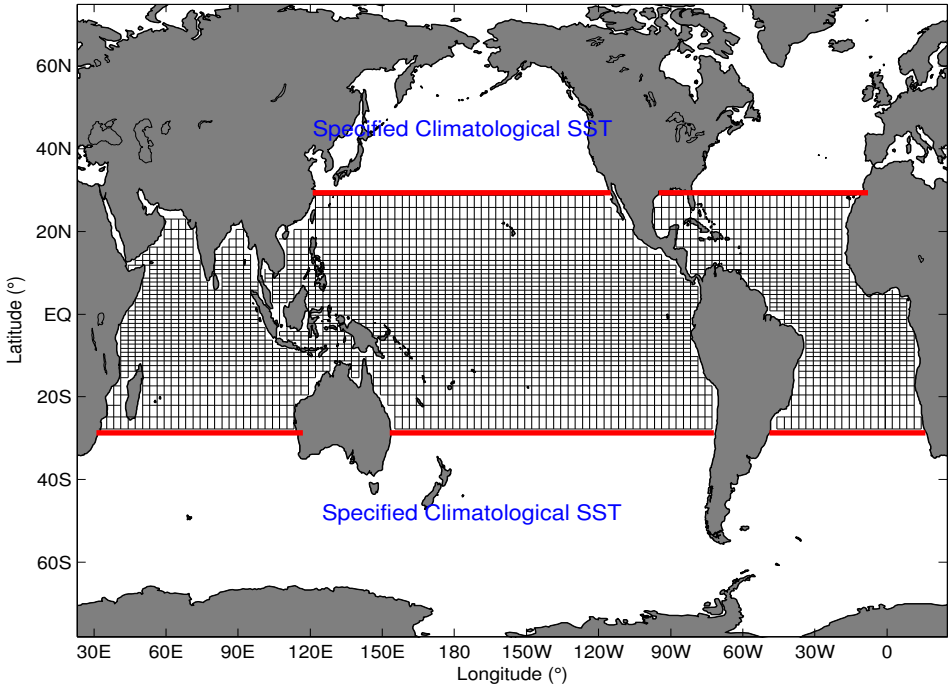

Figure 2.1 Coupled model domain and ocean grids (plotted every two grids at x and y directions). In the high latitudes, climatological SST is specified. The thick red lines denote transition zone where the coupled model SST is damped towards the specified SST.

CCM3 is coupled to the tropical MOM3 through an anomaly coupling methodology (Yeh et al., 2004). The ocean model affects the atmosphere model only through the SST anomalies, and the atmosphere provides surface wind stress and heat flux anomalies to the ocean. Before exchanging the anomalous fields between the two components, the observed climatological annual cycles are added to these corresponding anomalous fields to form the complete fields that the models need. Outside of the ocean domain of 30°S and 30°N, only the prescribed observed climatological SST is passed to the atmosphere. There is a 2°-wide transition zone near the open boundaries where the anomalies in the tropics are gradually damped to zero to provide a smooth transition between SSTs within the ocean model and prescribed SSTs outside the ocean domain. The oceanic and atmospheric models exchange the anomalous fields once per model day. A flux correction is also used in the ocean model to correct model biases and uncertainties in surface fluxes. This coupled model contains a set of comprehensive physics for simulating coupled climate variability in the tropics. Hereafter, we refer to this tropical coupled model as the CCM3-trMOM3 model (Figure 2.1).

To investigate the effect of AMOC changes on coupled climate variability in the tropics, we force the CCM3-trMOM3 through its open boundaries at 30°S and 30°N with the output from a global MOM3 (hereafter referred to as the gMOM3). The gMOM3 used here is the same as the tropical channel version trMOM3 used in the tropical coupled model except that it covers a global domain between 74°S and 65°N. The model physics and parameterization between gMOM3 and trMOM3 are identical. The gMOM3 and CCM3-trMOM3 are the primary modeling tools used in this dissertation.

B. Datasets and Data Analysis

The datasets used to tune and validate model simulations include:

1) GFDL Ocean Data Assimilation (ODA) dataset: this ODA run spans from 1980 to 1999, and includes 3-D temperature, salinity and velocity data.

2) ECMWF ERA-40 Reanalysis Product: this is an atmospheric reanalysis product provided by the European Center for Medium-Range Weather Forecasts (ECMWF). The variables used in this study include monthly surface wind stresses, surface heat fluxes and sea level pressure from 1958 to 2000.

Several commonly used statistical analyses are used to analyze model simulations and observations. These analyses include but are not limited to Empirical Orthogonal Function (EOF), linear correlation and composite analysis to identify coupled ocean-atmosphere patterns, the associated temporal variability and the key processes that control the tropical responses to AMOC changes.

C. Experimental Design

As mentioned earlier, the main purpose of this study is to examine the response of the tropical coupled system to changes in the AMOC. Our approach is to systematically examine the questions and test our hypotheses laid out in the previous chapter by carrying out a set of numerical experiments using CCM3-trMOM3 with lateral open boundary conditions derived from gMOM3 simulations in which the AMOC is weakened by freshwater forcing in high-latitude North Atlantic Ocean. This approach of combining a tropical coupled model with a global ocean GCM allows us to investigate separately contributions of different physical processes associated with AMOC changes to SST changes in the tropics. For example, as shown in recent studies, the cooling in the

high-latitude North Atlantic produced by a weakening in the AMOC can be transmitted into the tropical Atlantic via both atmospheric processes that involve interactions between atmospheric boundary layer and upper ocean mixed layer (Chiang et al., 2008) and oceanic processes that involve interactions between the wind-driven and thermohaline circulation (Chang et al., 2008). Each of these processes can be isolated and studied individually by conducting the following set of CCM3-trMOM3 sensitivity experiments:

i) Control Experiment (trMOM3-CE): The atmospheric component of the CCM3-trMOM3 is forced with observed annual cycle of SST outside the tropical ocean domain and the oceanic component is forced with climatological inflow/outflow conditions at the open boundaries derived from gMOM3 control simulation forced by observed climatological annual cycle wind stress with restoring to observed climatological surface temperature and surface salinity at a 120-day damping timescale to ensure that the model is capable of realistically simulating a stable AMOC. The CCM3-trMOM3 control run examines the extent to which the coupled model can reproduce major features of ocean circulation and the major modes of climate variability. The run also provides a reference for other CCM3-trMOM3 sensitivity runs where the different outputs of the gMOM3 hosing experiments are used as lateral open boundary conditions or an extratropical surface cooling at the North Atlantic and North Pacific is added to observed SST climatology outside the tropical ocean domain to force the atmospheric component of the CCM3-trMOM3. Hereafter, we refer to this tropical coupled experiment as trMOM3-CE in this dissertation.

ii) Boundary-Forcing Experiment (trMOM3-BFE): Same as trMOM3-CE except that the inflow/outflow conditions at the open boundaries are derived from one of the gMOM3 hosing simulations where the AMOC is weakened by a freshwater input of 1.0 Sv. Although a weakening of the AMOC will have a global influence on SST outside the

tropics, this setup allows us to investigate the local processes and interactions among the tropical ocean basins. Hereafter, we refer to this run as trMOM3-BFE in this dissertation.

iii) Surface-Forcing Experiments (trMOM3-SFEs): Same as trMOM3-CE except that in the North Atlantic basin (north of 20°N) or the North Pacific basin (north of 20°N) a cold SST anomaly derived from an ensemble of GFDL fully coupled climate model (GFDL CM2.1) water hosing runs (Zhang, 2007) are superimposed onto the observed SST climatology to force the atmosphere (Figure 2.2). These two runs are designed to examine the effect of atmospheric processes on tropical SSTs. Again we refer to these experiments as trMOM3-SFE-NA for the Atlantic forcing and trMOM3-SFE-NP for the Pacific forcing in this dissertation.

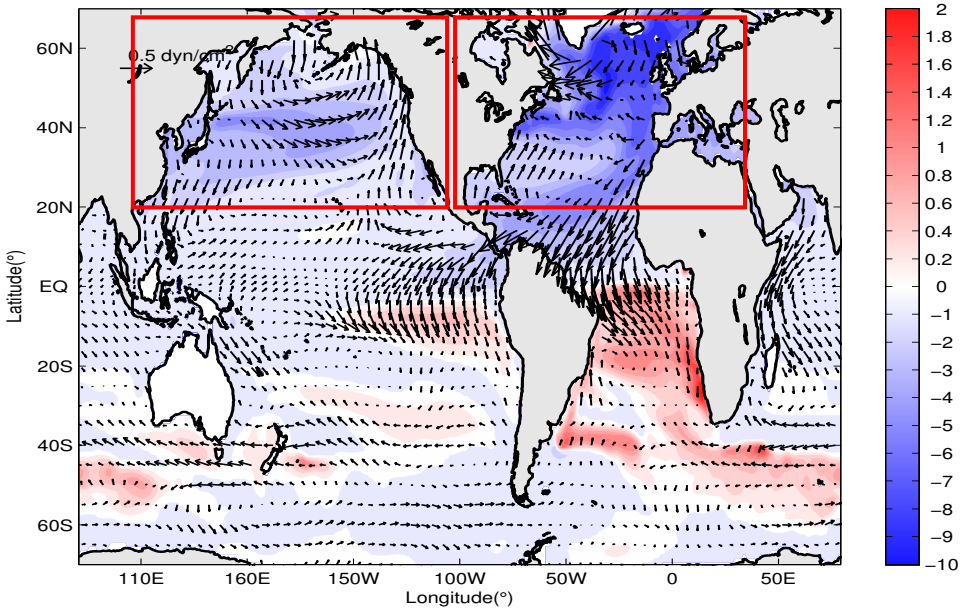

Figure 2.2 SST anomaly and wind stress anomaly from an ensemble of GDDL CM2.1 water hosing run (Courtesy of Dr. Rong Zhang). The temperature is in °C and wind stress is in dyn/cm^2. Cooling in the red boxes over the northern North Atlantic and North Pacific is used to forcing the CCM3-trMOM3 as surface boundary condition for the atmospheric model.

iv) Combined-Forcing Experiments (trMOM3-CFEs): There are two experiments in this set. First, the CCM3-trMOM3 is forced at both the surface of the North Atlantic Ocean and the North Pacific Ocean and along the open boundaries of the ocean model. This run is designed to examine the combined effect of the atmospheric and oceanic processes on tropical SSTs by comparing directly with trMOM3-SFE and trMOM3-BFE. We refer to this experiment as trMOM3-CFE-NH in this dissertation.

The second run is identical to the first run except that the surface cooling is applied only to the North Atlantic Ocean. This run is designed to examine the relative importance and the combined effect of the atmospheric and oceanic processes in the Atlantic sector on tropical SSTs. Using this run, we can quantify how much tropical climate changes is realized through processes in the Atlantic sector alone. We refer to this experiment as trMOM3-CFE-NA in this dissertation. For both runs, the inflow and outflow boundary conditions are derived from the 1.0 Sv gMOM3 hosing experiment.

Besides the trMOM3-CFE-NA, we also perform a set of similar experiments by varying the inflow and outflow boundary conditions using gMOM3 hosing simulations with freshwater forcing strength of 0.2Sv, 0.4Sv, 0.6Sv and 0.8Sv. This set of experiments is designed to explore the sensitivity of tropical coupled system to different AMOC strength under the same surface cooling condition in the North Atlantic. With these experiments we can test whether or not the AMOC change alone can indeed cause a substantial response in the tropical climate system. We can also evaluate the extent to which the regional coupled model is capable of reproducing the SST changes associated with a weakened AMOC simulated by the fully coupled GCMs (e.g. Zhang and Delworth, 2005). By comparing these experiments to the CCM3-trMOM3 control run (trMOM3-CE) we hope to better understand the physical processes associated with AMOC changes that affect the tropical climate variability.

To provide the open boundary conditions for trMOM3-CFEs and examine the

oceanic processes in AMOC-induced changes, a suite of ocean-only experiments using gMOM3 are also carried out and these experiments are divided into the following groups:

i) Control Experiment (gMOM3-Ctrl): The gMOM3 model is forced with the climatological annual cycle wind stresses taken from ECMWF ERA-40 reanalysis product, plus a restoring condition for SST and sea surface salinity (SSS) at 120-day damping timescale to ensure that the model is capable of realistically simulating surface ocean conditions and the AMOC. Hereafter we refer to this run as gMOM3-Ctrl. The output of this simulation provides the open boundary conditions for trMOM3-CE and serves as a baseline for other perturbation gMOM3 experiments.

ii) Hosing Experiments (gMOM3-Hosing): The set up of these experiments is the same as gMOM3-Ctrl except that the freshwater input in the high latitude North Atlantic between 63˚W~4˚E and 55˚N~65˚N is varied. We refer to these runs as gMOM3-Hosing-xSv, where x denotes the freshwater forcing strength. These experiments are to mimic one of the possible consequences of future global warming in high latitudes, causing ice sheets to melt. Considerable uncertainties exist in the projection of the amount of melt water input into the North Atlantic. In paleo climate studies, a freshwater hosing with a magnitude of approximately 1.0 Sv is considered to have occur during a typical Heinrich event. This can lead to a near collapse of the AMOC within a few decades and cool the subpolar North Atlantic by as much as 10ºC, according to fully coupled GCM hosing simulations (Stouffer et al. 2006). In our sensitivity experiments, we gradually increase the amount of fresh water input from 0.1Sv to 3.0Sv in 10 experiments. These experiments are intended to address the following scientific questions: How does the AMOC respond to the freshwater forcing? Is there a nonlinear threshold above which AMOC changes are insensitive to changes of freshwater input? These gMOM3 experiments also provide the open boundary conditions for the CCM3-trMOM3 model as described earlier.

iii) Wind-forcing Experiment (gMOM3-Winda): This experiment is also the same as gMOM3-Ctrl except that anomalous wind stresses derived from the ensemble of GFDL fully coupled climate model (GFDL CM2.1) water hosing runs with 0.6 Sv freshwater input (Zhang, 2007) are superimposed onto the ECMWF ERA-40 reanalysis wind stresses climatology to force the ocean (Figure 2.2). This experiment is designed to examine the effect of atmospheric circulation changes on the tropical oceans and is referred to as gMOM3-Winda.

iv) Combined-forcing Experiment (gMOM3-CFE): This experiment is the same as gMOM3-Winda experiment except that the gMOM3 is forced with both the anomalous wind stresses at the surface and the fresh water input of 1.0Sv in the North Atlantic. This experiment is designed to examine the combined effect of the atmospheric and oceanic processes on the tropical ocean SSTs. This experiment is referred to as gMOM3-CFE.

All the model experiments of gMOM3 and CCM3-trMOM3 described above are summarized in Table 2.1, including forcing configurations and strengths, as well as other information about each experiment.

The analysis presented in this dissertation is based on monthly mean output of these numerical simulations. Each of these experiments of gMOM3 and CCM3-trMOM3 consists of 100-year integrations. Unless indicated otherwise, the last 60 years of each simulation are used for model validation, analyses and comparisons with the control simulations.

Table 2.1 Summary of model configurations for the designed experiments

Experiments	Surface Forcing	Hosing Forcing	Number of Runs
trMOM3-CE	None	None	1
trMOM3-BFE	None	1.0Sv	1
trMOM3-SFE-NP	NP-SSTC	None	1
trMOM3-SFE-NA	NA-SSTC	None	1
trMOM3-CFE-NH	NH-SSTC	1.0Sv	1
trMOM3-CFE-NA	NA-SSTC	0.2 - 1.0Sv	5
gMOM3-Ctrl	None	None	1
gMOM3-Hosing	None	0.1-3.0Sv	10
gMOM3-Winda	Winda	None	1
gMOM3-CFE	Winda	1.0Sv	1

Note: 1) This table only lists main different features of each experiment. See details in text.
2) SSTC means SST cooling added for CCM3-trMOM3.
3) NP means North Pacific, NA means North Atlantic, NP means North Hemisphere (i.e., NP+NA)
4) Winda means wind stresses anomaly added for gMOM3.

D. CCM3-trMOM3 Model Validation

Before proceeding to the investigation of the effect of global ocean circulation changes on tropical coupled ocean-atmosphere system, it is necessary to demonstrate that the tropical coupled model is capable of simulating the main characteristics of the AMOC and the major modes of variability in the tropics. Therefore, we devote this section to a comparison of the CCM3-trMOM3 control simulation (trMOM3-CE) with

ocean data assimilation (ODA) products or observations.

1. Annual mean and annual cycle of the tropical oceans

The annual mean SST simulated by CCM3-trMOM3 is compared to the GFDL ODA reanalysis in Figure 2.3. The simulated SST climatology is very similar to the results of other anomaly coupled models (Schneider et al., 1997). It maintains an east-west temperature gradient along the equator in tropical Pacific Ocean with a slightly weaker strength than in observations. The eastern Pacific equatorial cold tongue is somewhat too narrow and extended too far westward. The annual mean SST difference between the simulated SST and the GFDL ODA SST is less than 1 °C over most of the tropical oceans except the central equatorial Pacific where the simulated SST is lower than the ODA value by approximately 2°C and for the western tropical Atlantic where the SST is slightly higher than ODA by more than 1 °C. The relatively small SST bias is attributed to the use of anomaly coupling methodology.

The annual mean subsurface thermal structure along the equator is examined in Figure 2.4, which shows the differences in the subsurface temperature and thermocline between the model and ODA. The model thermocline is clearly more diffused than that in the GFDL ODA. The 20 °C isotherm that is taken as a proxy for thermocline depth has a shallower-than-observed depth in the equatorial western Pacific, while its depth in the eastern equatorial Pacific seems to agree well with the ODA. Below the thermocline, the simulated temperature is about 2 °C warmer than the ODA temperature, while it is slightly colder than observations above the thermocline.

Along the north-south transect at 165°W (Figure 2.5), the model thermocline depth has a smaller south-north slope than the ODA thermocline depth. The latter has a steep slope running from the South Tropical Pacific to the thermocline ridge at 10°N, whereas the former has a more gentle slope and the ridge at 10°N is less pronounced. The

subsurface temperature is up to 3°C warmer than that in the GFDL ODA below the diffused thermocline. In spite of these deficiencies, the coupled model seems to capture reasonably well the nearly symmetric temperature distribution about the equator above the thermocline. A similar feature is also found along the north-south transect at 30°W of the upper Atlantic ocean (not shown).

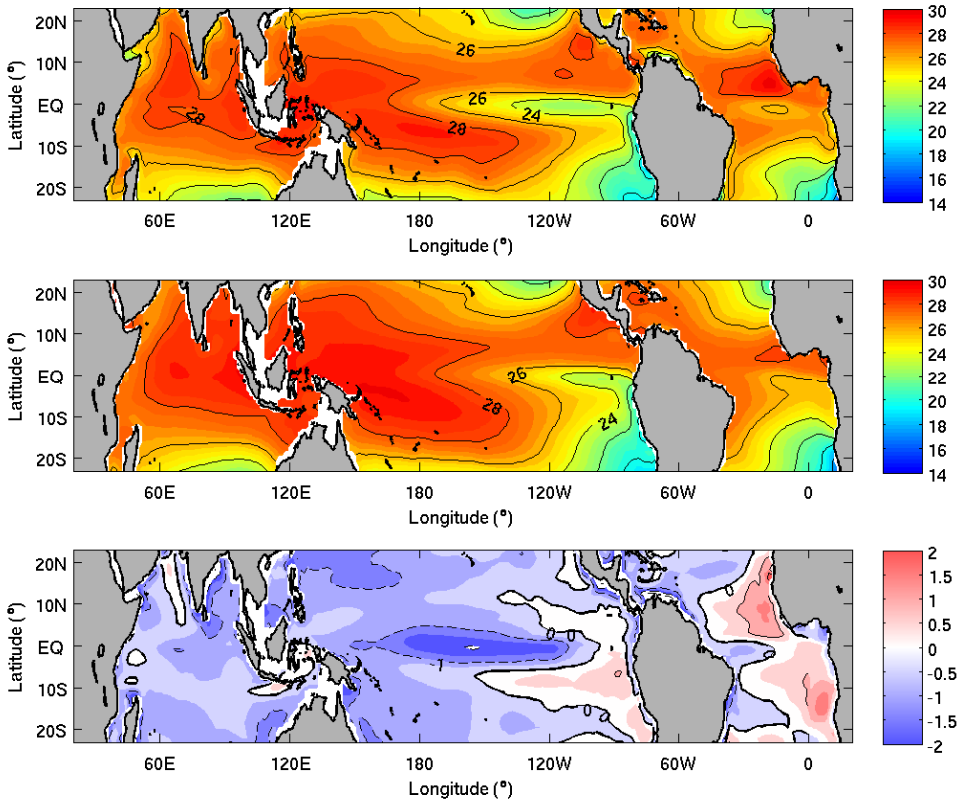

Figure 2.3 Annual mean SST (°C). Top: coupled model control integration averaged over the last 60 years from trMOM3-CE. Middle: GFDL ODA. Bottom: difference between model and GFDL ODA SST.

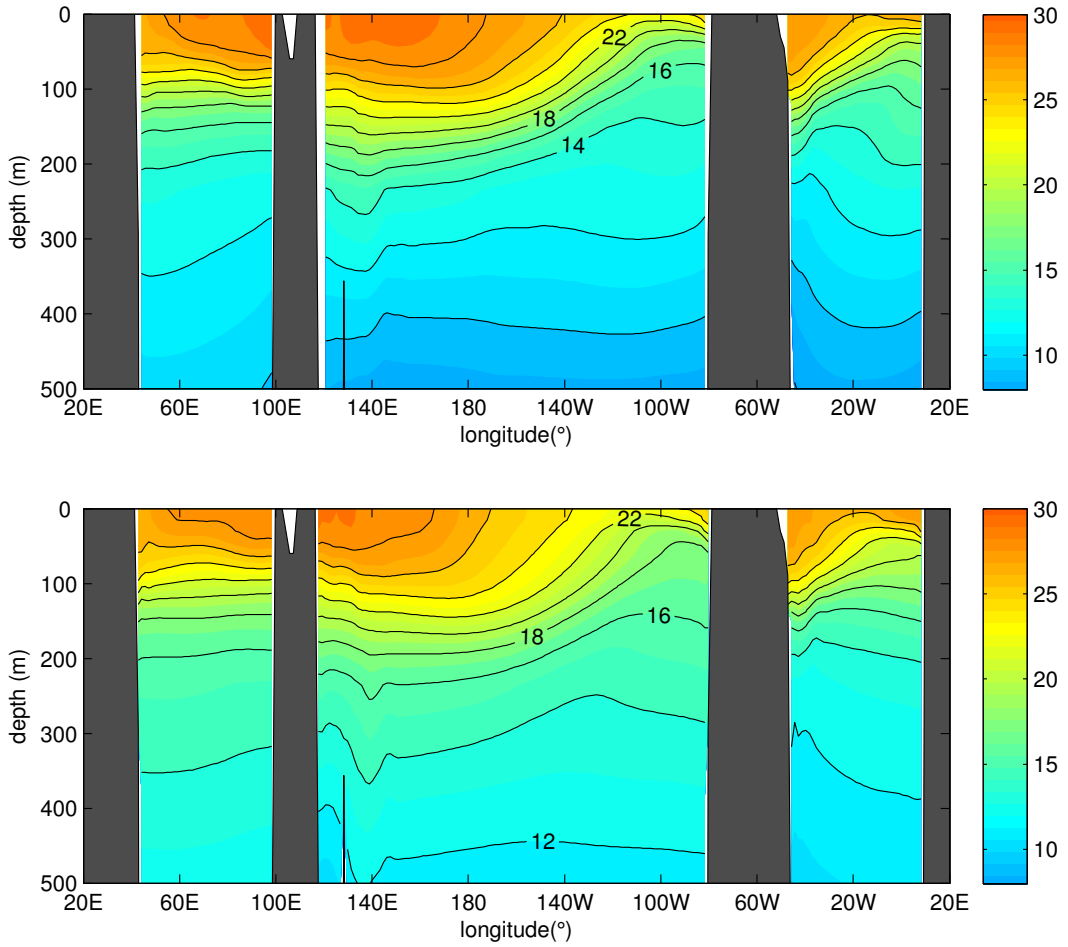

Figure 2.4 Annual mean temperature (°C) in the upper ocean along the equator as a function of depth. Top: GFDL ODA. Bottom: trMOM3-CE averaged over 60 years.

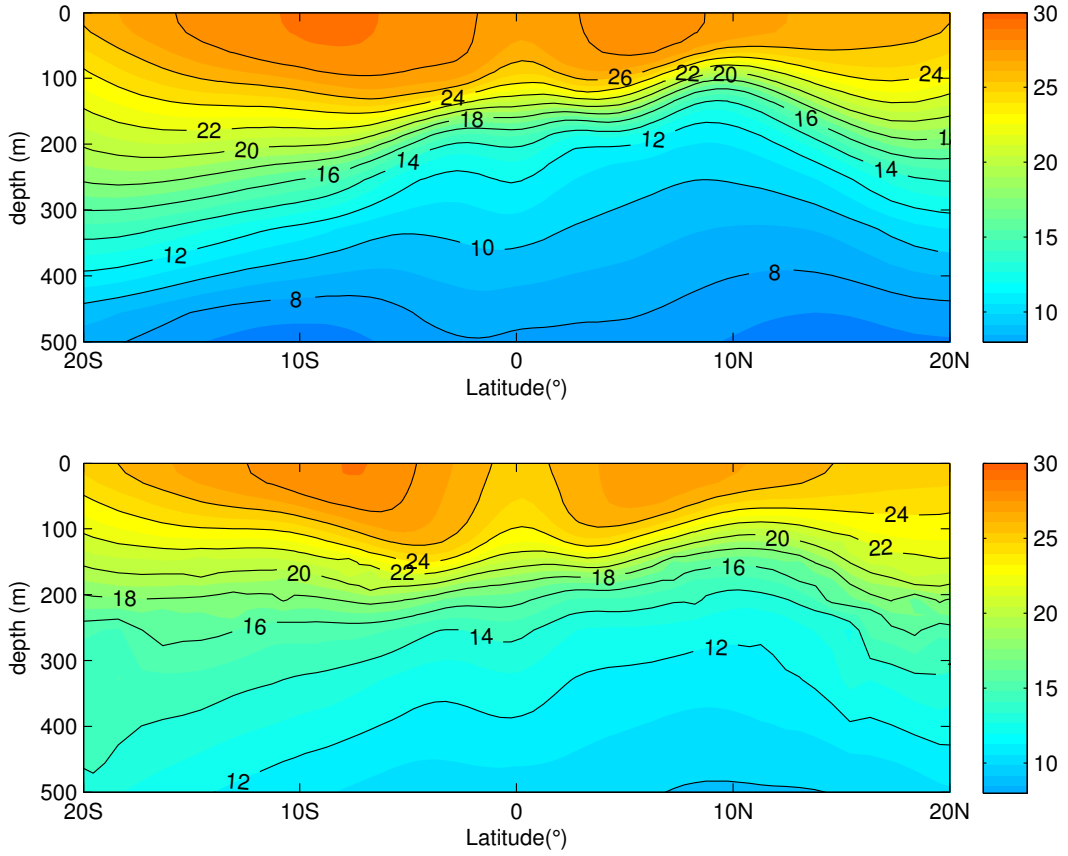

Figure 2.5 Annual mean temperature (°C) in the upper ocean along 165 °W as a function of depth. Top: GFDL ODA. Bottom: trMOM3-CE.

Annual mean subsurface temperature and ocean current averaged between 100m and 200m in the Atlantic for the coupled model and the GFDL ODA reanalysis are compared in Figure 2.6. In general, the coupled model gives a reasonably realistic simulation of the oceanic circulation except that the eastern tropical Atlantic is too warm compared to the ODA and the equatorial undercurrent (EUC) is weaker than that of the ODA. The North Brazil Current (NBC) along the western boundary of the Atlantic basin, carrying southern hemispheric water across the equator into the northern hemisphere is

also weaker than that estimated by the ODA. It also can be seen clearly that the subtropical gyre waters are almost 5°C warmer than the tropical gyre water near the equator, giving rise to strong temperature fronts separating the subtropical gyres from the tropical gyre. The front between the northern subtropical gyre and tropical gyre in the model is not as sharp as the one in the ODA.

Figure 2.7 shows the annual mean AMOC streamfunction and Atlantic zonally averaged temperature in trMOM3-CE simulation. The subtropical-tropical gyre temperature front near 10°N is again clearly visible. The mean AMOC gives a value of about 12 Sv at the equator in the upper 1000 m and this northward interhemispheric flow is the upper ocean return flow of the AMOC. Its value is roughly in line with the observed estimate and other state-of-the-art GCM simulations. The bottom overturning cell, however, is very weak in the model. In spite of the deficiencies, we consider that the simulation is sufficiently realistic for us to use this model to assess the tropical ocean-atmosphere response to changes in the AMOC.

The annual mean winds and precipitation from the atmospheric model in the control experiment is shown in Figure 2.8. The precipitation and wind stress fields bear close resemblance to the observed fields in many respects, owing again to the use of the anomaly coupling. The results shown in Figure 2.8 are similar to those presented by Schneider et al. (1997).

The observed and modeled annual cycles of SST at the equator in the Atlantic are compared in Figure 2.9. The structure of the model annual cycle is similar to that in the observations. In both model and observations, maximum variations are found near 12°W.

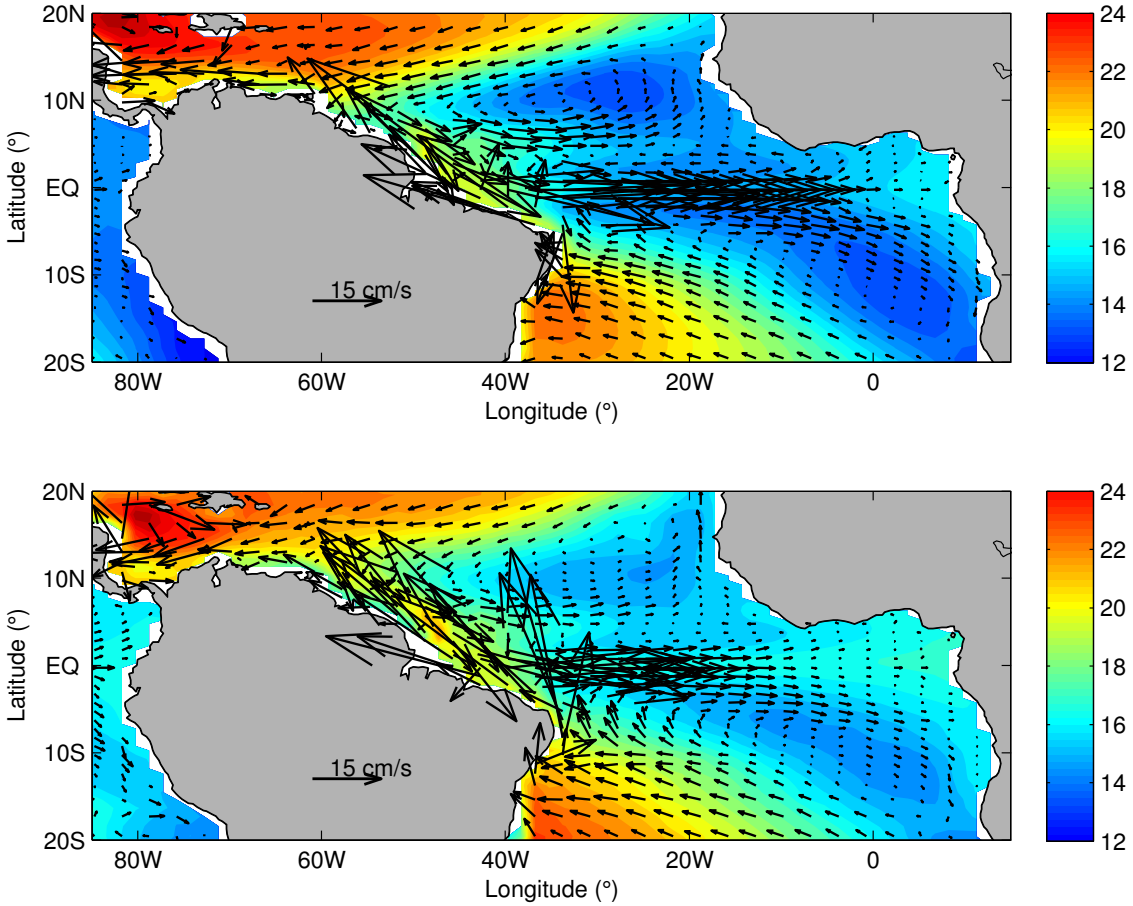

Figure 2.6 Annual mean temperature (°C; contour) and ocean current (vector) averaged between 100m and 200m over Atlantic Ocean. Top: GFDL ODA. Bottom: trMOM3-CE.

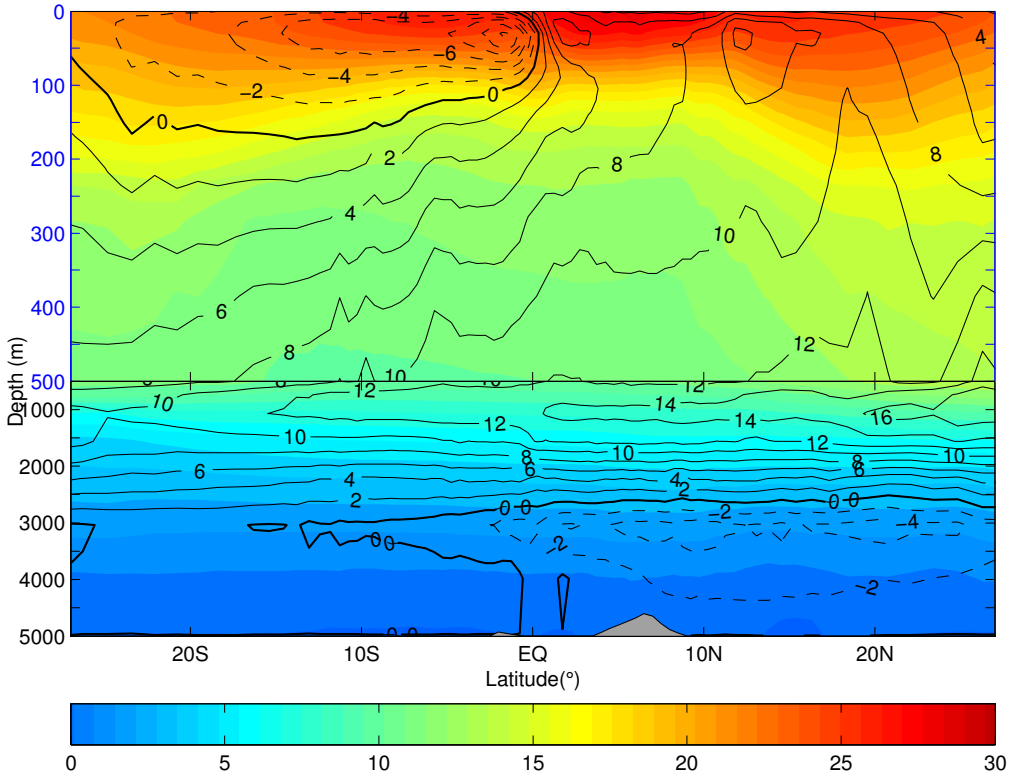

Figure 2.7 Annual mean AMOC (Sv; contour) and Atlantic zonally averaged temperature (°C; color) for trMOM3-CE.

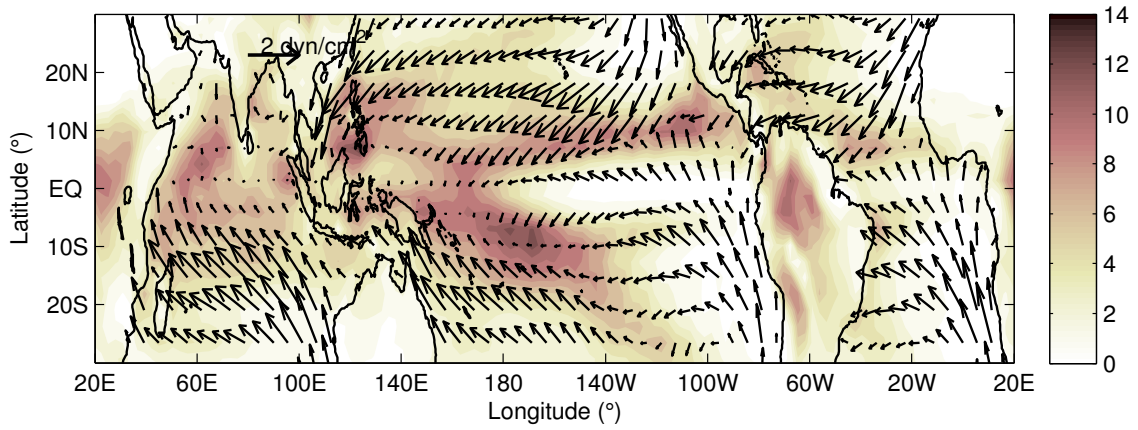

Figure 2.8 Annual mean surface wind stress (dyn/cm2; vector) and precipitation (mm/day; contour) for trMOM3-CE.

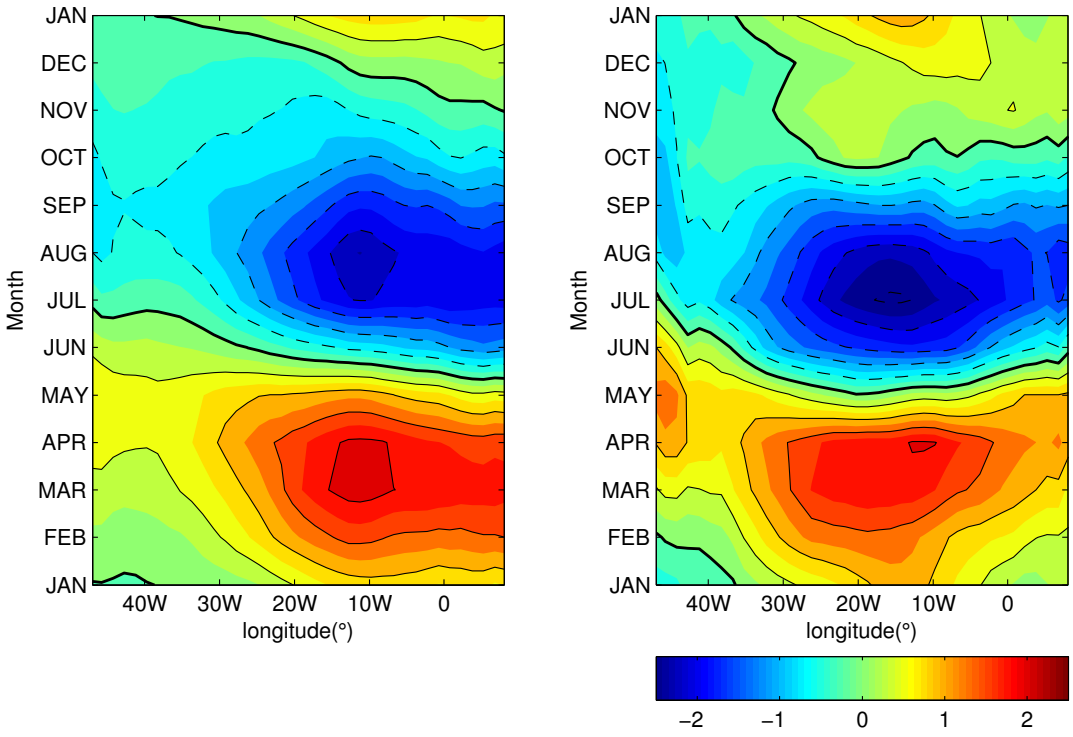

Figure 2.9 Annual cycle of SST (°C) at the equator (annual mean removed). The contour interval is 0.5 °C. Left: GFDL ODA. Right: trMOM3-CE.

2. Tropical variability

The EOF analysis provides an effective way to present the dominant pattern of variability of a dynamical system. Figure 2.10 shows the first two leading EOFs of simulated Atlantic SST anomaly, which compares favorably to the corresponding EOFs of the observed SST. The first EOF represents the so-called zonal mode of tropical Atlantic variability (TAV), while the second EOF represents the meridional mode. These results suggest that the model captures the basic spatial structure of TAV-related SST variability.

The first EOF of SST anomalies over the tropical Pacific region (120ºE-75ºW, 20ºS-20ºN) is displayed in Figure 2.11 for the coupled model simulation and observations, respectively. The primary feature of the leading SST EOF in the model shows a basic resemblance to that in the observations, with a few exceptions: 1) the simulated SST signature is more equatorially confined than the observed, especially in the northern tropical Pacific region; 2) the center of the simulated SST maximum variability is shifted westward along the equator and the SST variance extends further westward in comparison with the observations; 3) the explained variance of the leading EOF is 33% in the model, that is considerably less than the value of 64% found in the observation and the simulated SST maximum variability is also weaker than that of the observed.

Overall, we conclude that CCM3-trMOM3 gives a reasonable representation of ENSO variability in comparison with many other coupled GCM simulations, although the model ENSO does share many common flaws found in other coupled GCMs. We believe that this model presents us a useful numerical tool with which we can explore various physical mechanisms underlying the impact of AMOC changes to tropical climate variability.

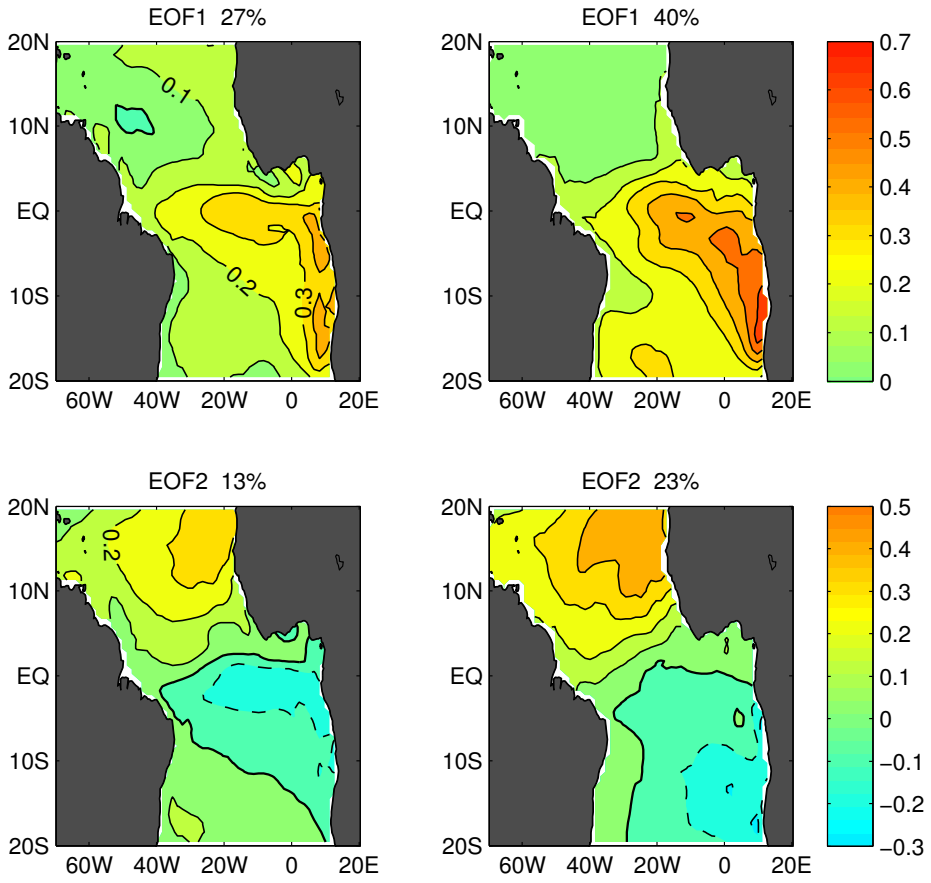

Figure 2.10 Tropical Atlantic Variability simulated by trMOM3-CE (left panel) and GFDL ODA (right panel)

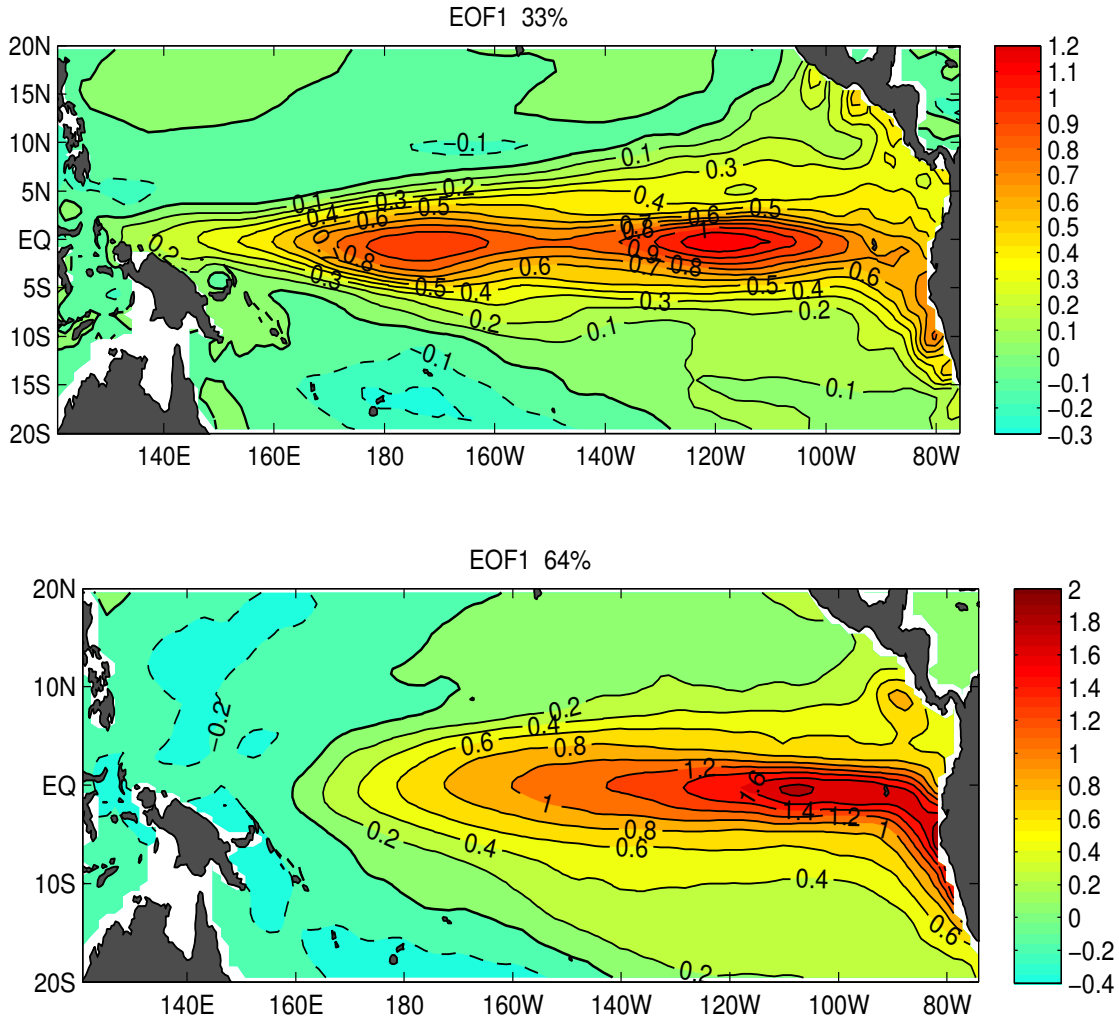

Figure 2.11 The first EOF of SST anomaly over tropical Pacific from trMOM3-CE (upper) and GFDL ODA (bottom)

CHAPTER III
OCEANIC RESPONSE TO NORTH ATLANTIC FRESHENING SIMULATED BY gMOM3

A. Introduction

It has long been noticed that the AMOC is a key element of the ocean climate system, changes in which can significantly affect the atmospheric and oceanic conditions on a global scale. The AMOC is a key component of the global ocean conveyor belt that transports large amounts of heat and water through wind-driven upper ocean circulation and the deeper oceanic thermohaline circulation. Analysis of ocean observations and model simulations suggests that there have been changes in the AMOC during the last century that may have profound implications on the tropical variability and climate change (Bryden et al., 2005; McPhaden and Zhang, 2002; Dong and Sutton, 2002; Vellinga and Wood, 2002; Zhang and Delworth, 2005). In almost all coupled climate model experiments, the Atlantic SST response to the weakening of the AMOC is characterized by a dipole with surface cooling in the northern hemisphere and warming in the southern hemisphere. In spite of the robustness of the modeling result, many fundamental questions have not been fully answered: What physical processes are responsible for the SST dipole? Does ocean-atmopshere interaction play a role in generating the SST dipole? If so, how does the feedback mechanism work? Does the AMOC respond linearly to freshwater forcing? Is there a threshold value below which the AMOC response to freshwater forcing changes drastically? Although many previous studies have examined the AMOC response to freshwater forcing (i.e., Stouffer et al., 2006), it remains unclear how different physical processes contribute to the formation of the dipole SST. This is because it is often difficult to isolate the causality in fully

coupled GCM experiments (Wu et al., 2007).

Meanwhile, paleoceanographic records suggest that the AMOC exhibits oscillations on the order of several time-scales during the last glacial cycle and its mode changes have been linked to abrupt climate changes over the North Atlantic region (Clark et al., 2002, 2004). Hubeny et al. (2006), for example, show evidence of multidecadal cycles of Late Holecene North Atlantic climate variability preserved by estuarine fossil pigments. Decadal-to-multidecadal AMOC variations are also indicated by observed changes in several variables, including sea surface height (Häkkinen and Rhines, 2004), surface heat and freshwater flux (Marsh, 2000), Atlantic Ocean salinity changes (Belkin et al., 1998; Curry et al., 2003) and the overflow from Nordic seas (Hansen et al., 2001) during the last 50 years. Similar multidecadal oscillations are also found in many coupled general circulation models (CGCMs) (Delworth et al., 1993; Timmermann et al., 1998; Saravanan et al., 2000; Knight et al., 2003; Cheng et al., 2004; Dai et al., 2005; Danabasoglu, 2008) and in simple, idealized models (Weaver and Sarachik, 1991; Greatbatch and Zhang, 1995; Saravanan and Mcwilliams, 1997; Capotondi and Holland, 1997; Neelin and Weng, 1999; Colin de Verdiere and Huck, 1999; Teraa and Dijkstra, 2002). These oscillations are mostly irregular and have a wide range of periods among different models, ranging from 25-30 years (Cheng et al., 2004; Dai et al., 2005) to 70-80 years (Timmermann et al., 1998).

The multidecadal AMOC oscillations are thought to be one of the main drivers of multidecadal SST variation over the North Atlantic that has significant regional and hemispheric climate impact (Enfield et al., 2001; Zhang and Delworth, 2006). This multidecadal SST variability is often referred to as the Atlantic Multidecadal Oscillation (AMO) named by Kerr (2000). It is one of the dominant modes of climate variability in the North Atlantic and its variability can be measured by a so-called AMO index which was introduced by Enfield et al. (2001) and defined as a 10-year running mean of the

detrended Atlantic SST anomaly averaged over the entire North Atlantic. The AMO has been documented extensively in literature (Moron et al., 1998; Tourre et al., 1999). Kushnir (1994) found that the difference of the SST pattern between the relatively warm years 1950-1964 and the relatively cold years 1970-1984 shows negative anomalies near Newfoundland and positive anomalies over the rest of the basin. Delworth and Mann (2000) extended the instrumental record with proxy data and demonstrated that there is a significant spectral peak in 40-70 year frequency band.

Although many mechanisms have been proposed to interpret the origin of the multidecadal AMOC oscillations, most of them have focused on the high latitude sinking region where the North Atlantic deep water formation (DWF) occurs because of the intense atmospheric cooling during the boreal winter. It has been proposed that the oscillations are maintained by the phase delay between temperature and salinity contributions to the total density in this DWF region. The difference among different proposed mechanisms mainly lies in what causes the changes in temperature and salinity associated with density changes in the DWF region.

Delworth et al. (1993) showed that the density anomalies in the sinking region of the North Atlantic drive the multi-decadal AMOC oscillation in the GFDL CGCM with an estimated time scale of 50-60 years. This density anomaly in the North Atlantic is induced by salinity fluctuations that arise from the AMOC oscillation itself. Using an updated version of the GFDL coupled model, Delworth and Greatbatch (2000) further suggest that the AMOC fluctuation in the new model is in principle thermally driven and excited by internally generated, low-frequency atmospheric noise, especially that associated with the North Atlantic Oscillation (NAO) (Danabasoglu, 2008).

In contrast to above studies, multidecadal oscillations are also interpreted to occur through the enhanced transports of relatively fresh water and sea ice from the Arctic into the sinking region (Delworth et al., 1997), the storage and release of freshwater from the

central Arctic and circulation changes in the Nordic Seas (Jungclaus et al., 2005). The coupling of the Atlantic and Pacific Oceans via an atmospheric teleconnection mechanism might also play a role (Timmermann et al., 1998). However, the basic mechanism that drives multidecadal oscillations remains the same as in the above studies, i.e., the oscillation is generated by changes in density structure in the sinking regions through advection of temperature and salinity anomalies.

According to the advective mechanism, the formation rate of the North Atlantic Deep Water (NADW) in sinking regions should change over multidecadal time scales. However, an analysis of surface heat and freshwater fluxes suggests little change of NADW formation rates in the Labrador Sea from 1980 to 1997 (Marsh, 2000), whereas observations do suggest a change in the AMOC over the last century (Bryden et al., 2005, Zheng, 2007). This implies that there may be other existing mechanisms causing the multidecadal AMOC oscillations. Zheng (2007) shows the mean AMOC difference between the periods 1958-1980 and 1981-2001 based on SODA data and shows that there are significant AMOC changes between the middle latitude band 20°N-45°N and layer 500m-2000m. In a model simulation, Dai et al. (2005) found that the upper-ocean density changes in the middle latitude North Atlantic lead the AMOC variation by about 6 years resulting in the AMOC multidecadal oscillation through an advective mechanism. This means that AMOC variations may also be generated by localized changes in middle latitude Atlantic regions that are often poorly simulated in ocean models.

Hence, the primary objectives of this chapter are 1) to isolate and elucidate oceanic processes and atmospheric processes in linking tropical SST response to AMOC changes, and 2) to investigate potential mechanisms for multi-decadal oscillations of the AMOC using gMOM3 experiments described in Chapter II. The fundamental questions to be addressed are: 1) How important are the oceanic processes for the SST response to a weakening of the AMOC due to the freshening of the North Atlantic? 2) Is there a

different mechanism for the multi-decadal AMOC oscillation that is independent of the changes in the sinking region?

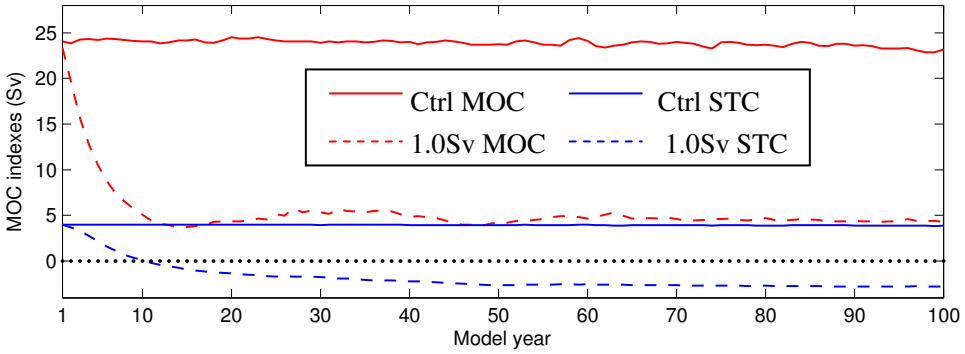

Figure 3.1 The time series of the maximum strength of the AMOC (maximum value of the annual Eulerian mean overturning streamfunction over the domain 30°N-50°N and 400m-2000m depth) in the gMOM3-Ctrl run (solid red line) and the gMOM3-Hosing-1.0Sv experiment (dashed red line), respectively. The blue lines indicate the mass transport in the low branch of the north STC averaged across the Atlantic basin along 8°N from 100 to 400m for the gMOM3-Ctrl run (solid blue line) and the gMOM3-Hosing-1.0Sv experiment (dashed blue line).

B. Tropical Ocean Response to a Shutdown of AMOC

In this section, we present the response of the tropical ocean to a near shutdown of the AMOC in a strong hosing experiment – gMOM3-Hosing-1.0Sv where the North Atlantic is freshened at a rate of 1.0 Sv ($10^6 m^3/s$) continuously for a period of 100 years. Figure 3.1 shows the time series of the maximum AMOC in the control run and the

perturbation experiment. In the control run, the maximum AMOC stabilizes at about 24 Sv for the whole simulation period within the reasonable ranges of most models' maximum AMOC strength. In the perturbation run, the maximum AMOC rapidly weakens from 24 Sv to about 5 Sv after 10 years and reaches an equilibrium state through the rest of the simulation.

Figure 3.2 is the vertical structure of the annual mean AMOC streamfunction for gMOM3-Ctrl run and the gMOM3-Hosing-1.0Sv experiment superimposed on the zonally averaged temperature. It shows the mean structure and change of the AMOC captured by the model simulations. The AMOC streamfunction has a maximum value near 45°N and 800m. The wind-driven subtropical cells (STCs) can be identified in the upper ocean. They are clearly asymmetric about the equator in the control run, but become nearly symmetric in the 1.0Sv experiment when the AMOC is nearly shutdown. Accompanied with the circulation change, there is a change in ocean temperature. In the 1.0Sv experiment, the substantial weakening of the AMOC due to the high latitude freshening weakens the northward heat transport in the Atlantic (Haarmas et al., 2008) and results in a cooling of mid-high latitudes of the North Atlantic (Figure 3.3), because most of the heat transport change occurs within the upper ocean (Boccaletti et al., 2005). Below the surface cooling, there is a subsurface warming in the deep water formation region where the surface freshening reduces deep convection and prevents the deep-penetration of the cold surface water (Chang et al., 2008). Within the tropics, there is a secondary warm anomaly maxima with 3°C temperature change between 100m and 400m near 8°N. This subsurface warming is an important source for the surface warming in the equatorial south Atlantic, as shown by Chang et al. (2008).

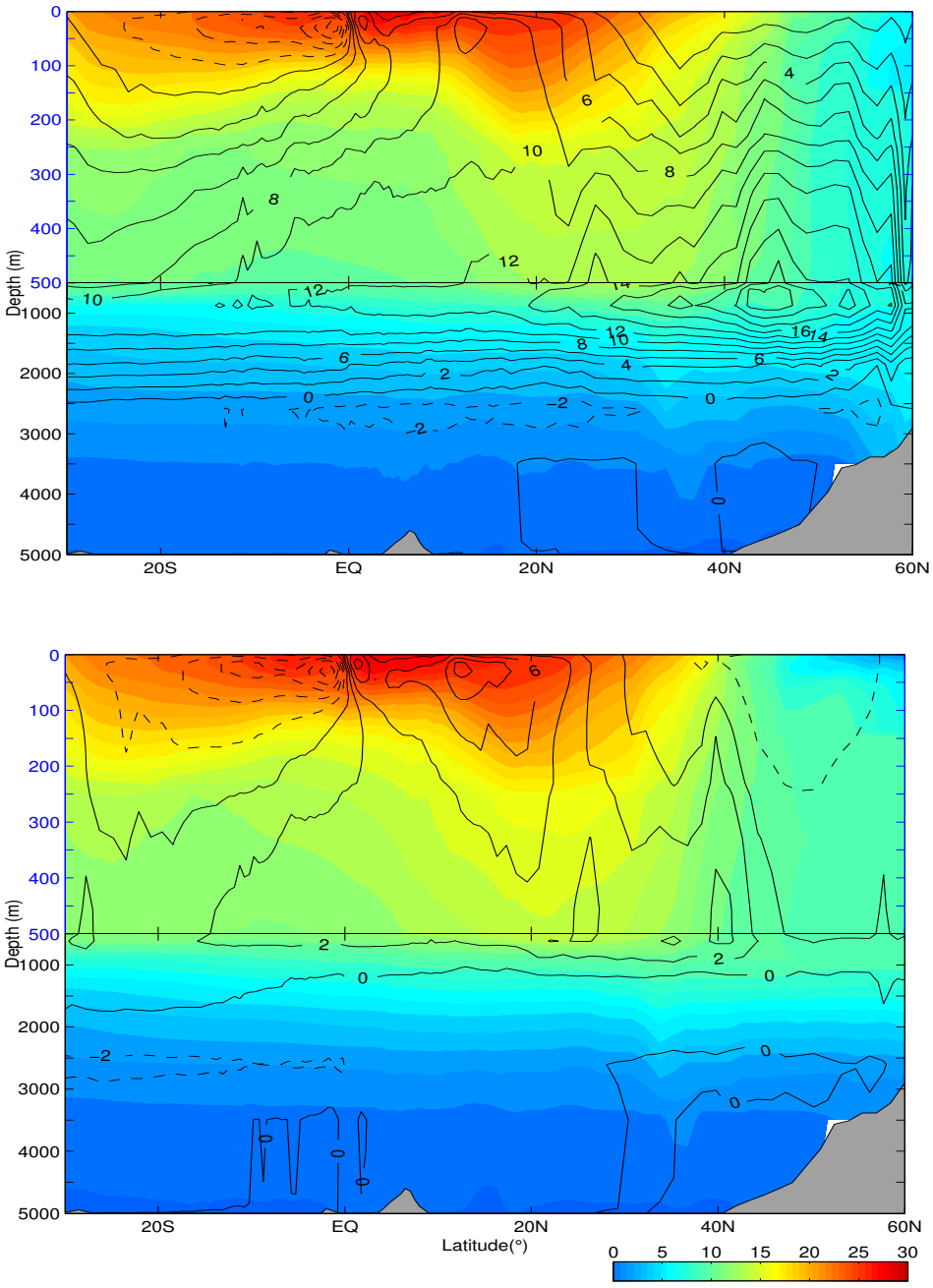

Figure 3.2 AMOC streamfunction (contour) superimposed on zonally averaged temperature (color) in the Atlantic Ocean for the gMOM3-Ctrl run (top) and the gMOM3-Hosing-1.0Sv experiment (bottom). The AMOC streamfunction is in Sv and the temperature is in °C.

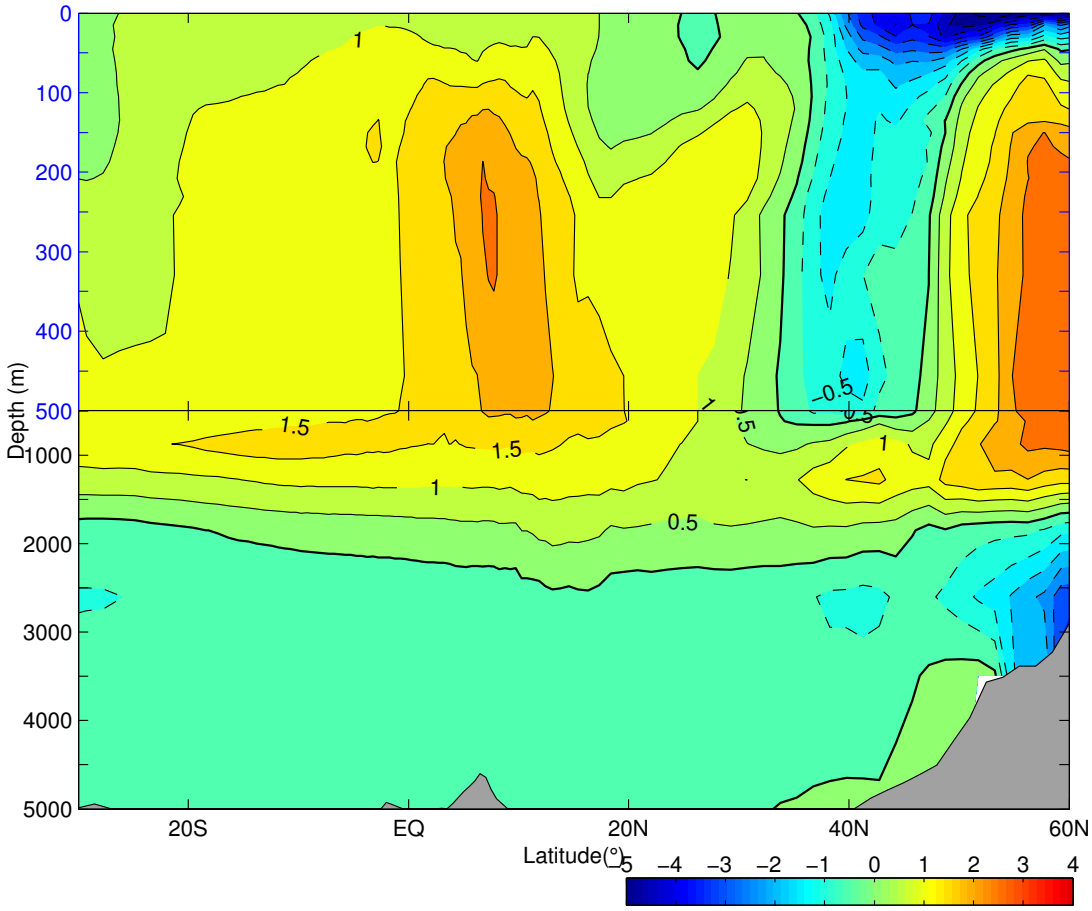

Figure 3.3 Zonally averaged temperature anomaly in the Atlantic Ocean derived by differencing between the gMOM3-Ctrl run and gMOM3-Hosing-1.0Sv experiment. The temperature is in °C.

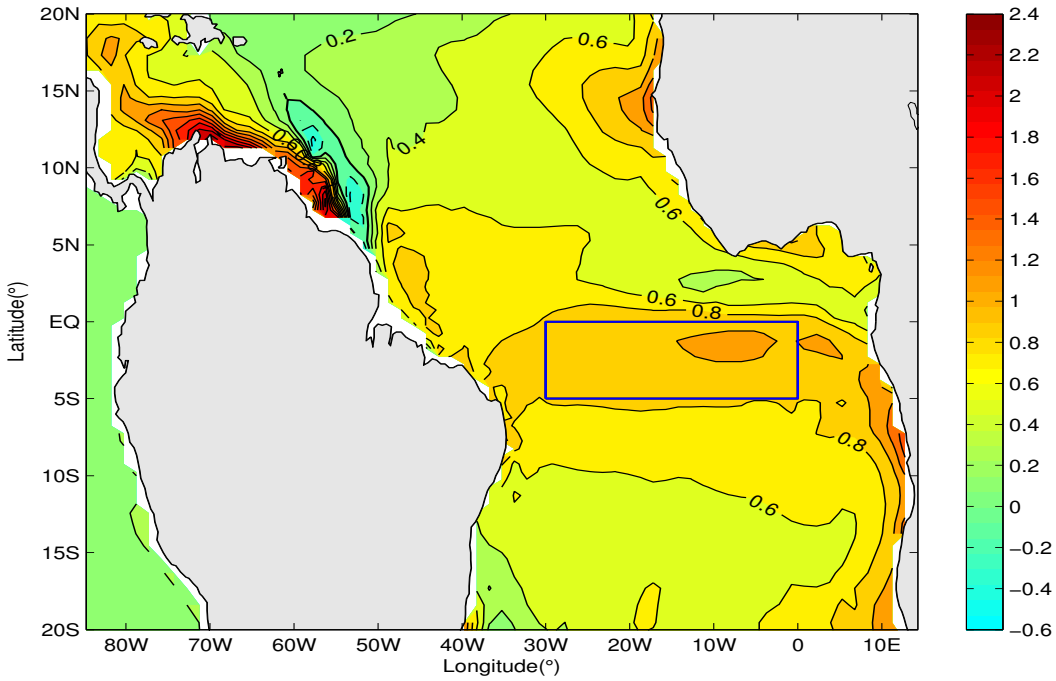

Figure 3.4 Tropical Atlantic SST anomaly derived by differencing between the gMOM3-Hosing-1.0Sv experiment and the gMOM3-Ctrl run. The temperature is in °C.

We next examine how the circulation change affects the tropical SST response. Figure 3.4 shows the annual mean tropical Atlantic SST difference between the 1.0Sv experiment and gMOM3-Ctrl run. It shows a basin-wide warming in the entire tropical Atlantic except for a small region off north Brazilian coast. Intense warming occurs near the upwelling zones off the west coast of Africa and along the equator, indicating that the warming signal may originate from the subsurface. Consistent with the oceanic pathway change mechanism proposed by Chang et al. (2008), the reduction in the interhemisphere flow in the upper ocean (Figure 3.2) causes the western boundary current along the northeastern coast of South America (the return branch of the northern STC, Figure 3.1) to reverse its direction from polarward to equatorward. This circulation

change gives rises to a rapid increase in subsurface temperature near the strong temperature front around 8°N (Figure 3.3). The warm anomaly is then carried equatorward along the western boundary.

In addition to the oceanic pathway change mechanism, oceanic wave adjustment also contributes to the surface warming. Figure 3.5 shows the time evolution of monthly temperature anomalies at 200m depth along the equator for the first 20 years. There are well-defined warm temperature pulses that appear to be initiated along the western boundary during late spring and summer and propagate rapidly eastward. The eastward propagation speed is estimated to be approximately 1.2 m/s and roughly coincides with theoretical phase speed of the second vertical mode of the equatorial Kelvin wave. We hypothesize that the wave generation is associated with the seasonal change of the North Brazil Current and North Equatorial Counter Current system. In each May, the southeast trades intensify, which has a dramatic effect on the North Brazil Current. It abruptly veers off the Brazilian coast and turns eastward to feed the North Equatorial Counter Current. This seasonal change in the ocean circulation excites Kelvin/Rossby waves and the waves, particularly the coastal and equatorial Kelvin waves, carry the warm anomalies from the temperature front region near 8°N to the equator and then along the equator to the eastern equatorial Atlantic. Further experiments are needed to separate the effect of the wave adjustment from the advection due to the circulation change. These experiments are beyond the scope of this dissertation. Instead, we carry out an analysis in an attempt to separate wave effect and advective effect. We assume that temperature change at a given depth can be decomposed into a part that is associated with isopycnal surface fluctuations and another part that is associated with the temperature change along the given isopycnal surface. The former can be considered as wave-induced, while the latter as advection-induced. Figure 3.6 is the time evolution of monthly temperature anomalies along the equator on the 26.45 isopycnal surface, which is in the depth range

between 150 m and 210 m. It is clear that the advective contribution occurs at much longer time scales than the wave contribution. This result needs to be further validated by future numerical experiments.

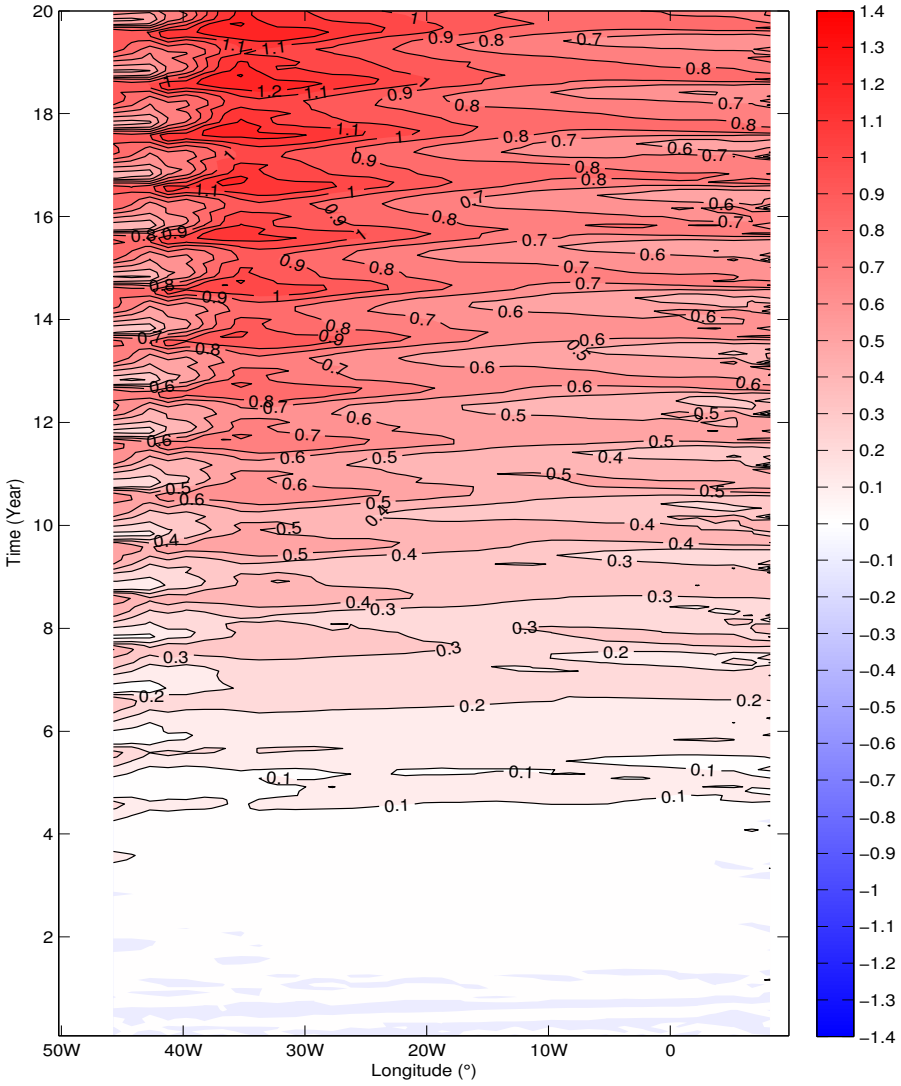

Figure 3.5 Time evolution of monthly temperature anomaly at 200m depth along the equator derived by differencing between the gMOM3-Hosing-1.0Sv experiment and the gMOM3-Ctrl run for the first 20 years. The temperature is in °C.

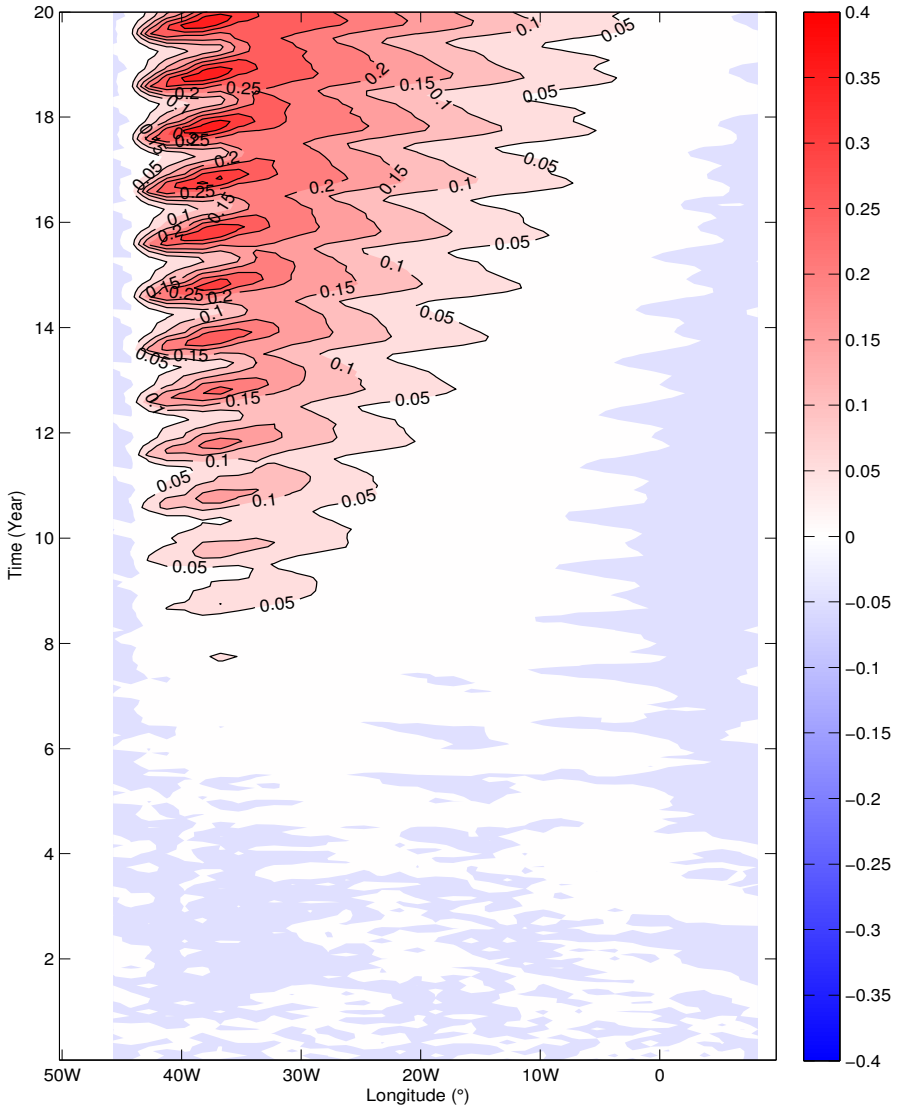

Figure 3.6 Time evolution of monthly temperature anomaly on the 26.45 isopycnal surface along the equator derived by differencing between the gMOM3-Hosing-1.0Sv experiment and the gMOM3-Ctrl run for the first 20 years. The temperature is in °C.

The large subsurface warming along the boundary between the subtropical and tropical gyre and its subsequent development along the equator and along the African coast is consistent with coupled GCM water-hosting simulations (Stouffer et al., 2006; Dahl et al., 2005; Chang et al., 2008; Wu et al. 2008) and a 2-1/2 layer reduced gravity ocean model study (Wen et al., 2009, submitted to J. Climate). In contrast, the strong surface cooling in the tropical North Atlantic simulated by coupled GCMs is absent in our stand-alone ocean model simulation, suggesting that the surface cooling is largely attributed to atmospheric processes, which is excluded in our simulations. The effect of the surface cooling in the North Atlantic will be investigated in the next chapter. Therefore, the direct influence of the AMOC-induced circulation changes on SST appears to be confined to the equatorial and South Atlantic Ocean. This finding supports the results of previous modeling studies that the atmospheric boundary layer process and its interaction with the ocean mixed layer are mainly responsible for transmitting the surface cooling from high latitude north Atlantic to the tropics (Chiang et al., 2003, 2008), whereas the oceanic teleconnection is responsible for the warming in equatorial south Atlantic (Chang et al. 2008; Wu et al. 2008). Without the participation of atmospheric processes, the high latitude cooling extending to the extratropical region hardly penetrates into the tropical region.

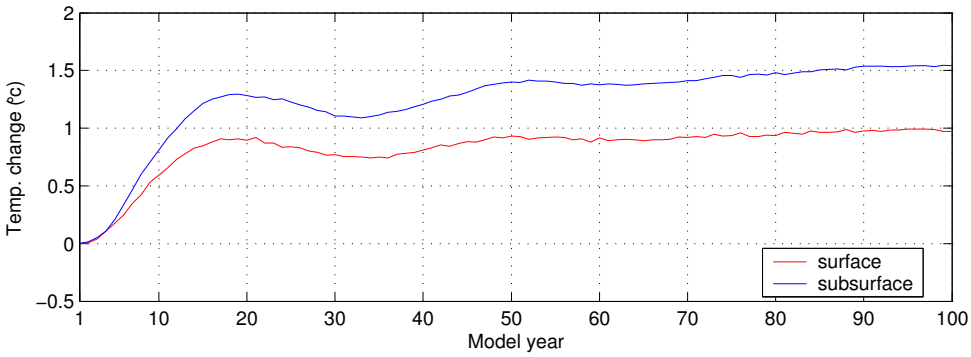

Figure 3.7 Time series of SST anomaly and subsurface temperature anomaly at 100m depth averaged over 30°W~0°W and 0°S~5°S indicated by the blue box in Figure 3.4.

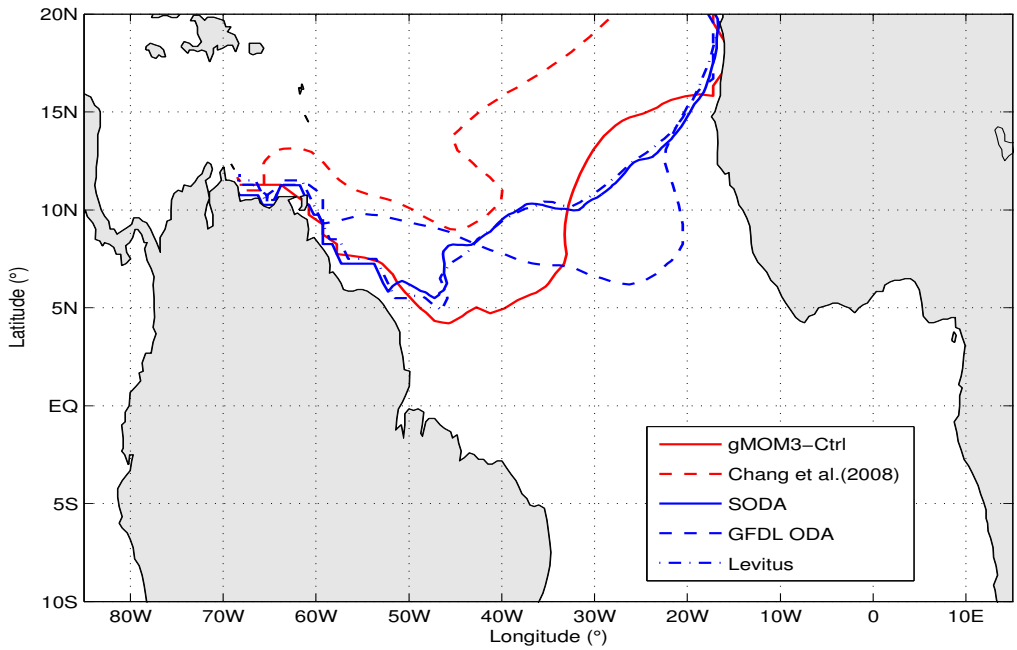

Figure 3.8 Location of the 17°C isotherm on 26.05 isopycnal for Levitus data, SODA data, GFDL ODA and the model data used in Chang et al. (2008) and the gMOM3-Ctrl run.

Figure 3.7 shows that the temperature anomaly averaged over 30°W~0°W and 0°S~5°S has a rapid increase by about 0.9°C during the first 20 years of freshening and the subsurface temperature increases by an even higher value than the surface temperature. This is consistent with previous findings that the surface warming in this region is caused by the subsurface temperature change. However, in our experiment, the temperature increase occurs in a relatively short period of time after the freshening when compared to the experiments conducted with the GFDL CM2.1 analyzed by Chang et al. (2008) in which it takes about 20 years after the freshening for the rapid temperature increase to occur. This may be due to the difference in strength and location of the temperature front between the northern subtropical and tropical region that determines how fast the warming anomaly propagates to the equatorial region (Wen et al., 2009, submitted to J. Climate.). Figure 3.8 shows the location of the 17°C isotherm on 26.05 isopycnal for Levitus data, SODA data, GFDL assimilation and the GFDL CM2.1 simulation used in Chang et al. (2008) and the gMOM3-Ctrl run. Compared to the observations, the GFDL CM2.1 simulation places the front too far away from the equator, while the gMOM3-Ctrl simulation places the front too close to the equator. This difference may help explain the difference in the temperature response to the fresh water forcing simulated by the GFDL CM2.1 and gMOM3.

Previous coupled GCM studies have shown that a sudden weakening of the AMOC also leads to persistent changes in the Tropics outside the Atlantic (Dong and Sutton, 2002; Zhang and Delworth, 2005) and a weakening of the Indian and Asian summer monsoons, which is consistent with the global synchronization of abrupt climate change indicated by paleorecords (Wang et al., 2001; Altabet et al., 2002). Although the main mechanism linking the response from the Atlantic to the tropical Pacific is thought to be through the atmosphere (Zhang and Delworth, 2005; Xie et al., 2008), it is not clear whether the ocean plays any role in the remote response over the tropical Pacific. To

investigate this question, we analyze gMOM3-Winda and gMOM3-CFE simulations, both of which are described in Chapter II, section C. We compare these simulations to gMOM3-Hosing-1.0Sv experiment to assess the relative importance of atmospheric versus oceanic contributions to changes in the tropical Pacific Ocean.

The upper Pacific MOC shown in Figure 3.9a is symmetric about the equator and presents no significant changes in the hosing run (Figure 3.9b), suggesting that the upper Pacific MOC is not strongly affected by the Atlantic circulation change forced by the fresh water. However, an antisymmetrical subsurface temperature anomaly pattern with warming north of the equator and cooling south of the equator occurs in gMOM3-Winda and gMOM3-CFE. This indicates strongly that the atmospheric changes are mainly responsible for the Pacific changes in response to the Atlantic freshening (Zhang and Delworth, 2005; Xie et al., 2008). The question is how the atmospheric processes work to cause the opposite sign of subsurface temperature anomalies.

As mentioned previously, the depth of 20ºC isothermal is a good proxy for the tropical thermocline depth. Figure 3.10 shows the tropical thermocline depth anomaly and the Pacific subsurface temperature anomaly at depth of 150m for gMOM3-Hosing-1.0Sv, gMOM3-Winda and gMOM3-CFE. Again, the gMOM3-Hosing-1.0Sv experiment, where only the fresh water forcing is used to force the model, produces no significant changes in the Pacific (Figure 3.10a). The other two experiments where wind stress anomalies are introduced produce significant subsurface anomalies (Figure 3.10b and 3.10c). North of the equator, the positive wind stress curl anomaly (Figure 3.11) produces an enhanced Ekman pumping, which deepens the tropical North Pacific thermocline to result in subsurface warming there, while the tropical South Pacific thermocline is shallowed owing to the positive wind stress curl anomaly there, causing the subsurface cooling south of the equator.

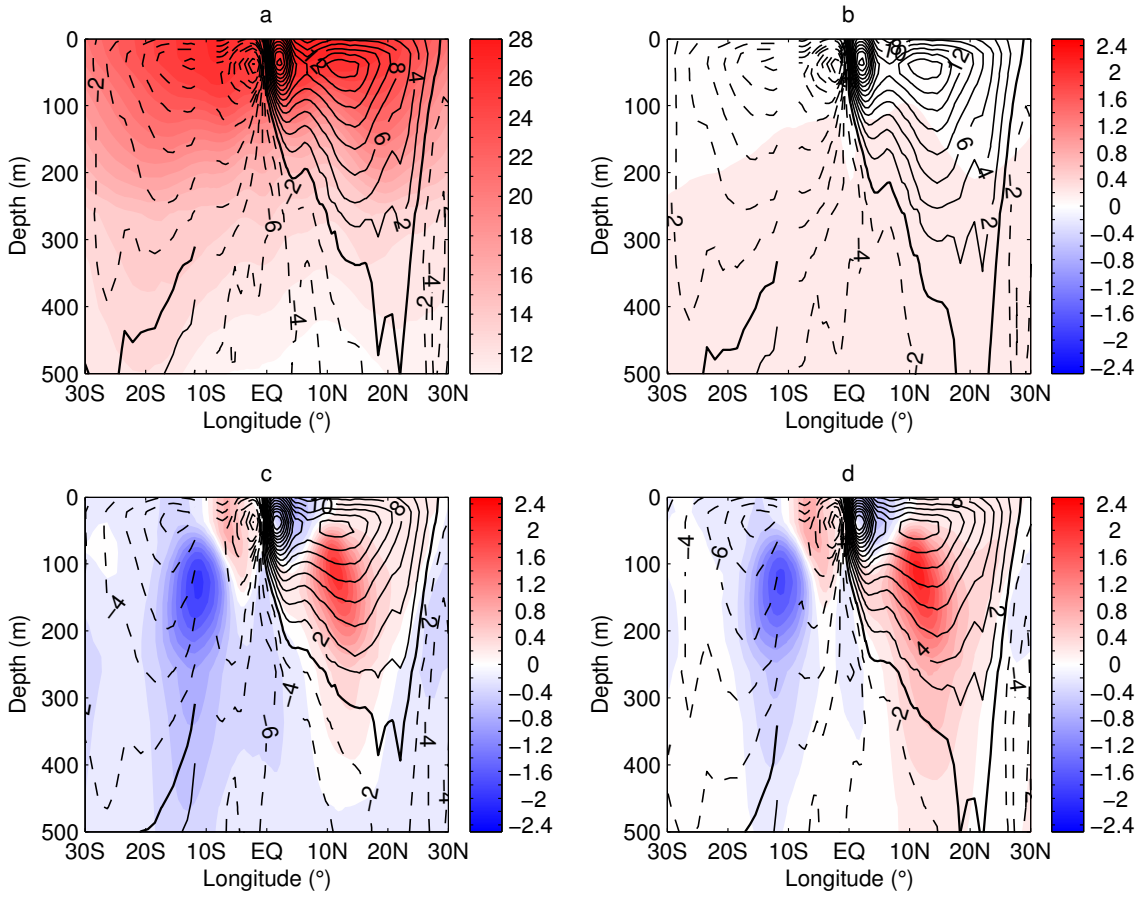

Figure 3.9 Upper Pacific MOC (contour) and zonally averaged temperature (color) for the run of gMOM3-Ctrl (a), gMOM3-Hosing-1.0Sv (b), gMOM3-Winda (c) and gMOM3-CFE (d). In (b), (c) and (d) superimposed onto the MOC streamfunctions are temperature anomalies (color), instead of temperature, in °C. The MOC streamfunction is in Sv.

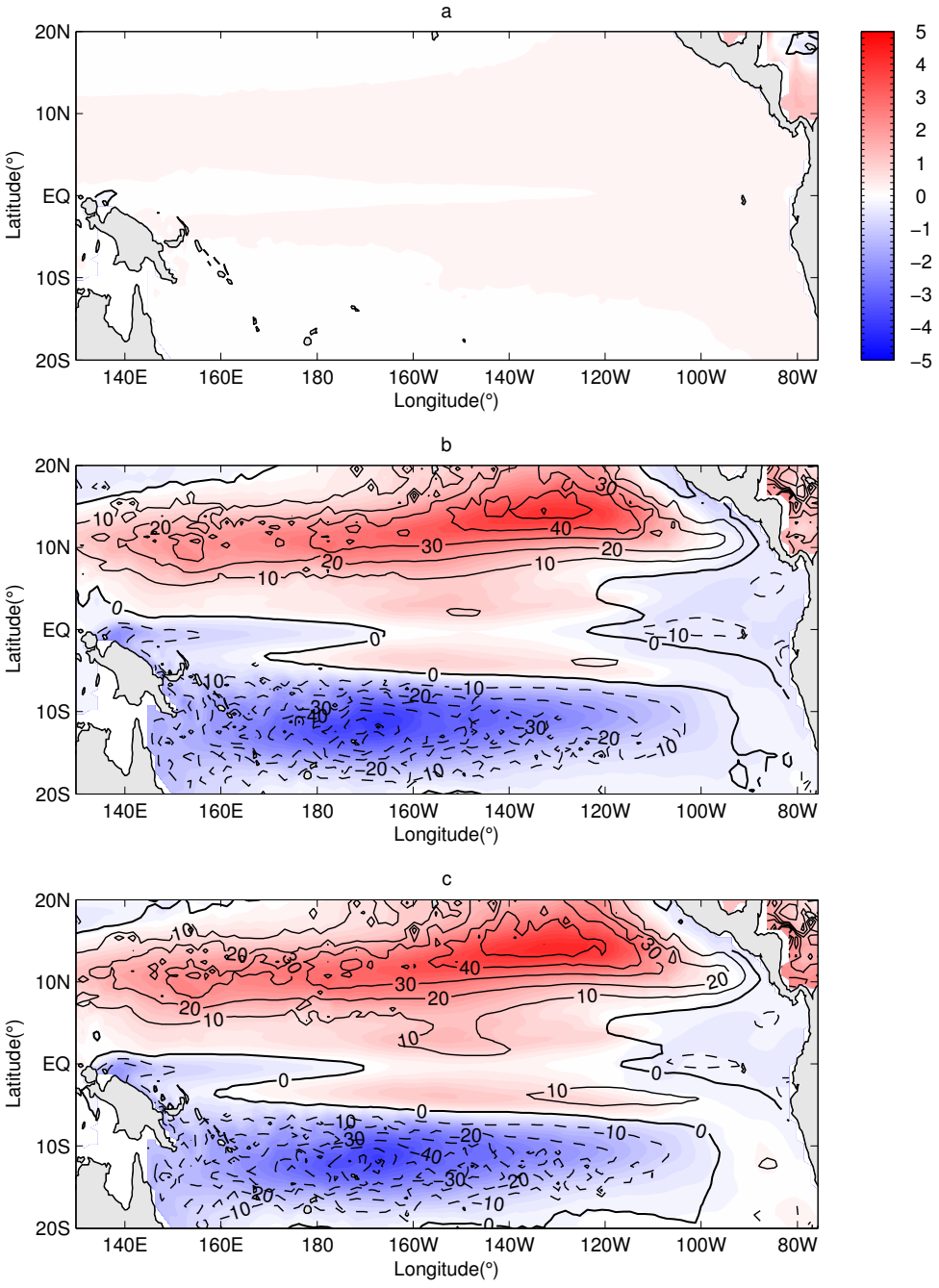

Figure 3.10 Pacific subsurface temperature anomaly (color) and the thermocline depth anomaly (contour) for the runs of gMOM3-Hosing-1.0Sv (a), gMOM3-Winda (b) and gMOM3-CFE (c). The temperature is in °C and the depth is in meter.

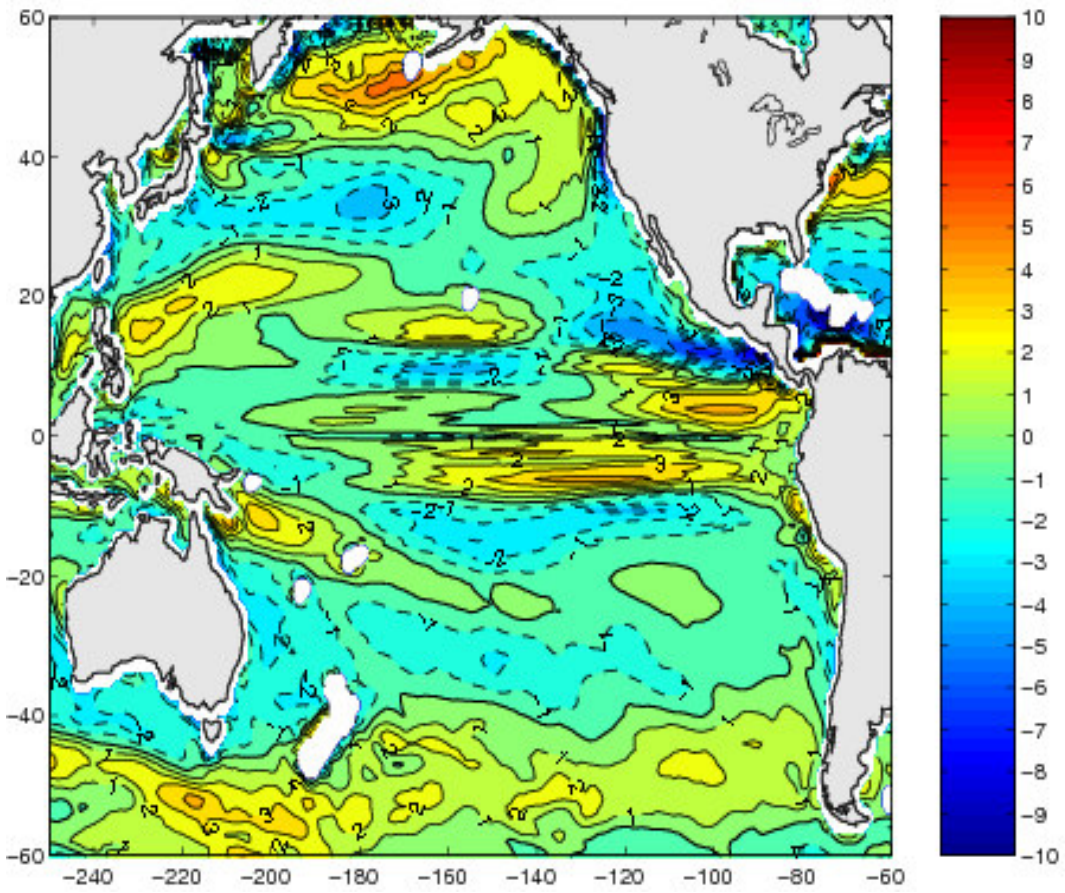

Figure 3.11 Wind stress curl anomaly over Pacific Ocean used in gMOM3-Winda experiment. The wind stress curl is in 10^{-8} N/m^3.

C. Tropical Response to Different Strengths of AMOC

To explore the sensitivity of the tropical response to changes in the AMOC, we carried out a set of sensitivity experiments where the freshwater input in the northern North Atlantic is increased systematically from 0.1Sv to 3Sv. We are particularly interested in examining the questions, such as, does the AMOC respond linearly or nonlinearly to the changes in freshwater forcing? What are the tropical responses to different strengths of the AMOC induced by the freshwater hosing? Is there a threshold value in the AMOC strength below or above which the AMOC strength becomes insensitive to the hosing freshwater? The control simulation of gMOM3-Ctrl serves as a reference for all other sensitive experiments. The details of the experimental design and method are described in section B of Chapter II.

If we measure AMOC strength using the maximum value of the annual Eulerian mean overturning streamfunction over the domain 30°N-50°N and 400m-2000m depth in each experiments, we can track AMOC changes as a function of the magnitude of the freshwater forcing as shown in Figure 3.12. For weak freshwater forcing (0Sv to 0.6Sv), the AMOC strength decreases nearly linearly with the freshwater forcing. After that, the AMOC decreases at a slower rate, suggesting that it is less sensitive to the freshwater input. The change of the return branch of north STC follows a similar trend in response to the AMOC changes, while it reverses its direction with a freshwater input of 0.3 Sv.

The relationship between the freshwater forcing strength and tropical Atlantic SST changes measured by a SST index averaged over an equatorial box of 30°W-0°W and 5°S-0°S from each experiment is shown in Figure 3.13. The SST responds similarly to AMOC changes. For relative weak freshwater forcing (0.1Sv to 0.6Sv) the SST increases linearly with the freshwater forcing. Beyond 0.6 Sv, the SST becomes insensitive to freshwater forcing, as shown in Figure 3.14.

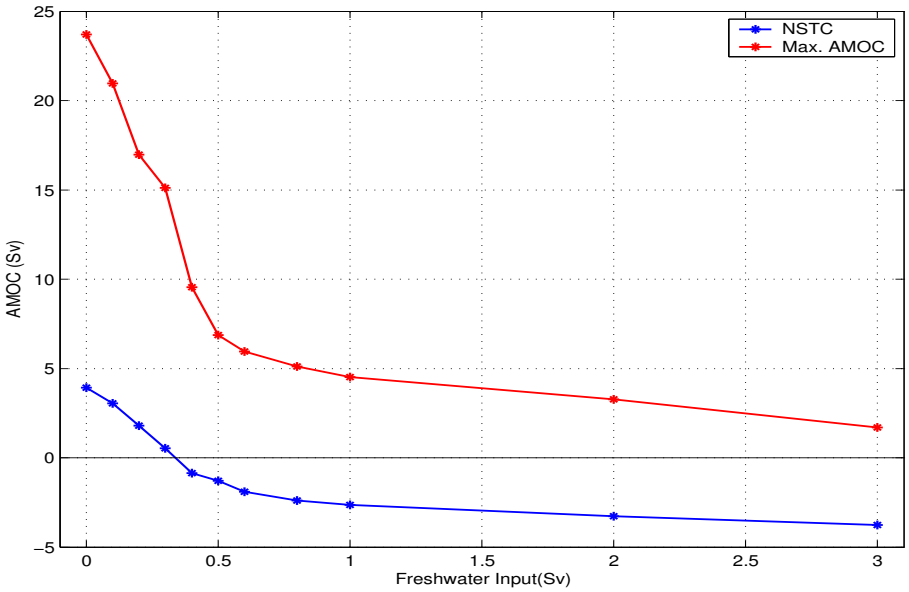

Figure 3.12 Maximum AMOC and the return branch of northern STC averaged for the last 60 years of the simulations in response to different strength of the freshwater input over northern North Atlantic.

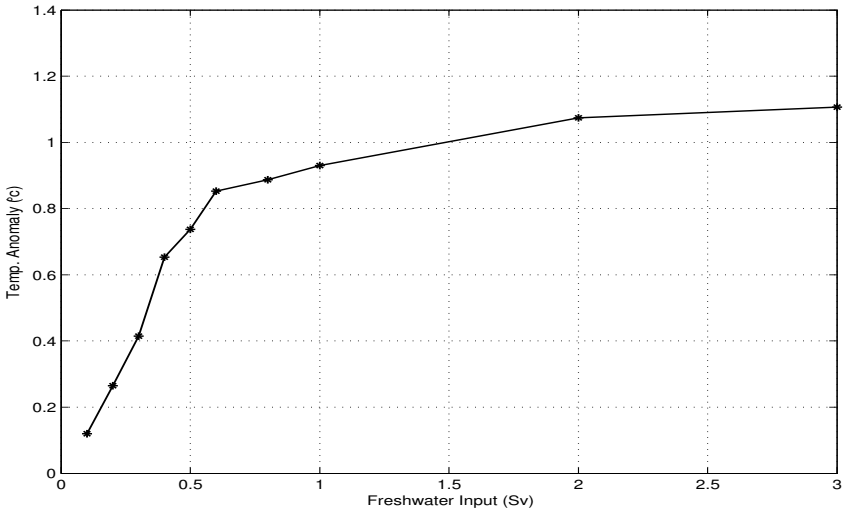

Figure 3.13 Relationship between the freshening strength and the changes of tropical Atlantic SST anomaly.

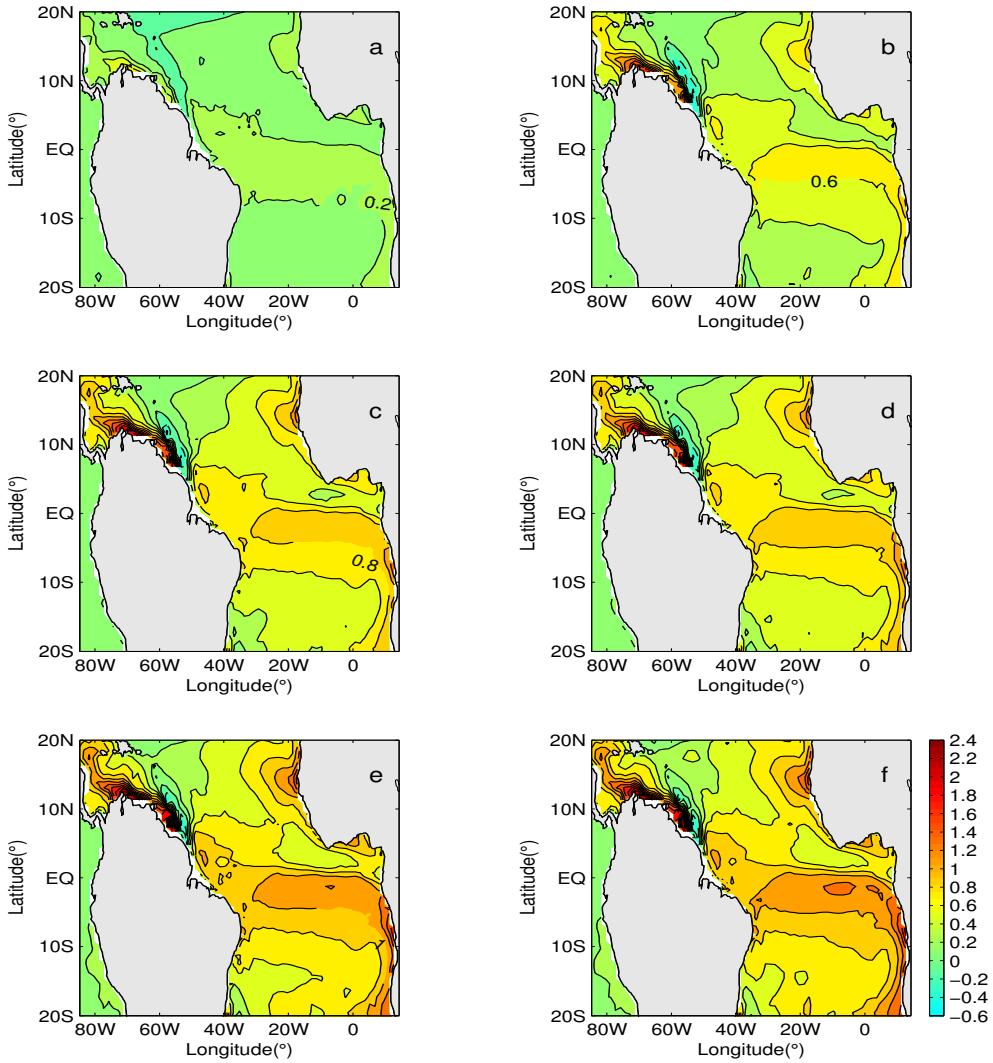

Figure 3.14 Tropical Atlantic SST anomalies between the gMOM3-Ctrl run and (a) the gMOM3-Hosing-0.2Sv experiment, (b) the gMOM3-Hosing-0.4Sv, (c) the gMOM3-Hosing-0.6Sv, (d) the gMOM3-Hosing-0.8Sv, (e) the gMOM3-Hosing-2.0Sv, (f) the gMOM3-Hosing-3.0Sv.

Overall, the configuration of our gMOM3 permits a systematic exploration of the response to different rates of freshening and the sensitivity experiments indicate a threshold value in the neighborhood of 0.3Sv-0.4Sv beyond which the NSTC return flow reverses its direction (Figure 3.12). For weak freshwater forcing (0.1Sv-0.3Sv), the reduction in the intensity of the AMOC and the warming of tropical Atlantic are modest and may be dominated by the Kelvin/Rossby wave adjustment process excited by the high latitude freshwater input. Yang (1999), Knutti et al. (2004), and Cessi et al. (2004) explored this oceanic linkage between the high and the low latitude Atlantic and suggested that the freshwater forcing can excite Kelvin and coastally trapped waves that travel along the western boundary and then along the equator. Once they reach Africa, the Kelvin wave splits into a northern and southern branch. While propagating poleward, they radiate Rossby waves that readjust the ocean interior. These processes have an adjustment time scale on the order of one or two decades (Johnson and Marshall, 2002). This process manifests itself in the sea surface height in our run. Figure 3.15 shows the sea surface height anomaly in gMOM3-hosing-0.1Sv. It indicates that it takes approximately 7 years for the wave signal reaching the equator, causing changes in the equatorial thermocline.

As the forcing strength reaches a certain threshold in the neighborhood of 0.3Sv-0.4Sv, the oceanic teleconnection mechanism proposed by Chang et al. (2008) may become more dominant. In this parameter range, the change in the NSTC pathway that causes the warm subtropical gyre water to enter the equatorial thermocline contributes to the warm SST anomaly in the equatorial Atlantic. For large values of the freshwater forcing (0.8Sv-3.0Sv), the changes of AMOC and NSTC become independent of the forcing strength while the tropical SST change is also insensitive to the freshwater inputs.

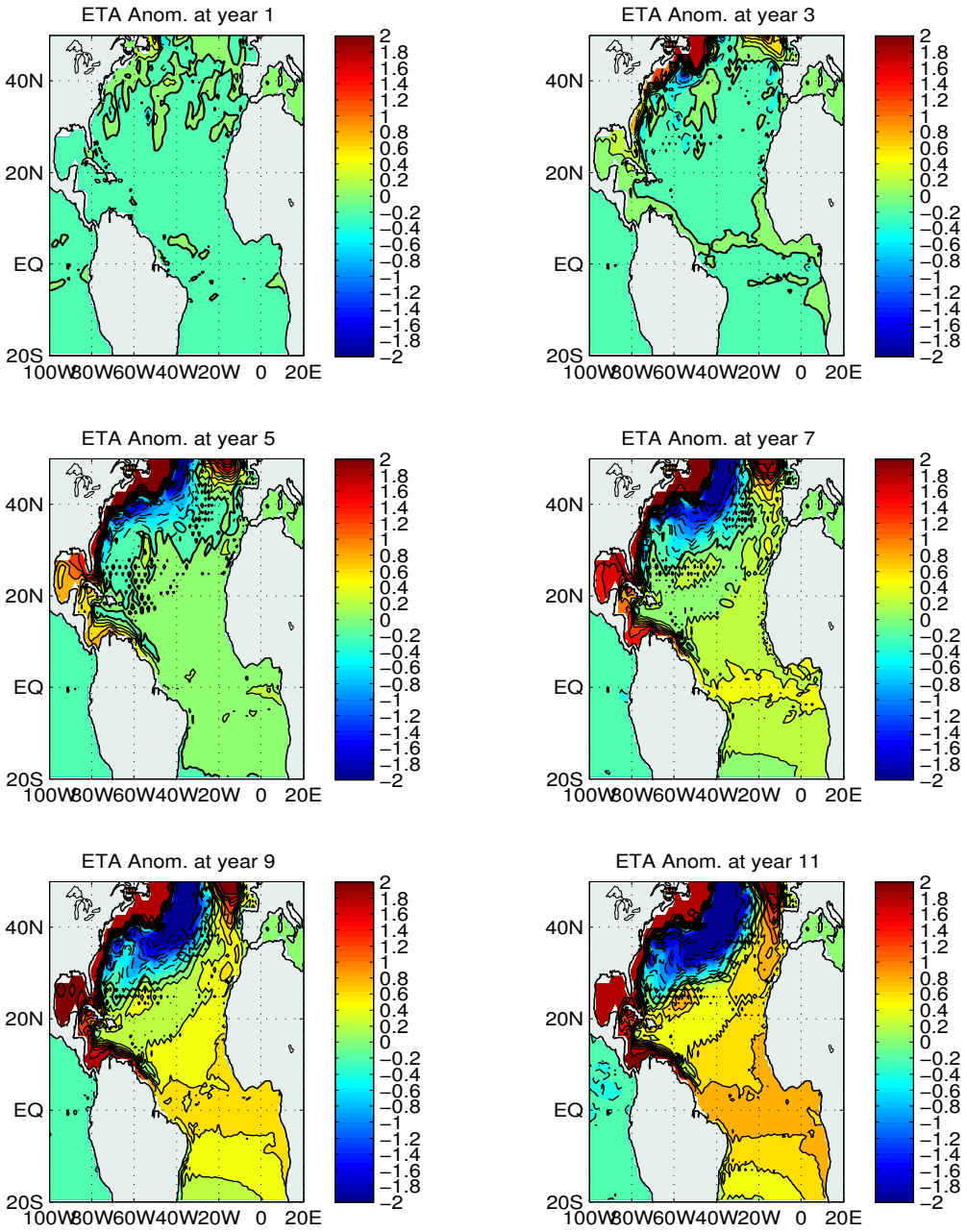

Figure 3.15 Difference of sea surface height between gMOM3-hosing-0.1Sv and gMOM3-CTRL. The sea surface height is in cm.

Using a 2-1/2 layer reduced gravity ocean model, Wen et al. (2009) show that the tropical Atlantic SST responds nonlinearly to AMOC changes. For small decreases in AMOC strength, the tropical Atlantic SST response is weak and is insensitive to the changes in AMOC strength while its response increases drastically when the AMOC strength is decreased below a threshold value. The cause of the different behavior in the reduced gravity ocean model and the gMOM3 model simulation may be attributed to the difference in model configurations. In the reduced gravity ocean model, the AMOC strength is regulated by the imposed northward mass transport at the open boundaries of 30ºS and 30ºN to mimic the return flow of AMOC. This configuration may overestimate the importance of circulation changes while weakening the role of the Kelvin/Rossby wave adjustment.

D. Multidecadal Oscillation of AMOC

One interesting feature that deserves further exploration in the gMOM3 hosing sensitivity experiments is a multidecadal AMOC oscillation that develops after about 10 years into the simulations, particularly with the freshwater forcing in the range of 0.3Sv and 0.4Sv. In this section, the characteristics of the decadal oscillation are documented and the physical mechanism responsible for the oscillation is explored. We focus on our study of the gMOM3-Hosing-0.4Sv experiment and restrict our analysis to the last 80-year segment of the 100-year simulation.

Figure 3.16 shows the corresponding time-mean AMOC of 0.4Sv hosing simulation. Due to the freshwater input, the circulation associated with the North Atlantic Deep Water (NADW) only has a maximum strength of about 9 Sv, which is about 40% of the control run. In the upper ocean, the NSTC is also enhanced and the STCs become more symmetric about the equator. The sinking occurs in a broad region north of 50°N, down

to a depth of about 2000m.

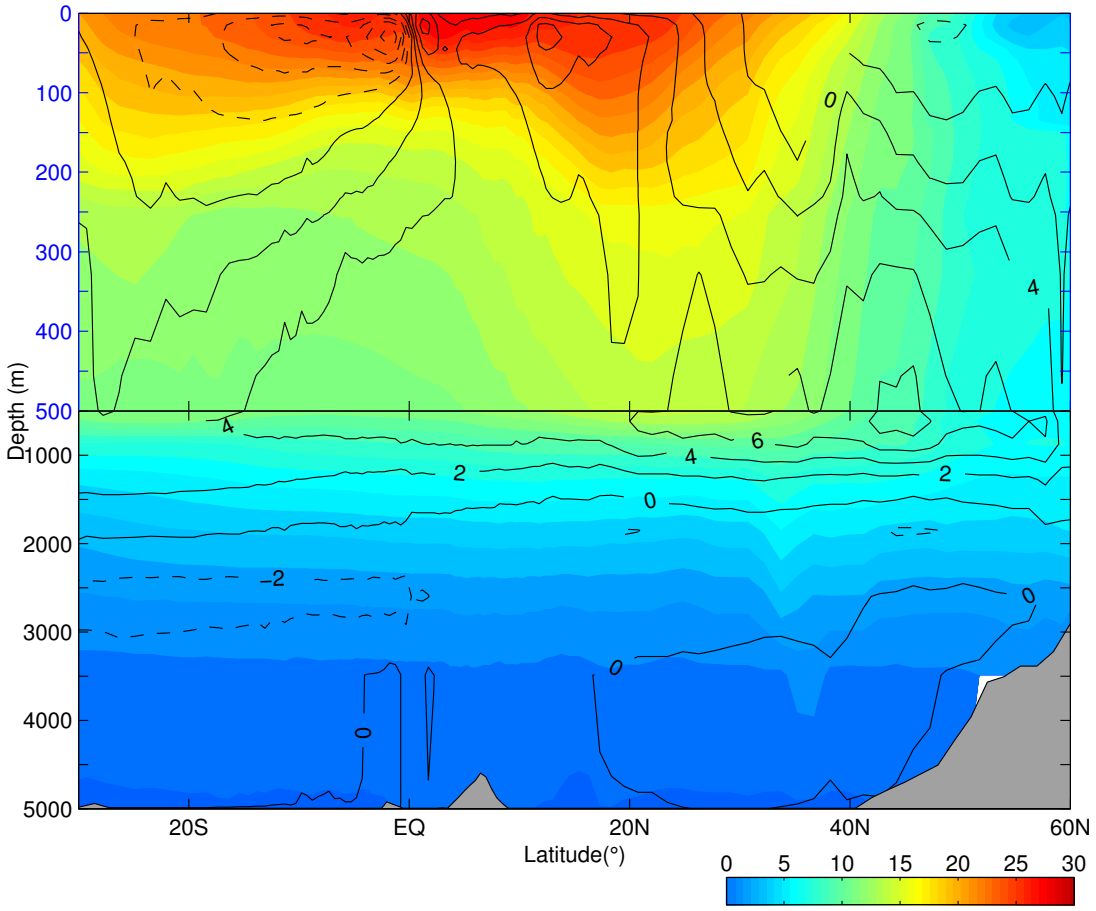

Figure 3.16 Time-mean AMOC (contour) and zonal averaged Atlantic temperature (color) in gMOM3-Hosing-0.4Sv experiment. The temperature is in °C and AMOC streamfunction is in Sv.

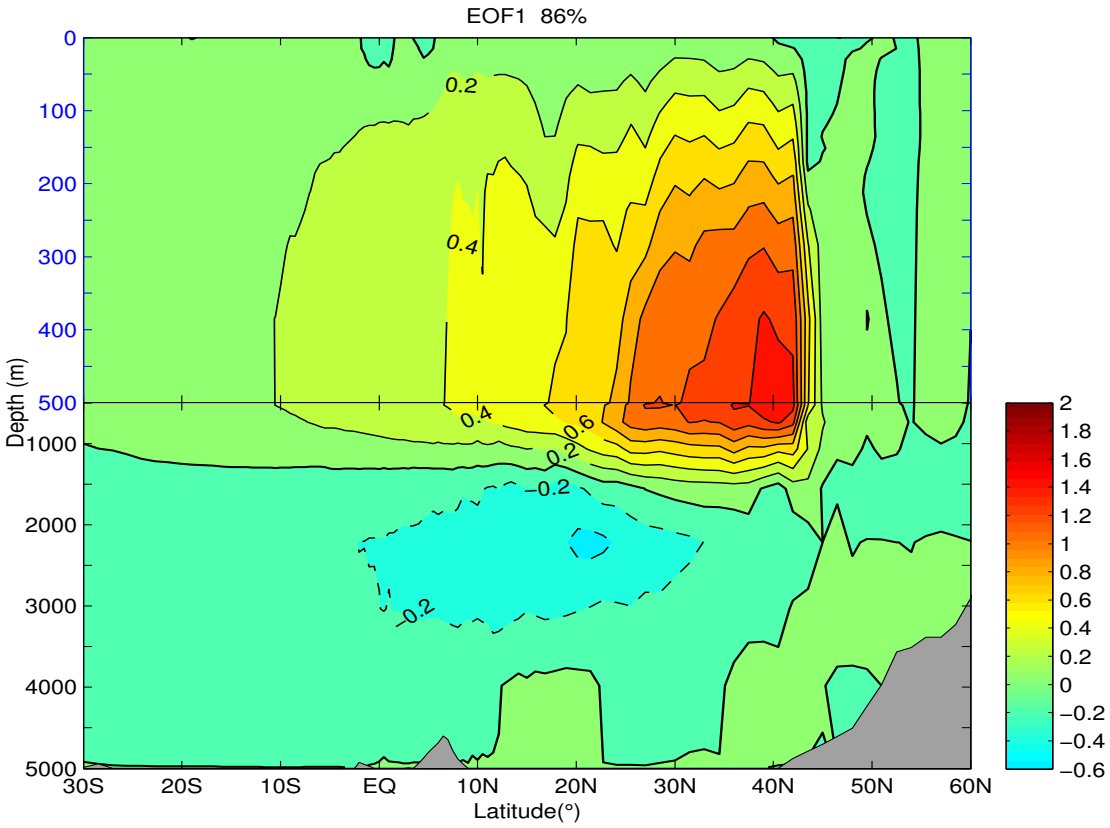

Figure 3.17 The EOF1 of the AMOC oscillation in gMOM3-Hosing-0.4Sv.

The first EOF of the AMOC is shown in Figure 3.17 and explains 86% of the total variance. Its spatial structure is different from the time-mean AMOC, shown in Figure 3.16, in that the circulation associated with the decadal oscillation is shallower (upper 1500 m) and more equatorward with no structure north of 45°N. The maximum variability is around 40°N near the Gulf Stream extension region. This positive pattern indicates a strengthening of the overturning circulation centered near the Gulf Stream extension region.

Figure 3.18 shows the leading principal component (PC), which is highly correlated

with the AMOC index. We use the first EOF and its PC time series to characterize the decadal oscillation simulated by gMOM3.

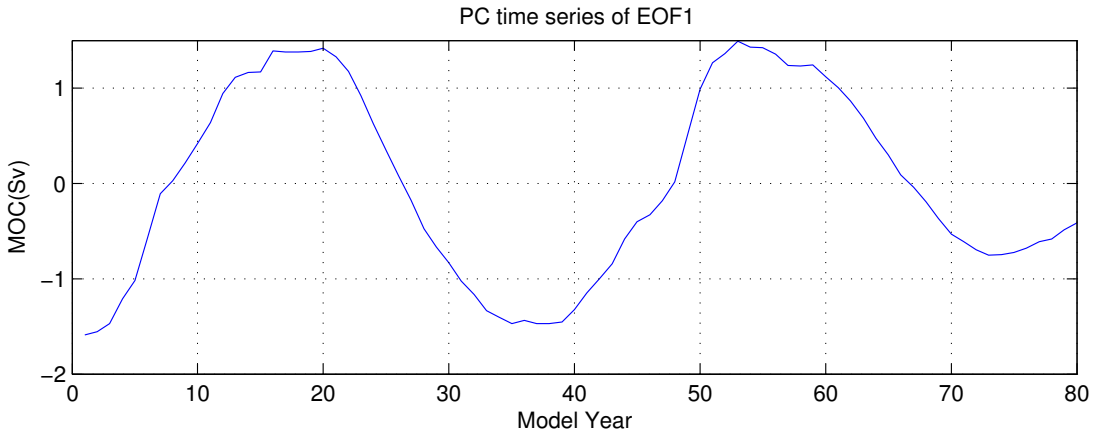

Figure 3.18 The leading principal component of the AMOC oscillation in gMOM3-Hosing-0.4Sv.

Figure 3.19 shows the leading EOF of SST anomalies and the associated PC time series. The SST EOF accounts for 66% of the total SST variance and the PC time series correlates highly with the PC time series of the AMOC (Figure 3.19b). Lag-correlation function between the AMOC and SST PC time series shows that the largest correlation occurs when the SST leads the maximum AMOC by 5-6 years (Figure 3.19c). The composite of SST anomalies corresponding to high AMOC states minus those of low AMOC states is shown in Figure 3.19d. The pattern bears a strong resemblance to the leading SST EOF and suggests that a strong AMOC corresponds to a strong surface

cooling in the Gulf Stream extension region and warming in the region to the east and to the south. Regressions of SST anomalies onto the first PC time series of the AMOC (Figure 3.20) at different time lags reveal a pattern very similar to that of the SST composite when the SST leads the AMOC PC time series by 5-6 years. Figure 3.20 also shows that the intense surface cooling near the Gulf Stream extension region is associated with a southward shift of the Gulf Stream, suggesting that the surface cooling may be associated with the ocean circulation change in the region.

To investigate this possibility, we focus on the Gulf Stream extension region. Figure 3.21 shows lag regressions of temperature, salinity and density anomalies over the region 50°W-70°W and 35°N-45°N against the AMOC PC1 time series. Again one can see that the anomalies lead the AMOC by about 5-6 years. Figure 3.22 shows the lag regressions of the 200m density anomaly onto the AMOC PC1 time series, indicating that the maximum density anomaly occurs about 5-6 years prior to AMOC maximum. This identifies the mid-latitude North Atlantic near the Gulf Stream extension region as the source for the AMOC decadal oscillation in the model.

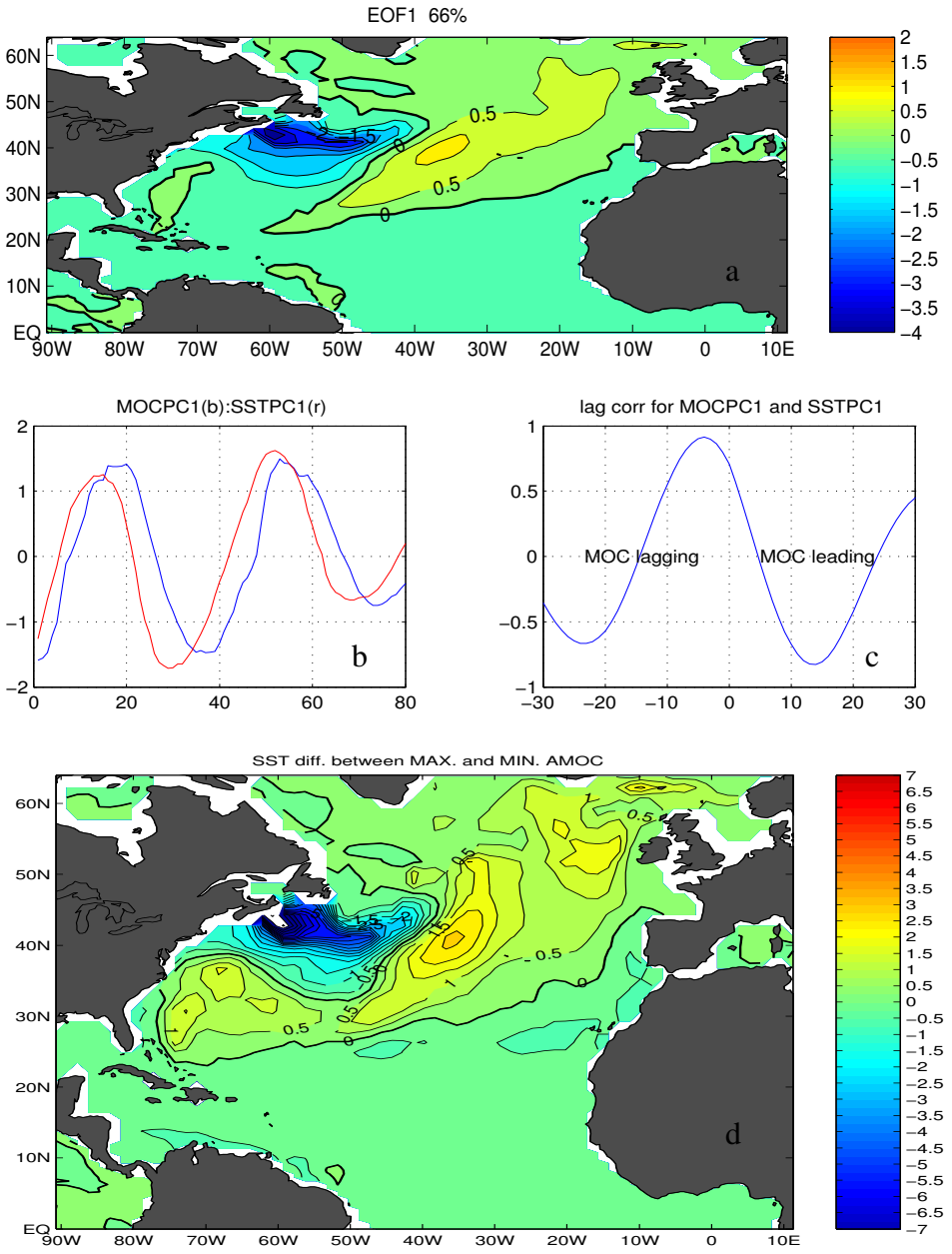

Figure 3.19 (a) Leading EOF of SST anomaly, (b) the corresponding PC time series (red) overlaid onto the AMOC PC1 (blue), (c) Lag correlations between SST PC1 and AMOC PC1, (d) composite of SST anomalies corresponding to high AMOC states minus those of low AMOC states.

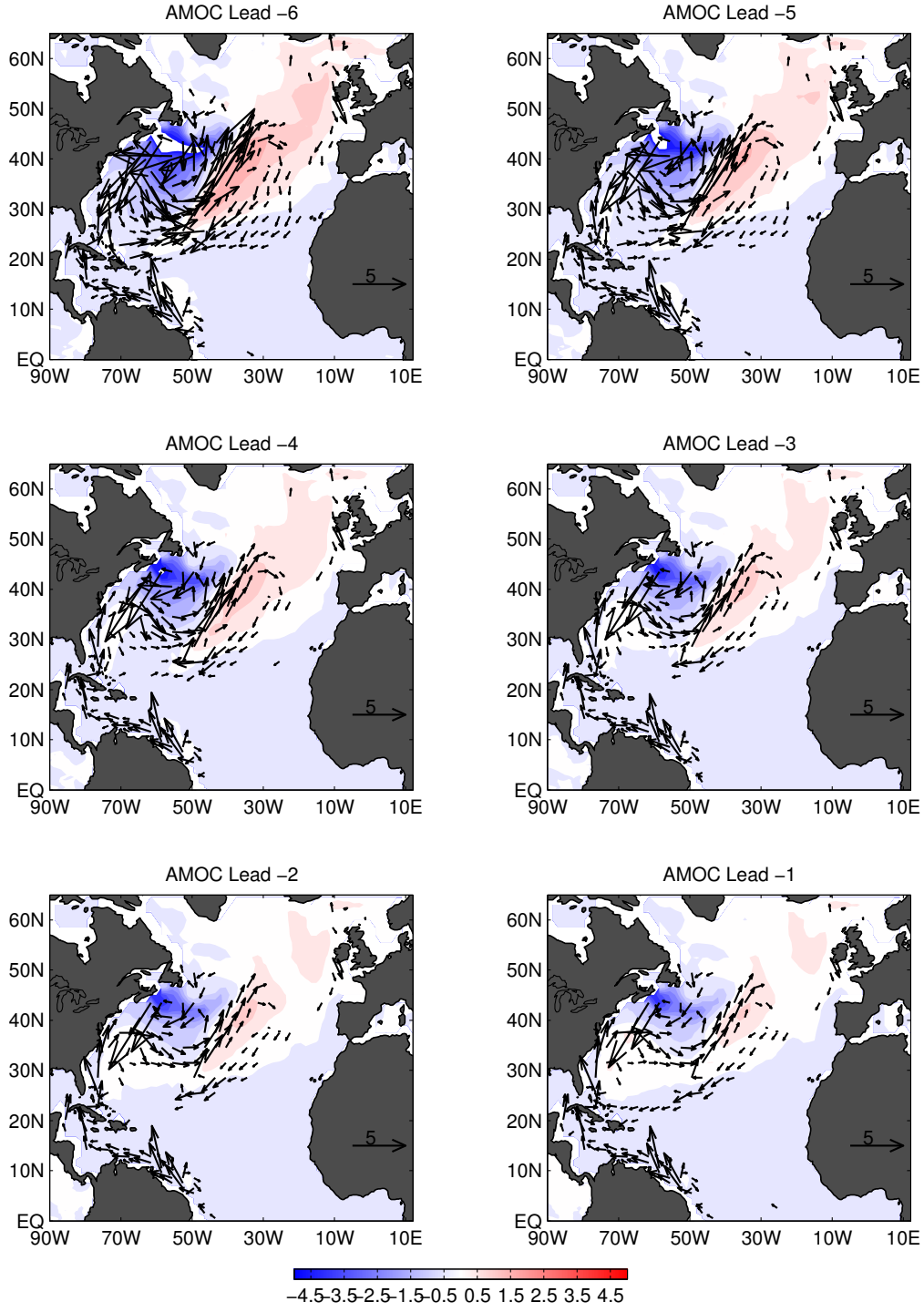

Figure 3.20 The lag regressions of the SST anomalies with the AMOC EOF1 time series.

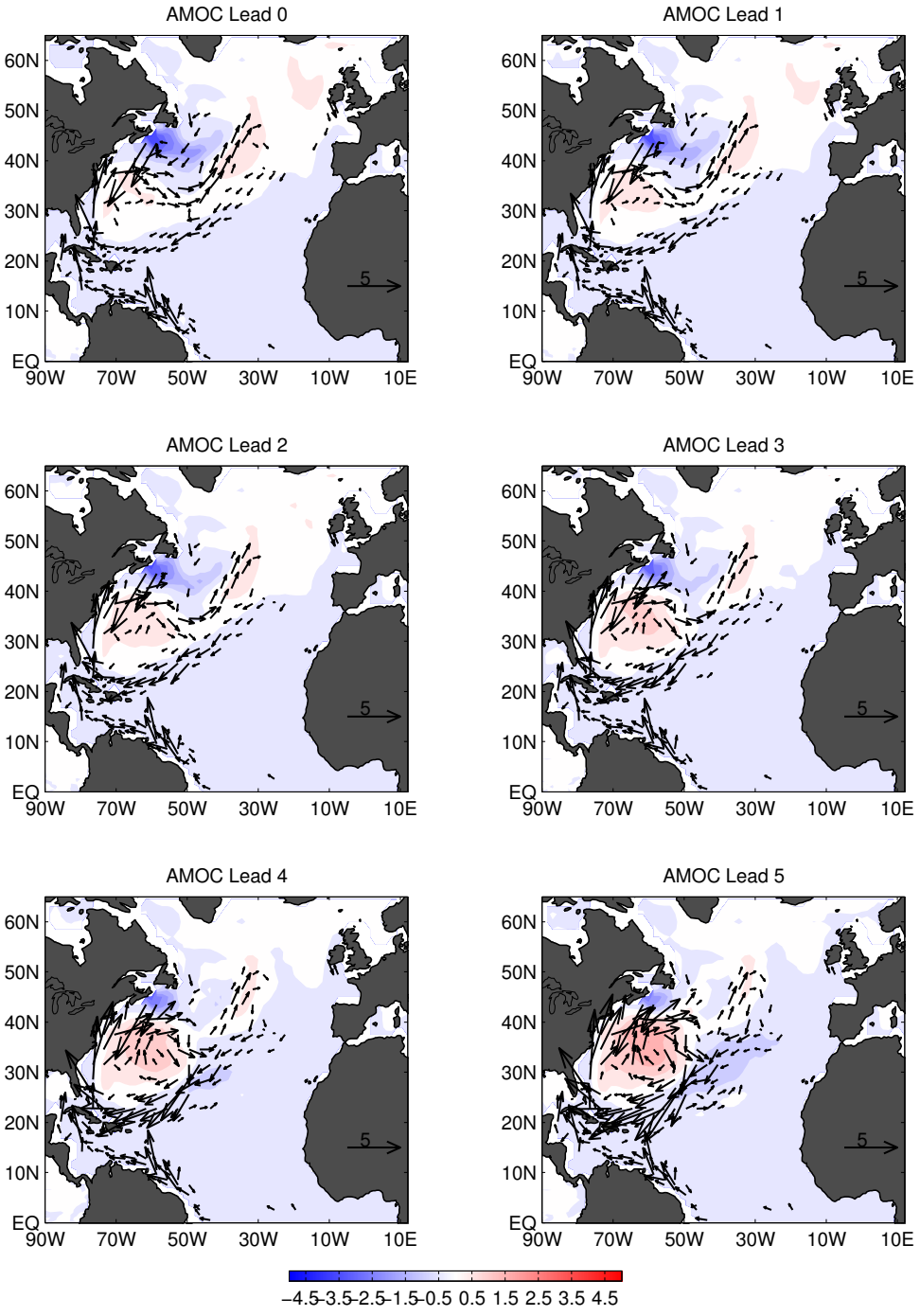

Figure 3.20 (Continued.)

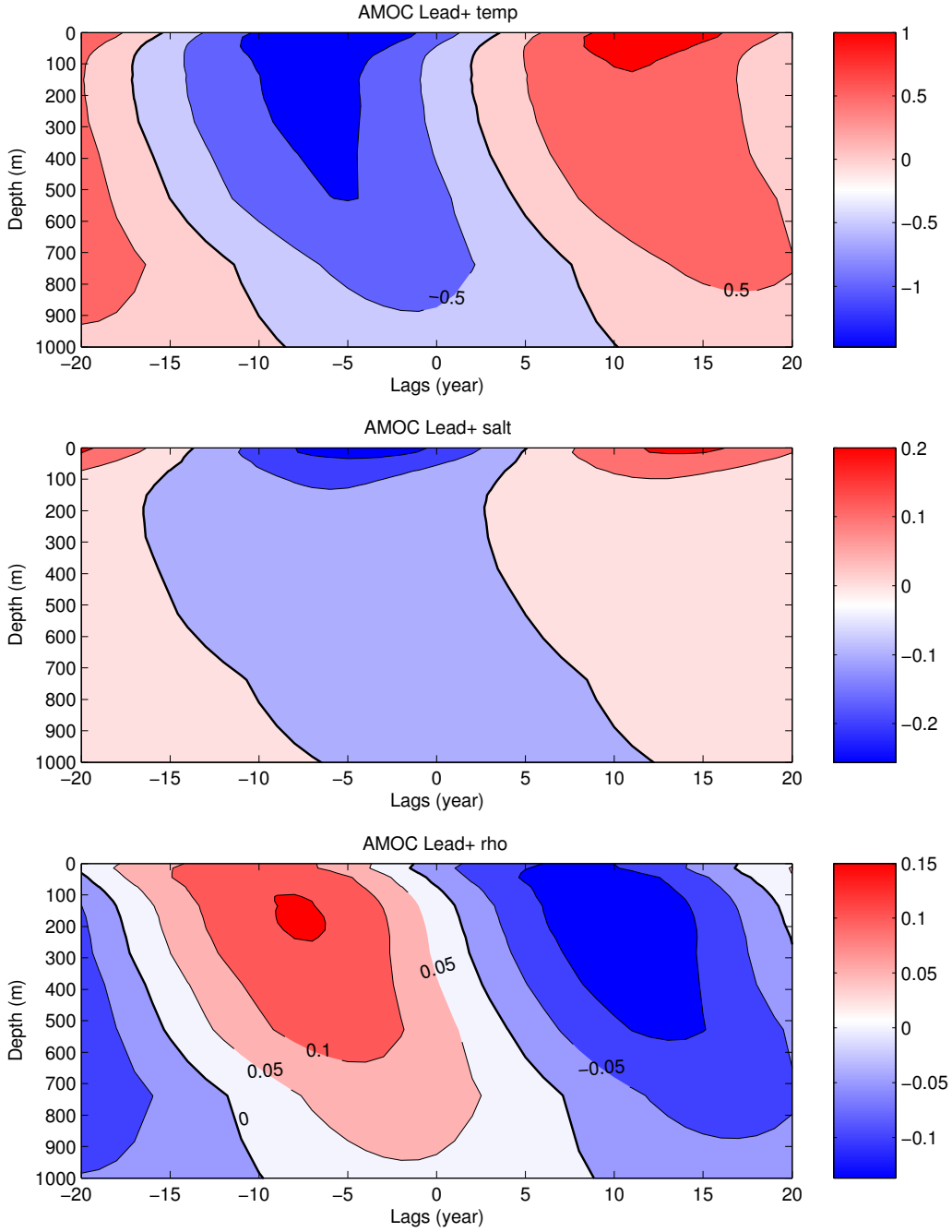

Figure 3.21 Lag regressions of temperature (upper), salinity (middle) and density (lower) anomalies averaged over the region 50°W-70°W and 35°N-45°N onto the AMOC PC1 time series.

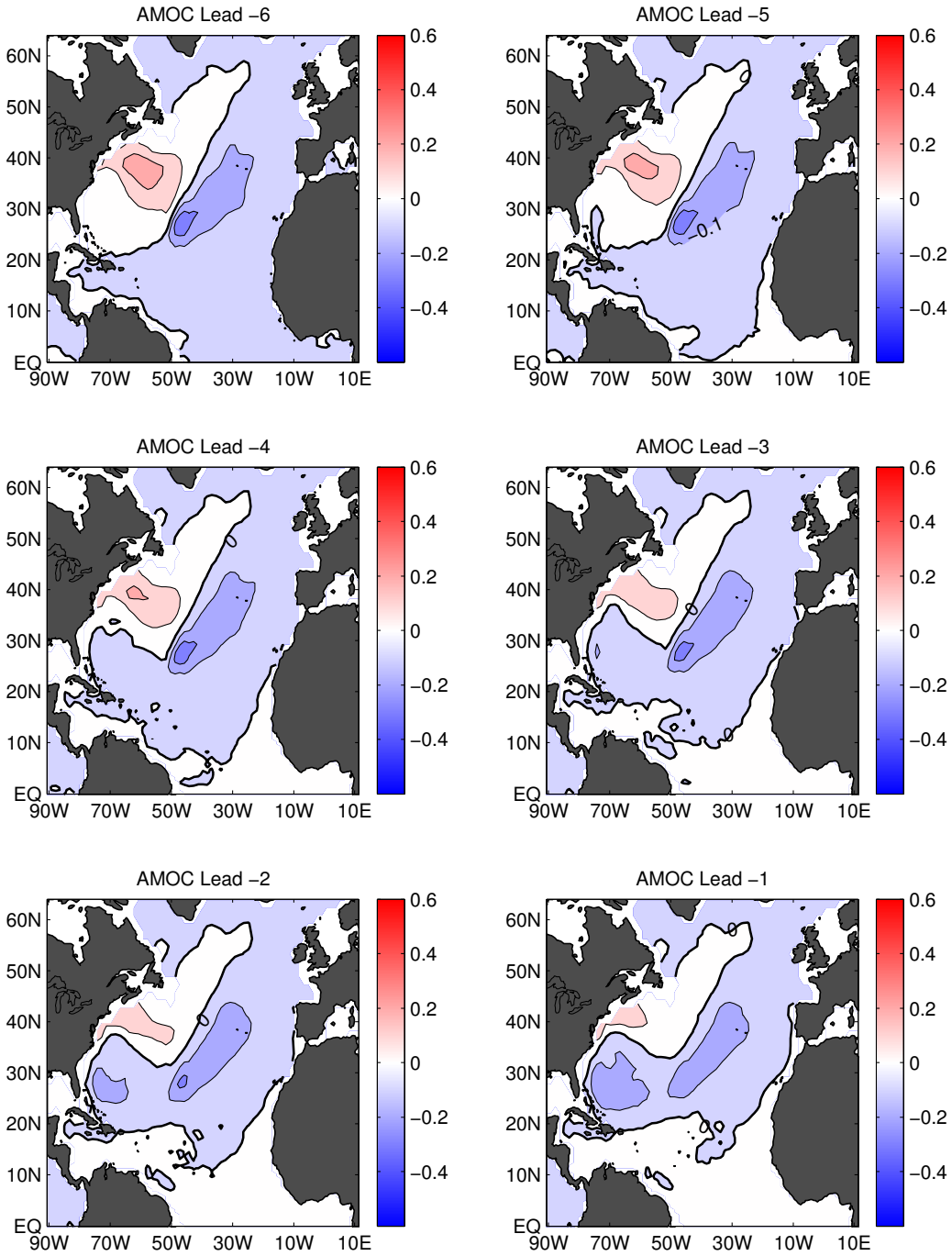

Figure 3.22 Lag regression of density anomalies at 200 m onto the AMOC PC1 time series. The contour interval is 0.1.

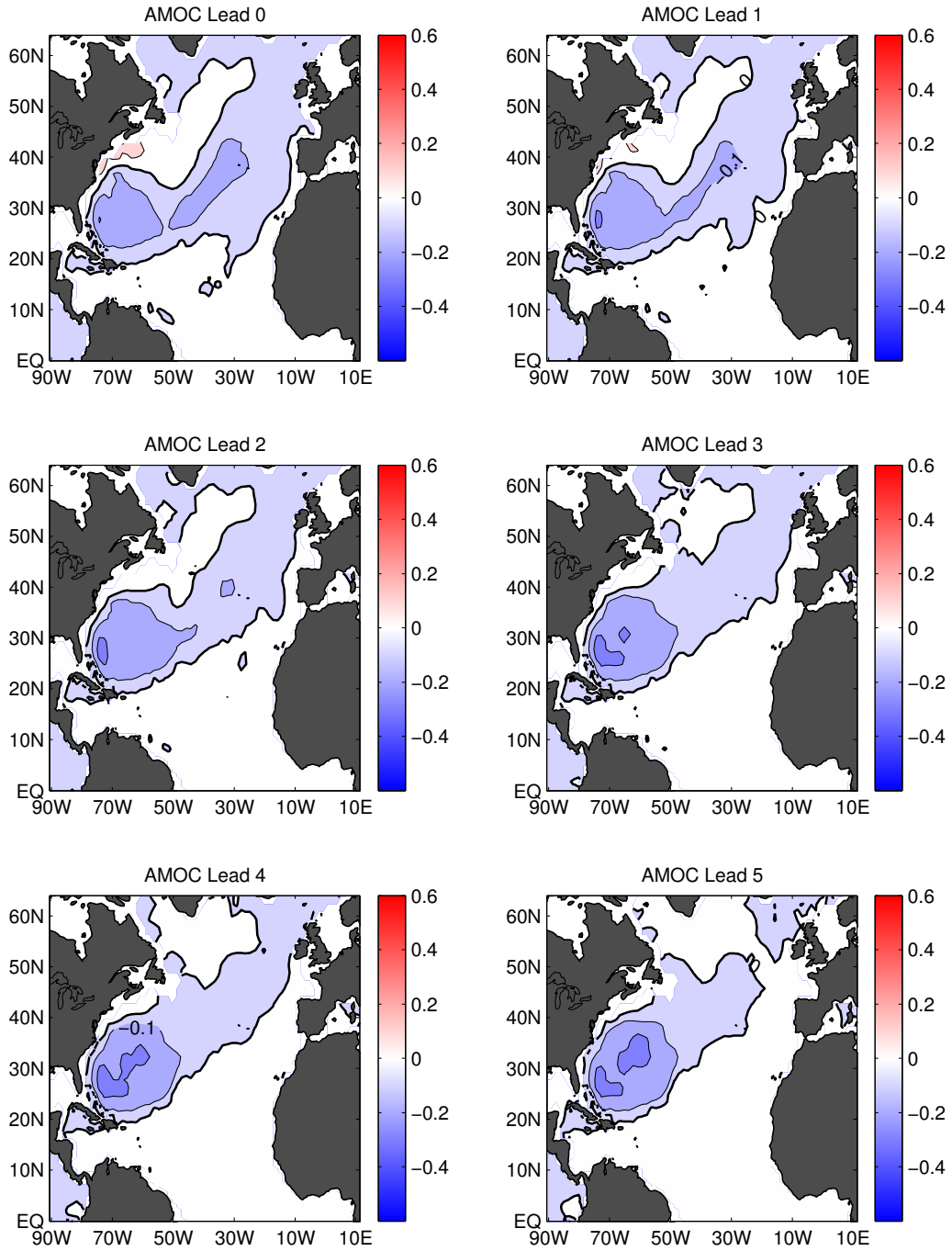

Figure 3.22 (Continued.)

Based on these preliminary analyses, we propose the following mechanism for the multi-decadal AMOC oscillation. As the freshwater forcing increases, the AMOC continues to weaken, causing the weakening of the Gulf Stream which allows cold subpolar gyre water to expand southward and the cold surface water accumulates near the Gulf Stream exit region. As the freshwater input reaches a certain strength, the regional cooling is sufficiently strong such that it becomes hydrostatically unstable and deep convection occurs. Figure 3.3 provides an illustration of the new convective site, which shows a cold temperature anomaly near 40°N that penetrates to a depth of about 1000 m, which indicates deep convection. As a result, a cyclonical recirculation gyre is developed surrounding the core of the cold temperature anomaly, forcing the warm water carried by the Gulf Stream to stay in the southern and eastern side of the recirculation gyre and forming warm anomalies along its path, as shown in Figure 3.19 and 3.20. The deep convection drives an anomalous AMOC, which acts to intensify the Gulf Stream and push the Gulf Stream exit region northward. This has a negative impact on the cold anomalies. On the other hand, the warm anomalies are advected slowly by the subtropical-tropical gyre circulation and eventually return to the Gulf Stream, reinforcing the northward heat transport by the Gulf Stream. Both these processes act to counteract the surface cooling and cease the deep convection. If these counteractive processes are sufficiently strong, the cold anomalies can be replaced by warm anomalies along the Gulf Stream exit region, causing the whole processes to reverse. The Gulf Stream will be weakened again, causing southward intrusion of the cold water to occur again. The advection of the cold water by the subtropical gyre will reinforce the surface cooling and reinitiate the deep convection. Therefore, the oscillation is a result of a delicate balance among several physical processes and can only occur when freshwater forcing reaches a certain critical point. If the forcing is too weak, the deep convection can't occur and thus no oscillation will take place. On the other hand, if the forcing is

too strong, the deep convection can't be overcome by the anomalous warm advection and no oscillation will occur either.

A detailed examination of this hypothesis is beyond the scope of this dissertation. However, an analysis of the GFDL CM2.1 hosing simulation (Zhang, 2008, personal communication) suggests the existence of similar oscillations. The leading EOF of the AMOC streamfunction that explains 37% variance shows maximum variability around 40°N with a period of around 21 years (not shown). Figure 3.23 shows a lag regression analysis of temperature, salinity and density anomalies averaged over 30°W-70°W and 40°N-50°N against the AMOC PC1 time series as a function of depth. It shows maximum anomalies at 400 m depth, leading AMOC PC1 time series by 2-3 years. A lag regression analysis of temperature anomaly at 400 m where the anomaly is strongest against the AMOC PC1 time series shows that the cold temperature anomalies along the Gulf Stream extension region leads AMOC by about 3 years (not shown). The gMOM3 simulation shows similar lead-lag relationship except that the maximum temperature and salinity anomalies are trapped near the surface and the lead is about 5-6 years. The other difference between the two simulations is that there is a distinct downward propagation of density anomaly in the gMOM3 simulation that is absent in the GFDL CM2.1 simulation. The inter-model comparison study is one way to gain understanding of the oscillation mechanism, because the gMOM3 simulation involves much simpler physics than the fully coupled GFDL CM2.1 simulation. If one can determine that the oscillations in the two models are governed by similar mechanisms, it is likely that the multi-decadal AMOC oscillation in the fully coupled GFDL model has its origin in the ocean and that the ocean-atmosphere interactions might play a secondary role. The analysis presented here hints at this conclusion, but does not provide a definitive answer.

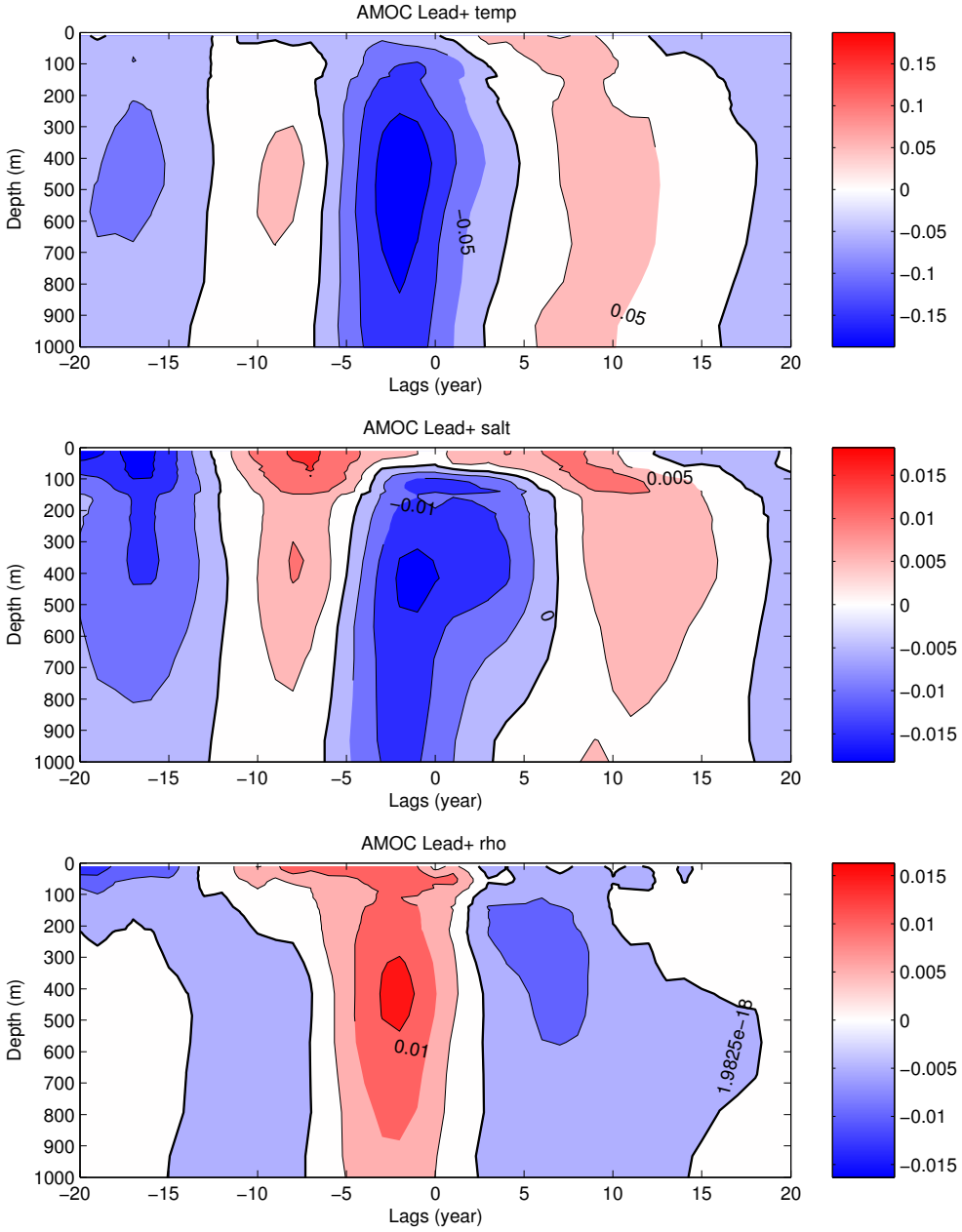

Figure 3.23 Same as Figure 3.21 except that the anomalies are averaged over the region 30°W-70°W and 40°N-50°N from the GFDL CM2.1 simulation.

E. Discussion

In this chapter, we investigated the oceanic processes linking the tropical SST response to AMOC changes caused by the freshwater input over the northern North Atlantic. The modeling approach that we adopted is, in many ways, similar to that of Stouffer et al. (2006) where the freshwater is hosed into the northern North Atlantic, mimicking the melting of glaciers in response to the global change. Different from Stouffer et al. (2006), our emphasis is on the effect of AMOC changes on tropical SST through oceanic processes. By varying the strength of the imposed freshwater input in a stand-alone ocean GCM, we conducted a large number of numerical simulations to shed light on detailed oceanic processes controlling tropical SST response and its sensitivity.

Whether a freshening of the north Atlantic results in a significant tropical SST response depends critically on the magnitude of the freshening through several mechanisms. The results presented here indicate that the oceanic processes are of prime importance for the tropical Atlantic SST warming. The oceanic teleconnection proposed by Chang et al. (2008) operates when the necessary freshwater input into the northern North Atlantic exceeds 0.3Sv in order to make the North Brazil Undercurrent to reverse its direction and flow equatorward. This threshold is probably model dependent. Nevertheless, the current rate of freshening over North Atlantic is so small (Dickson et al., 2002; Curry and Mauritzen, 2005) that this threshold may not be reached in the near future. Even with the great salinity anomaly, a large near-surface pool of freshwater that appeared off the east coast of Greenland in the late 1960s (Dickson et al., 1988), the surface freshening in the high latitude of the North Atlantic only amounts to about 0.07Sv during a 5-year period (Curry and Mauritzen, 2005). As reported in previous studies, and comfirmed here, such rates will have a small effect on the AMOC, and will unlikely produce a significant tropical SST response in the Atlantic.

Should future global warming rapidly accelerate the melting of glaciers and freshening rate of the northern North Atlantic, it is then possible that a substantial weakening, even shut down of the AMOC would occur, with far-reaching climatic consequences. The first sign of such a climate change would be a sharp decrease in the SST of the high-latitude North Atlantic Ocean, followed by warming in the deeper layer of the North Atlantic Ocean. A significant subsurface warming will be initiated along the gyre boundary of the northern subtropical and tropical gyres and then will spread into the equatorial south Atlantic, giving rise to warm SST anomalies in the Gulf of Guinea and off the coast of western Africa. This is a likely scenario for a climatic condition such as the Younger Dryas, as hypothesized by Chang et al. (2008).

In our ocean-only experiments, a shutdown of the AMOC has no significant effect on the tropical Pacific Ocean. Hence, a decrease in the strength of the AMOC will leave the Pacific thermohaline circulation unaffected through the oceanic teleconnection in our model, but it will influence the shallow wind-driven circulations through Atmospheric teleconnections, and hence can induce changes of the equatorial thermocline. Our results show a dipole-like thermocline response in the tropical Pacific with a deepened thermocline in the northern tropical Pacific and a shallowed thermocline in the southern tropical Pacific.

In contrast to the water hosing experiments carried out by fully coupled climate models (Stouffer et al., 2006), our ocean-only model simulations show no prominent SST changes in the Pacific Ocean and opposite sign SST changes in the northern tropical Atlantic, suggesting that the SST changes over these regions are primarily attributed to atmospheric processes and the oceanic teleconnection mechanism dominates SST changes in the equatorial south Atlantic. These findings are in line with recent modeling studies (Chiang et al., 2008; Chang et al., 2008; Wu et al., 2008), indicating that the tropical SST response to AMOC changes is governed by a set of complex oceanic and

atmospheric processes. A comprehensive understanding of this issue requires the understanding of interactions between the wind-driven and thermohaline circulations along the western boundary, as well as a knowledge of ocean-atmosphere interactions. In subsequent chapters, we will use a tropical ocean GCM coupled to an atmospheric GCM to address the issue of how air-sea interactions may affect the tropical SST response to AMOC changes and evaluate the relative importance of the oceanic versus atmospheric processes in transmitting changes in high latitude North Atlantic to the tropics through a set of coupled model sensitivity experiments. An improved understanding of these issues may have a bearing on abrupt climate change prediction.

Another interesting topic discussed in this chapter is the multidecadal oscillation of the AMOC. We found that large, mid-latitude SST and SSS anomalies near the Gulf Stream extension region are directly associated with the AMOC oscillations when freshwater forcing into the North Atlantic reaches a certain critical value of about 0.4 Sv. In contrast to previous CGCM studies (Delworth et al., 1993; Dong and Sutton, 2005; Dai et al., 2005), our study does not show the existence of an ocean mode suggested by Delworth et al. (1993) that relies on the lagged phase relationship between the temperature and salinity contributions to the total density in the DWF regions. Instead, we found that the density anomaly formed along the Gulf Stream exit region is critical in maintaining a decadal oscillation with a 40-year period. However, this oceanic mode may be sensitive to model resolution, physical parameterizations and surface forcing. More investigation is needed to test its robustness and to fully understand its physical mechanism.

CHAPTER IV

AMOC IMPACT ON COUPLED OCEAN-ATMOSPHERE SYSTEM *

A. Introduction

Paleoceanographic proxy records indicate that the AMOC was substantially weakened during the Younger Dryas (12.8 and 11.5 cal. kyr BP) (Boyle, 2000; McManus et al., 2004; Hughen et al., 2004; Piotrowski et al., 2005) resulting in a wide-spread surface cooling over the Northern Atlantic sector (Zhao et al., 1995; Bard et al., 2000; Guilderson et al., 2001) and warming in the tropical South Atlantic (Mulitza and Rühlemann, 2000; Arz et al., 1999; Weldeab et al., 2006) (Table 1.1; Figure 4.1). This dipole-like Sea Surface Temperature (SST) pattern is perceived as a robust response to a weakening in AMOC and is well simulated by a range of coupled climate models in the so-called water-hosing experiments where fresh water is hosed into the high latitude North Atlantic, mimicking melt water discharge (Stouffer et al. 2006).

Although the overall paleo-temperature reconstructions over a broad geographic scale are consistent with the occurrence of this SST dipole during the Younger Dryas, there are some inconsistent findings about the temperature changes in the southern Caribbean region and in the western Tropical Atlantic. When an updated age model for ODP site 1002C (10°42.73'N, 65°10.18'W) (Peterson et al., 2000) is applied to the alkenone unsaturation-based SST record from Herbert and Schuffert (2000), little or no temperature change is observed at the initiation of the Younger Dryas (temperatures

*Parts of this chapter are reprinted with permission from "On the interpretation of Caribbean paleo-temperature reconstructions during the Younger Dryas" by Wan X., P. Chang, R. Saravanan, R. Zhang and M. W. Schmidt, *Geophys. Res. Lett.,* 36, L02701, doi:10.1029/2008GL035805, 2009. Copyright 2009 by the American Geophysical Union.

remain about 24°C) and only a small warming of about 1°C is observed at the termination of the event at 11.5 kyr. In comparison, a Mg/Ca-SST record based on planktonic foraminifera in another Cariaco Basin core PL07-39PC (10º42´N, 64º56´W) suggests a 2-3ºC cooling at the start of the Younger Dryas with an average temperature of about 24°C during the cold event (Lea et al., 2003). Guilderson et al. (2001) inferred an even larger amount of cooling off the coast of Barbados (13ºN, 59º30´W) based on coral stable isotope values. In contrast, both alkenone-based (Rühlemann et al., 1999) and faunal-based (Hüls and Zahn, 2000) SST reconstructions from a Tobago Basin core (12° 05' N, 61°15'W) in the western Tropical Atlantic indicated an opposite response — a surface warming during the Younger Dryas. In addition, a Mg/Ca-SST record from the southwestern Caribbean (11° 34' N, 78°25'W) also indicated ~1.2°C of surface warming during the Younger Dryas (Schmidt et al., 2004) (Figure 4.1). Although these SST records are based on a variety of paleo-proxies, each with its own uncertainties which might be associated with seasonality, depth habitats or diagenesis etc., one wonders whether there is a physical explanation for the complex spatial structure of the reconstructed temperature change. In particular, it would be interesting to know if there are competing physical processes that can give opposing SST changes in response to a weakening in AMOC. One objective of this chapter is to shed light on this issue.

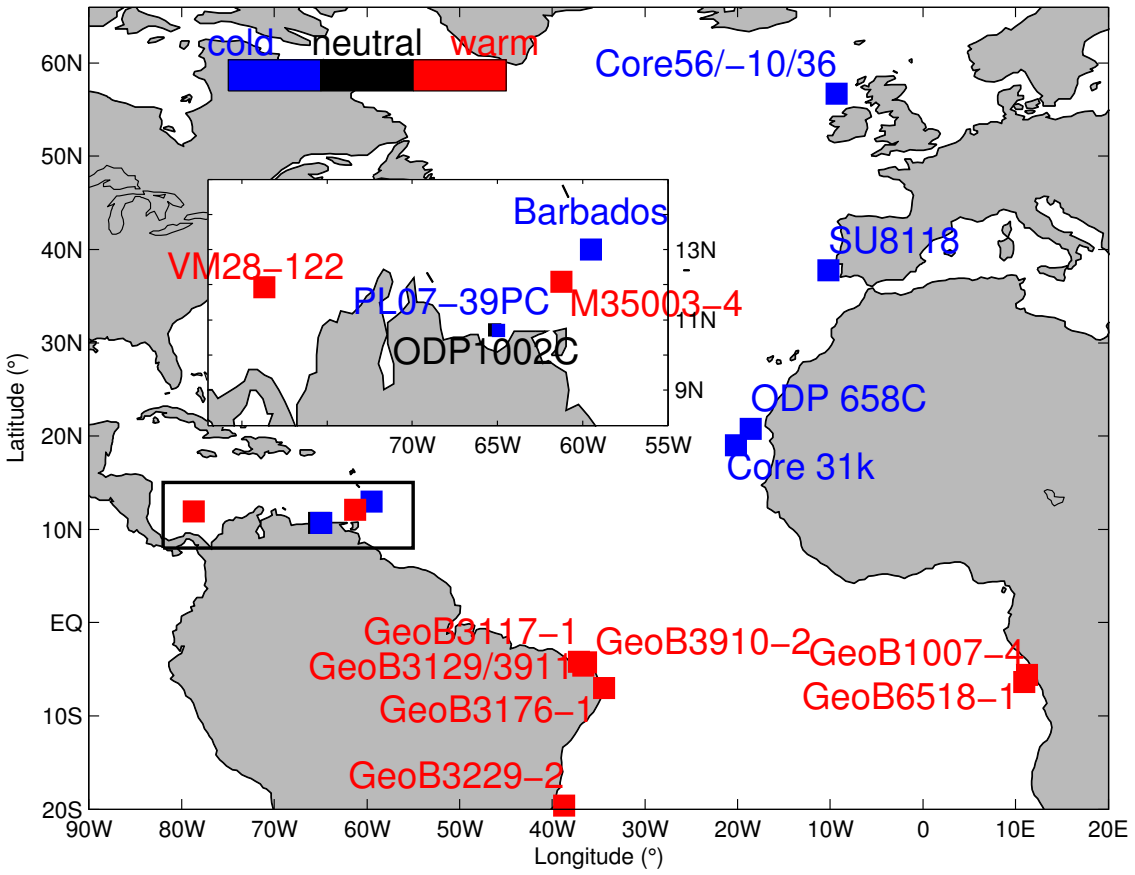

Figure 4.1 A summary diagram of paleo-SST reconstructions during the Younger Dryas over Atlantic Ocean: Core 56/-10/36, Kroon et al. (1997); SU8118, Bard et al. (2000); Core 31k, ODP658C, Zhao et al. (1995); Barbados, Guilderson et al. (2001); PL07-39PC, Lea et al. (2003); VM28-122, Schmidt et al., (2004); M35003-4, Rühlemann et al. (1999), Hüls and Zahn (2000); ODP1002C, Herbert and Schuffert (2000); GeoB1007-4, Mulitza and Rühleman (2000); GeoB3117-1, GeoB3176-1, GeoB3229-2, Arz et al. (1999); GeoB3910-2, Jaeschke et al. (2007); GeoB3129/3911, Weldeab et al. (2006); GeoB6518-1, Weijers et al. (2007). Blue denotes surface cooling and red denotes surface warming. The inset is an enlargement of black box in the Southern Caribbean.

The other objective of this chapter is to provide an explanation for the paleo salinity distribution in the tropical oceans during the Younger Dryas. Paleoceanographic proxy records provide evidence for wide-spread surface cooling over the Northern Hemisphere at times of reduced AMOC. Although the collapse of AMOC is associated with a freshening of surface waters at the sites of deep water formation in the northern North Atlantic, proxy records suggest a corresponding sea-surface salinity (SSS) increase in the entire tropical Atlantic (Schmidt et al., 2004, 2006; Weldeab et al., 2006; Carlson et al., 2008) and the eastern equatorial Pacific (EEP) Ocean around Central America (Benway et al., 2006; Leduc et al., 2007) (Figure 4.2). This basin-wide tropical Atlantic SSS change contrasts sharply to the dipole-like sea-surface temperature (SST) response to a slowdown of the AMOC (e.g. Stouffer et al. 2006) and its mechanism is not well understood.

Although the migration of the Intertropical Convergence Zone (ITCZ) in response to paleo glacial boundary (Peterson et al., 2000; Koutavas et al., 2002; Chiang et al., 2003) and the role of the moisture transport from the Atlantic to the Pacific (Zaucker et al., 1994; Leduc et al, 2007; Xie et al., 2008) are known, it seems paradoxical when they are used to explain the change of the paleo-salinity. For instance, the southward migration of Atlantic ITCZ associated with the North Atlantic cooling (Chiang et al., 2003) would lead to an increase in SSS over the western tropical Atlantic (WTA) and a decrease in the equatorial south Atlantic, while paleo-proxy records show that there is increased salinity in the latter (Weldeab et al., 2006; Carlson et. al., 2008). On the other hand, the change in mean ITCZ position could cause a roughly similar paleo-salinity response across both the WTA and the EEP because the EEP and the Caribbean Sea are in the same latitudinal band. However, the variation of the vapor transport from the Atlantic to the Pacific in maintaining the modern inter-ocean salinity contrast should yield salinity changes of the opposite sign across the Central America that is inconsistent

with paleo salinity records.

Therefore, it seems that each of these proposed mechanisms explains a certain feature of paleo salinity observations, but none of these offer an explanation for the basin-wide paleo-salinity response to AMOC changes. The second objective of this chapter is to demonstrate, through experiments with CCM3-trMOM3, that the basin-wide paleo-salinity response is attributed to a combined effect of the southward migration of the Atlantic ITCZ associated with the Northern Hemisphere cooling (Chiang et al., 2003) and an AMOC-induced oceanic pathway changes described by Chang et al. (2008).

Finally, as mentioned in the previously chapters, AMOC changes not only affect tropical Atlantic climate through both the oceanic (Chang et al., 2008) and atmospheric (Chiang and Bitz, 2005) teleconnections, but also affect tropical Pacific climate via mainly atmospheric processes. It is important to understand how the atmospheric teleconnection mechanism can operate in the Pacific sector. As both the North Pacific and north Atlantic cool in response to a weakening in the AMOC, one wonders whether the surface cooling in the North Pacific or in the North Atlantic exerts a stronger influence on the tropical climate variability. In particular, we would like to test a hypothesis put forward by Timmermann (2003) that the anomalous cooling in the Northern Hemisphere in response to a weakening in the AMOC can induce a change in ENSO. There are some indications in observations that the AMO and ENSO are linked, with a negative AMO phase being correlated with a strong ENSO variability (Figure 4.3). As the AMO is thought to be caused by the multidecadal oscillations of AMOC (Knight et al, 2005), Dong et al. (2006) suggest that changes in Atlantic SST induced by AMOC could modulate ENSO on multidecadal timescales. Therefore, the third objective of this chapter is to investigate the influence of the AMOC on ENSO variability.

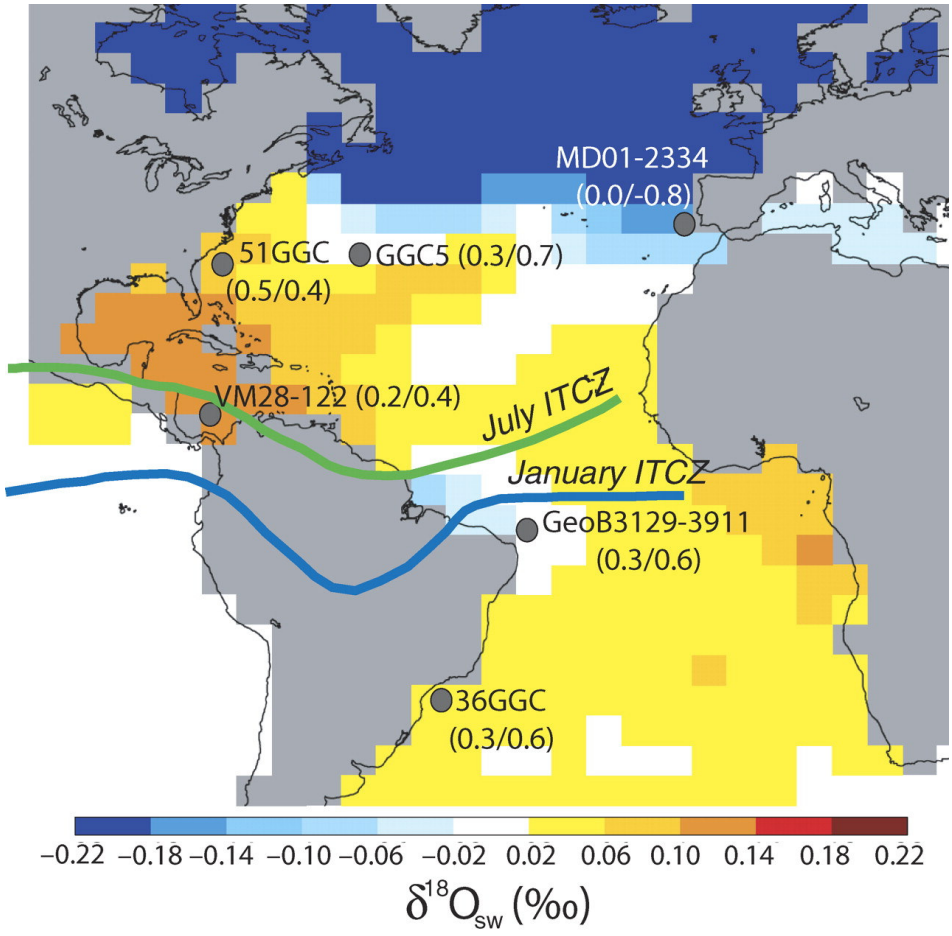

Figure 4.2 Modeled changes in surface $\delta^{18}O_{seawater}$ resulting from a 50% reduction in AMOC based on the coupled GCM NASA GISS ModelE-R (Schmidt et al., 2007). Because the $^{18}O/^{16}O$ ratio of seawater covaries linearly with surface salinity, increases in $\delta\ ^{18}O_{seawater}$ indicate increased SSS. Also shown are the locations of proxy reconstructions (locations indicated in circles) indicating significant increases in surface $\delta^{18}O_{seawater}$ during the Younger Dryas (first value) and for the Older Dryas (second value) for cores 51GGC, GGC5, 36GGC (Carlson et al., 2008), VM28-122 (Schmidt et al., 2004) and GeoB3129-3911 (Weldeab et al., 2006). The Green (blue) line is the modern July (January) ITCZ location. Reprinted with permission of the Geological Society of America from Carlson et al. (2008).

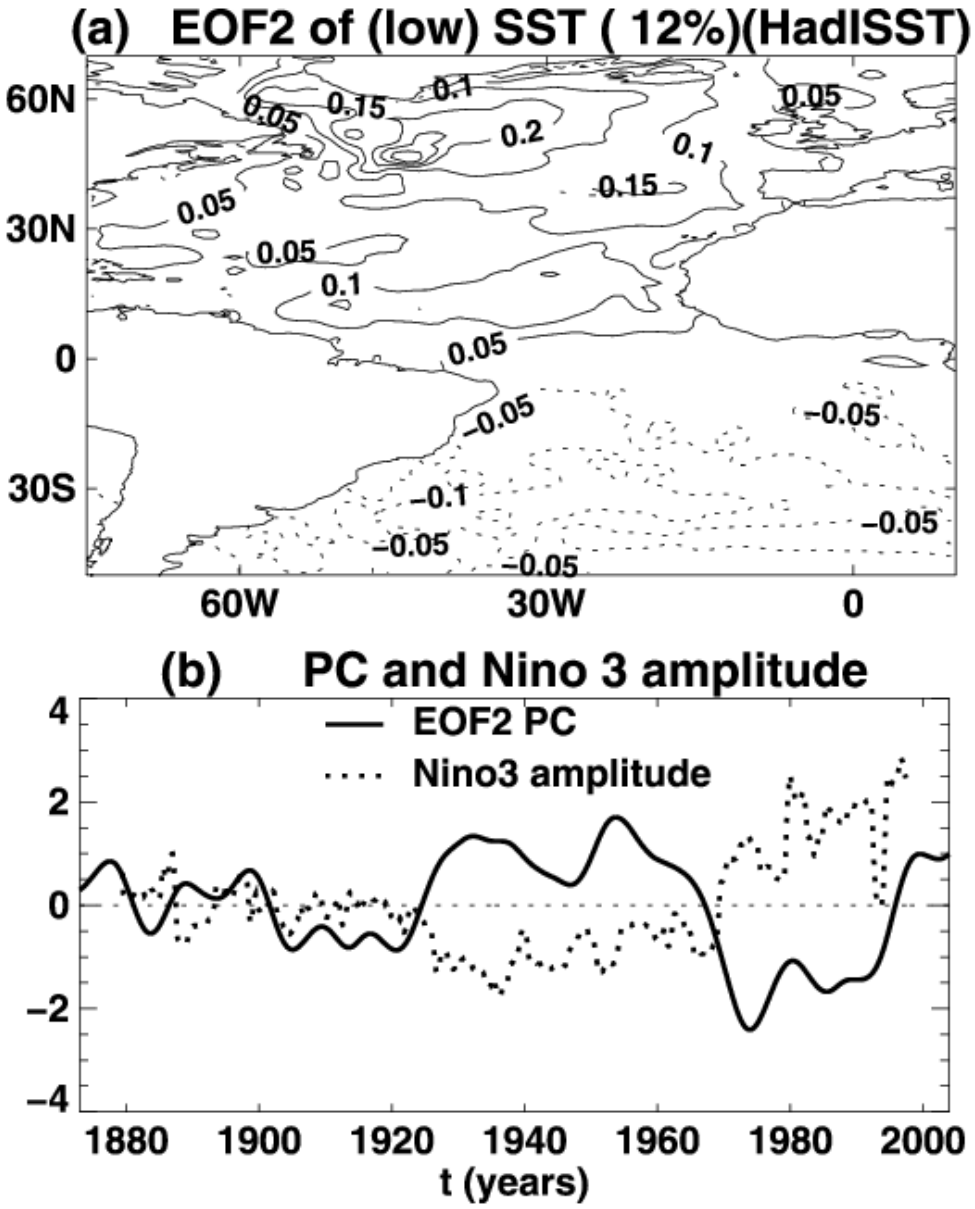

Figure 4.3 (a) EOF 2 of low frequency (low-pass filter with half power at period of 13.3 years) monthly SST variability (°C) over Atlantic, and (b) corresponding normalized principal component (full) and the normalized anomalous ENSO magnitude (defined as monthly Nino 3 index standard deviation in a running 13 year window) variation (dotted) based on observations (Rayner et al., 2003). Reprinted with permission of the American Geophysical Union from Dong et al. (2006).

Our investigation will be conducted in the framework of CCM3-trMOM3 model whose details, including its physical parameterizations, resolution and performance in simulating major modes of variability, are provided in Chapter II. In this chapter, we describe the results from a set of numerical simulations designed to systematically investigate the role of oceanic and atmospheric processes in transmitting climate change signal in the high latitude North Atlantic to the tropics. The construction of the CCM3-trMOM3 allows us to investigate separately contributions of oceanic and atmospheric processes involved in teleconnecting AMOC changes to the tropics.

B. Impact of AMOC on Mean Climate

1. Atmospheric vs. oceanic teleconnection in tropical SST response to AMOC changes

In most fully-coupled model hosing simulations, dominant features include a weakened AMOC and strong surface cooling over the Northern Hemisphere, including both the North Atlantic and North Pacific. These surface coolings presumably contribute to tropical SST changes. However, their relative importance remains unclear and is difficult to assess in a fully coupled simulation. Figure 4.4a shows the annual mean SST difference between trMOM3-CFE-NH and trMOM3-CE. Recall that in trMOM3-CFE-NH, both surface coolings in the North Atlantic and North Pacific and the AMOC-induced ocean circulation changes are imposed at the open boundaries. Therefore, one expects this simulation to reproduce the results of fully coupled GCM hosing simulations. Indeed, Figure 4.4a shows many features that are consistent with SST changes simulated by fully coupled GCM hosing experiments (Stouffer et al. 2006), including an Atlantic SST dipole with strong cooling in excess of 1ºC over the north tropical Atlantic and a moderate warming over much of the equatorial and south tropical

Atlantic, a warming pattern over the southeastern tropical Pacific and a moderate cooling over much of the Indian and northern tropical Pacific. When the surface cooling in the North Pacific is absent (Figure 4.4b), little change is observed in the tropical Atlantic sector, while the North Tropical Pacific becomes warmer. This suggests that the surface cooling in the North Pacific tends to cool the tropical Pacific in response to the AMOC change. To further verify this result, we turn to trMOM3-SFE-NP (Figure 4.4d) where only the surface cooling in the North Pacific is included in the boundary forcing. Figure 4.4d clearly shows that the whole tropics cool with a strong cooling of up to 1ºC in the equatorial and north tropical Pacific and a weak cooling over the tropical Atlantic. Interestingly, over the Indian Ocean, an IOD-like pattern emerges with cooling in the western basin and warming in the eastern basin.

In contrast, the surface cooling in the North Atlantic in response to the weakening of the AMOC causes strong cooling over much of tropical Atlantic, as revealed by trMOM3-SFE-NA experiment shown in Figure 4.4e. A moderate warming is observed over the equatorial and south tropical Pacific Ocean. Zhang and Delworth (2005) and Wu et al. (2008) argue that the Pacific warming is attributed to the atmospheric teleconnection. A direct comparison between Figure 4.4b and 4.4e shows a remarkably similar pattern of SST change with an exception of equatorial south Atlantic, suggesting that the effect of the oceanic teleconnection on tropical SST is mainly confined to this region. This finding is further supported by the results of trMOM3-BFE-1.0Sv experiment shown in figure 4.4c. When only the AMOC-induced ocean circulation change is specified along the open boundaries, strong SST response is largely confined to the equatorial south Atlantic. Over other tropical ocean basins SST changes are generally weak (~0.2 ºC), except in the equatorial Pacific where a 0.4 ºC warm SST is observed. The latter may be attributed to the Kelvin/Rossby wave mechanism proposed by Timmermann (2003). Overall, the results presented here are consistent with the

previous study by Chang et al. (2008) and with the results of the uncoupled experiments.

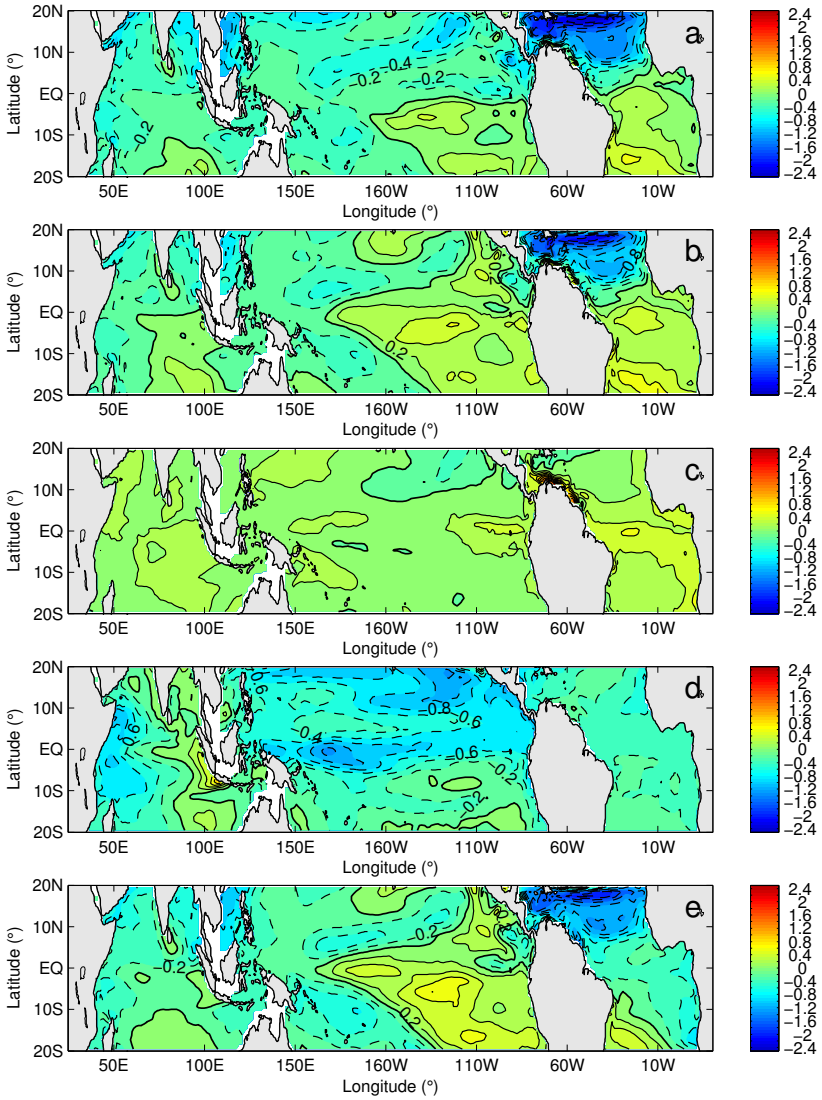

Figure 4.4 Annual mean SST difference between a) trMOM3-CFE-NH and trMOM3-CE, b) trMOM3-CFE-NA and trMOM3-CE, c) trMOM3-BFE and trMOM3-CE, d) trMOM3-SFE-NP and trMOM3-CE, e) trMOM3-SFE-NA and trMOM3-CE. The temperature is in °C.

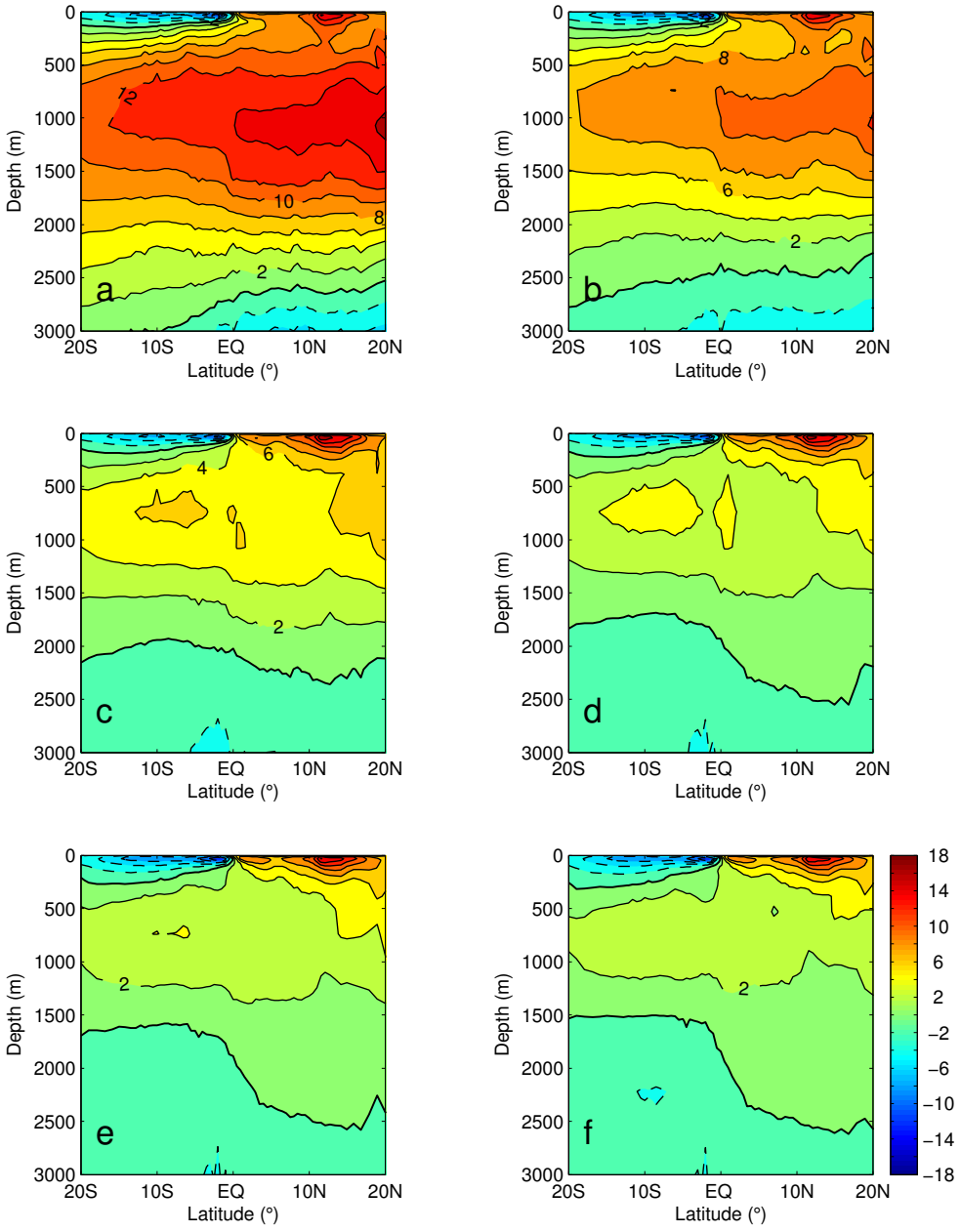

Figure 4.5 AMOC streamfunction in a) trMOM3-SFE-NA, b) trMOM3-CFE-0.2Sv, c) trMOM3-CFE-0.4Sv, d) trMOM3-CFE-0.6Sv, e) trMOM3-CFE-0.8Sv, f) trMOM3-CFE-NA. The AMOC streamfunction is in Sv.

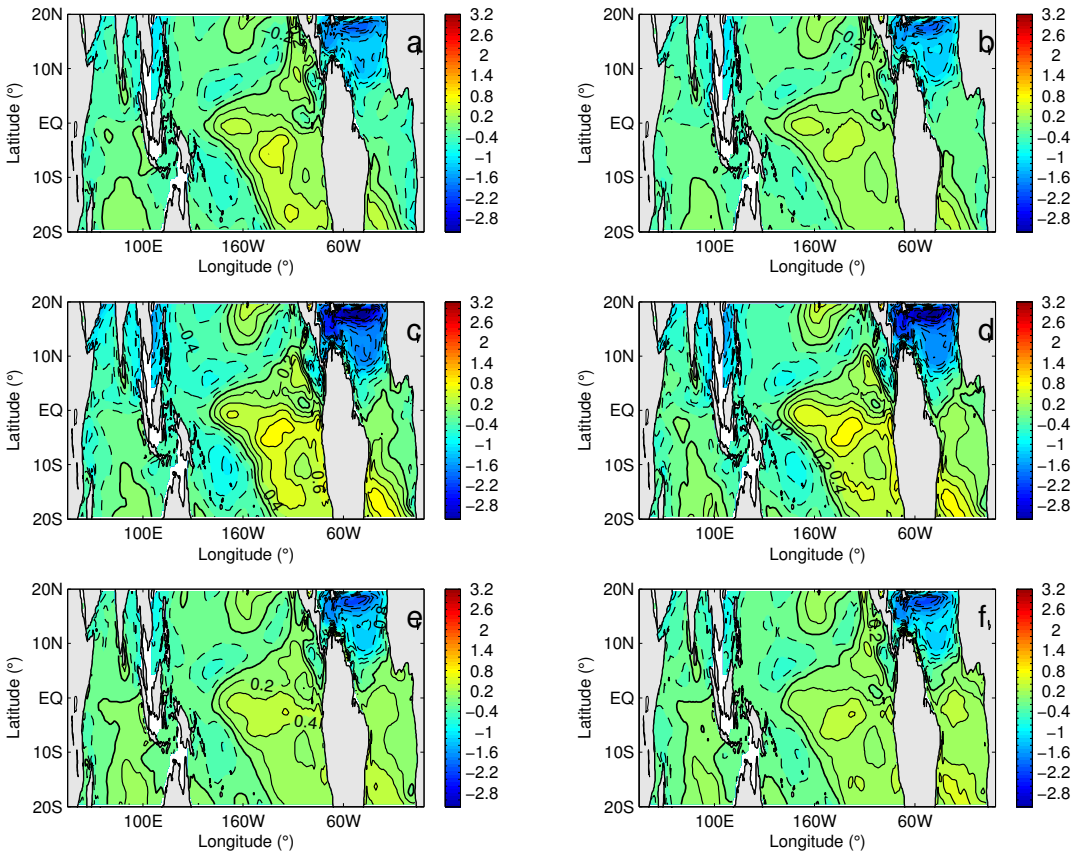

Figure 4.6 Annual mean SST difference between a) trMOM3-SFE-NA and trMOM3-CE, b) trMOM3-CFE-0.2Sv and trMOM3-CE, c) trMOM3-CFE-0.4Sv and trMOM3-CE, d) trMOM3-CFE-0.6Sv and trMOM3-CE, e) trMOM3-CFE-0.8Sv and trMOM3-CE, f) trMOM3-CFE-NA and trMOM3-CE. The temperature is in °C.

In the previous chapter, we examined the tropical SST response to different AMOC strengths by conducting a set of sensitivity experiments using gMOM3 without taking into consideration of atmospheric processes and ocean-atmosphere interactions. To assess the importance of these processes, we conducted a parallel set of sensitivity experiments using CCM3-trMOM3. In these experiments, we use the corresponding gMOM3 output as lateral boundary conditions to force the CCM3-trMOM3 while keeping the surface cooling in the North Atlantic unchanged (same as in trMOM3-CFE-NA). Figure 4.5 shows the AMOC from the six experiments where the AMOC transport changes at the open boundaries are derived from gMOM3 hosing experiments where the freshwater forcing strength increases gradually from 0.0Sv (control run) to 1.0Sv in step of 0.2Sv. As expected, the AMOC strength simulated by the CCM3-trMOM3 experiments drops systematically from about 15Sv to 2Sv at 20ºN and 1000m, confirming that the open boundary conditions work properly. Figure 4.6 shows the corresponding SST changes in the tropical oceans. It is evident that the SST is relatively insensitive to the imposed AMOC changes. This is particularly the case in the tropical Pacific and Indian Oceans where the pattern of the SST anomaly is nearly identical in all the experiments. The only region where the SST response changes significantly is in the South Tropical Atlantic where the SST anomaly changes its sign from negative to positive. It is worth noting that the transition from negative to positive SST anomaly takes place at around freshwater forcing of 0.4 Sv which coincides with the threshold value for the reversal of the NSTC as shown in Figure 3.10. These results confirm two earlier findings: 1) The surface cooling induced by AMOC changes in the high latitude North Atlantic is a dominant forcing for much of the tropical SST changes through atmospheric teleconnection; 2) The oceanic teleconnection is critically important for the surface warming in Tropical South Atlantic through changes in oceanic pathway as proposed by Chang et al. (2008).

These sensitivity experiments reveal not only that both the oceanic and atmospheric teleconnections contribute to tropical SST changes, but also they tend to compete with each other in certain areas of the tropical oceans. For example, atmospheric processes tend to cool the North Tropical Atlantic, while oceanic processes tend to warm it. Therefore, the effective SST change depends on the relative importance of these processes. This competing nature of the atmospheric and oceanic processes can help us interpret the paleo-temperature reconstructions and the paleo-salinity reconstructions during the Younger Dryas in this region. The following two sections are devoted for discussions on this topic.

2. On the interpretation of Caribbean paleo-temperature reconstructions during the Younger Dryas

As shown in Figure 4.1, paleo-temperature reconstructions in the Southern Caribbean suggest a complex SST change during the Younger Dryas that needs a dynamical explanation. In this section, we first demonstrate that this complex SST change is captured by our model simulation and then we dissect the underlying dynamical processes governing the SST response by separating atmospheric influences from oceanic effects.

Figure 4.7a shows the SST difference between trMOM3-CFE-NA and trMOM3-CE over the tropical Atlantic basin. Consistent with other model water hosing experiments (Stouffer et al., 2006), the combined effect of the surface cooling in the North Atlantic and the ocean circulation change is to produce an SST dipole with strong cooling in excess of 1ºC over the north tropical Atlantic, and a moderate warming over much of the equatorial and south tropical Atlantic. Interestingly, a narrow strip of warmer surface water also appears off the northern coast of South America, extending into the Southern Caribbean. This warming is surrounded by wide-spread surface cooling of the North

Atlantic, giving rise to a complex SST response pattern that is consistent with proxy reconstructions (Figure 4.1). Therefore, with both the surface forcing mimicking the cooling in the North Atlantic and boundary forcing driven by the AMOC change, the CCM3-trMOM3 is capable of reproducing the complex SST response in the southern Caribbean observed during the Younger Dryas. The question is what physical processes are responsible for this SST response.

To shed light on this issue, we turn first to the trMOM3-BFE where the SST change can only be attributed to ocean circulation change. As shown in Figure 4.7b, in the absence of surface cooling in the North Atlantic, the weakened AMOC produces surface warming in the entire tropical Atlantic basin with a strong warming along the northern coast of South America extending into the equatorial wave guide. This surface warming originates from the strong subsurface temperature gradient zone that separates the warmer and saltier subtropical water from the colder and fresher tropical gyre water along the boundary between the subtropical gyre and tropical gyre. As explained by Chang et al. (2008), the weakening of the AMOC causes the northward western boundary current to decrease, as most of the AMOC return flow is carried by the western boundary current (Fratantoni et al., 2000). The weakened western boundary current then produces a strong subsurface temperature warming near the strong temperature gradient zone due to horizontal heat advection by anomalous currents. Figure 4.8a shows that under present climatic conditions, there is roughly 12 Sv of cross-hemisphere flow in the upper 500 m of the tropical Atlantic Ocean. In the trMOM3-BFE, this flow is reduced to less-than 4 Sv accompanied with a subsurface warming of 2.5°C centered around 8°N and 300 m (Figure 4.8b). The warming extends into the surface mixed layer along the Atlantic coast of northern South America due to coastal upwelling (Figure 4.7b). Meanwhile, the subsurface warming also spreads southeastward along the western boundary and then along the equatorial wave guide, because the substantially weakened

AMOC causes the subsurface North Brazil Current (NBC) to reverse direction and enable warmer and saltier subtropical gyre water to penetrate into the equatorial zone (Chang et al., 2008) (Figure 4.7b). Equatorial upwelling subsequently brings the warming to the ocean surface and surface currents then spread the warm water over much of the tropical Atlantic. Therefore, the ocean circulation change alone tends to warm the tropical Atlantic Ocean.

In contrast, if we only permit North Atlantic surface cooling to occur without changing the ocean circulation, as in the trMOM3-SFE, then surface cooling prevails everywhere in the tropical Atlantic basin (Figure 4.7c). The cooling spreads into the tropics from the North Atlantic through a series of atmospheric processes and interactions with the ocean mixed layer. Chiang et al. (2008) argues that the wind-evaporation-SST (WES) feedback, which involves interactions between the wind-induced latent heat flux and SST changes (Xie and Philander, 1994; Chang et al., 1997), is particularly effective in transmitting the high-latitude SST changes to the tropics. The process sets in quickly and can transmit the cooling into the tropics within a decade. The cooling over the North Atlantic also enhances the northeasterly trade wind, which in turn strengthens the wind-driven STC. A comparison between the STCs in the trMOM3-CFE-NA (Figure 4.8b) and the BFE (Figure 4.8c) shows that the surface cooling causes the maximum strength of the northern STC to increase from 10 Sv in the trMOM3-BFE to 14 Sv in the trMOM3-CFE-NA. This 40% increase of northern STC enhances the subsurface warming at the strong temperature gradient zone near 8°N by 0.5°-1.0°C, owing to the enhanced anomalous heat advection. Therefore, the complex SST response pattern in the southern Caribbean can be attributed to the interplay between atmospheric process induced surface cooling and oceanic process induced subsurface warming. The relative strength of these processes determines the occurrence and strength of the opposing temperature changes in the region.

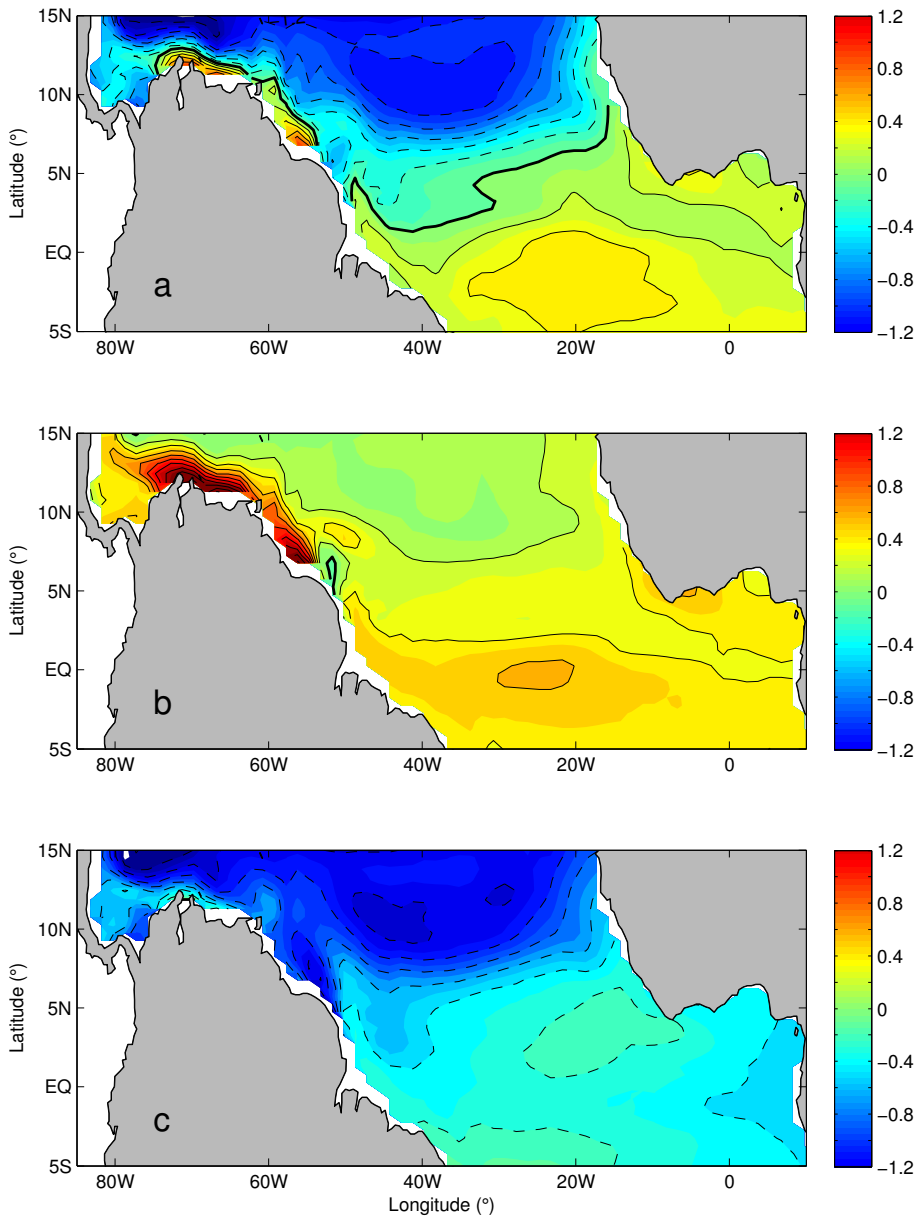

Figure 4.7 CCM3-trMOM3 simulated SST differences between (a) trMOM3-CFE-NA and trMOM3-CE, (b) trMOM3-BFE and trMOM3-CE, (c) trMOM3-SFE-NA and trMOM3-CE, respectively. Experiment details are given in the text. The interval of contour line is 0.2ºC.

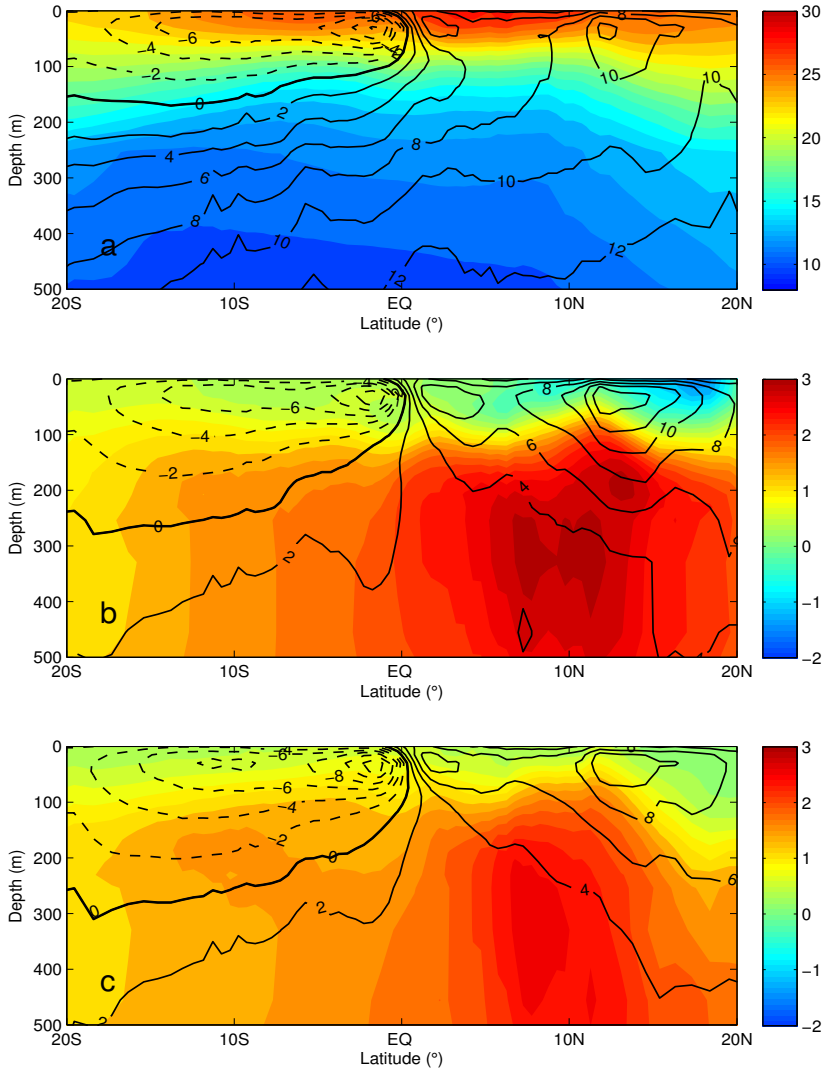

Figure 4.8 Upper Atlantic Ocean meridional overturning circulation streamfunction (contour) in trMOM3-CE (a), trMOM3-CFE-NA (b) and trMOM3-BFE (c), superimposed on zonally averaged temperature (color) in trMOM3-CE (a), zonally averaged temperature difference (color) between trMOM3-CFE-NA and trMOM3-CE (b) and between trMOM3-BFE and trMOM3-CE (c), respectively. The color bars indicate the temperature changes in ºC and the streamfunction contour interval is 2Sv, where 1Sv = $10^6 m^3 s^{-1}$.

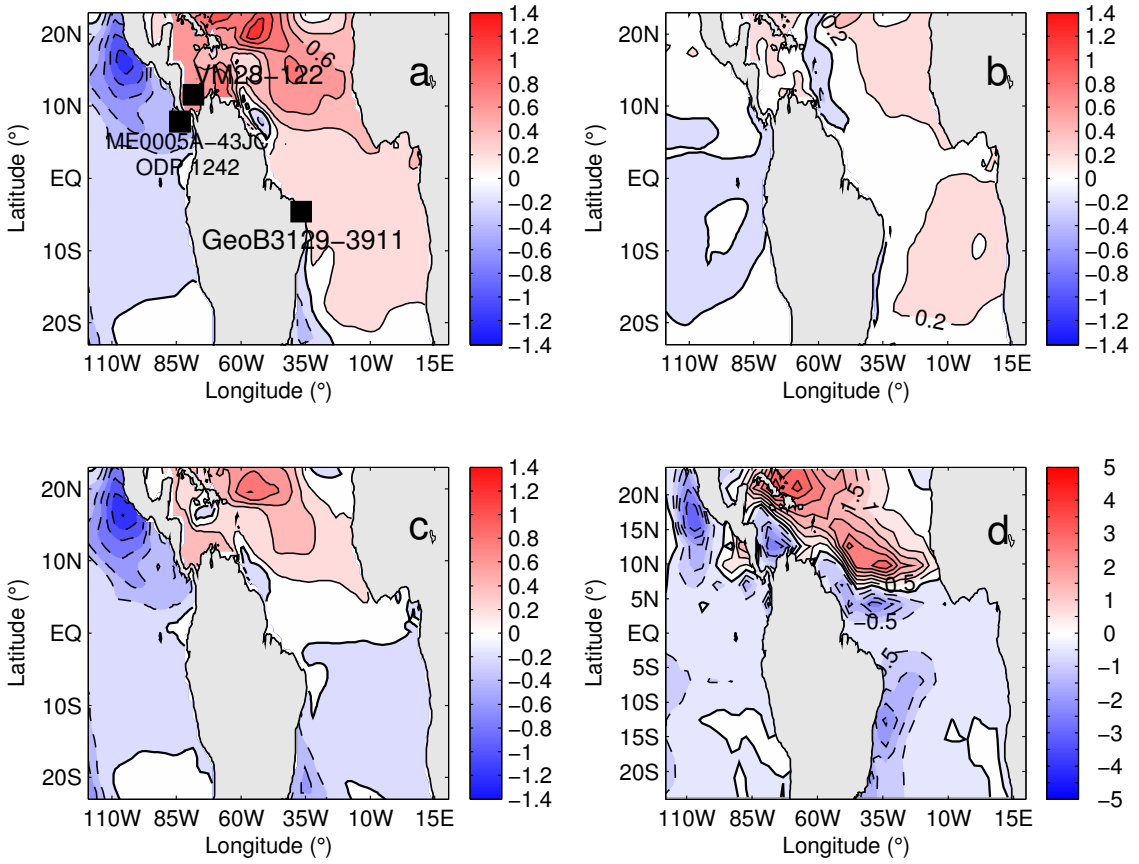

Figure 4.9 CCM3-trMOM3 simulated tropical surface salinity differences between (a) trMOM3-CFE-NA and trMOM3-CE, (b) trMOM3-BFE and trMOM3-CE, (c) trMOM3-SFE-NA and trMOM3-CE, respectively, and tropical precipitation difference between (d) trMOM3-CFE-NA and trMOM3-CE. The black squares in a indicate the locations of the proxy records that show the increased surface salinity in the model region during the period of the reduced AMOC (VM28-122 (Schmidt et al., 2004), ME0005A-43JC and ODP 1242 (Benway et al., 2006), GeoB3129-3911 (Weldeab et al., 2006)). Experiment details are given in the text. The interval of contour line is 0.2 for salinity and 0.5 mm/day for precipitation. Red (blue) color means positive (negative) values, saline (freshening) water for salinity and dry (wet) for precipitation.

3. On the interpretation of paleo-salinity reconstructions during the Younger Dryas

In the previous section, we show that the competing oceanic and atmospheric mechanisms associated with a weak AMOC may provide a physical explanation for the complex SST response in the northwestern tropical Atlantic and Caribbean region. Can the model also simulate the reconstructed paleo-salinity change during the Younger Dryas? If so, can it provide an explanation for the reconstructed paleo-salinity change?

Figure 4.9a shows the simulated surface salinity changes in trMOM3-CFE-NA experiment over the tropical Atlantic and eastern tropical Pacific in reference to the control run. Consistent with proxy $\delta^{18}O_{seawater}$ records for the tropical Atlantic (Figure 4.2) (Schmidt et al., 2004, 2006; Carlson et al., 2008; Weldeab et al., 2006), there is a basin-wide increase in sea-surface salinity (SSS) over the whole tropical Atlantic, although some differences exist with respect to magnitude and pattern of the salinity change. The largest salinity increase (in excess of 0.5) occurs in the tropical North Atlantic while an opposite salinity change occurs over the EEP region. This large salinity anomaly in the north tropical Atlantic is consistent with proxy-SSS records during cold periods in the North Atlantic on both orbital (Schmidt et al., 2004; Carlson et al., 2008) and millennial (Schmidt et al., 2006) time scales. Nevertheless, the modeled amplitude of the salinity change is less than what the proxy-SSS result suggests, possibly due to the coarse model resolution. With the design of coupled model experiments, we show that the SSS change over tropical region associated with rapid AMOC decrease involves several physical processes, including changes in both the atmosphere and ocean.

Figure 4.9d shows the corresponding model precipitation change between trMOM3-CFE-NA and trMOM3-CE. Over the WTA and EEP regions, we see consistency between the modeled SSS anomalies (Figure 4.9a) and the precipitation changes (Figure 4.9d), indicating that the surface freshwater flux is mainly responsible for the distribution of SSS anomalies. Over the equatorial and south Atlantic, however, there is an increase in

SSS in a region with elevated freshwater precipitation, suggesting that other mechanisms must be involved. We now demonstrate that the salinity increase in this region is caused by changes in the oceanic pathway in response to the weakening of the AMOC.

Figure 4.10a shows the AMOC in upper 500 m, superimposed on zonally averaged salinity in trMOM3-CE. Two maximum salinity cores at 20°S and 20°N are clearly revealed. Of particular interest is the strong salinity gradient along 10°N separating the maximum salinity water of the north Atlantic subtropical gyre from the low salinity water of the tropical gyre. The zonally averaged salinity difference between trMOM3-CFE-NA and trMOM3-CE, trMOM3-BFE and trMOM3-CE, trMOM3-SFE-NA and trMOM3-CE, are shown in Figure 4.10b, 4.10c and 4.10d, respectively. In trMOM3-BFE the AMOC weakens through changes in the open boundaries (Figure 4.10c), which causes the strength of the northward western boundary current (WBC) that carries the AMOC return flow to decrease. The anomalous advection of the reduced WBC acting on the strong salinity gradient near 10°N gives rise to a strong positive subsurface salinity anomaly (Figure 4.10c). Meanwhile, the subsurface branch of the northern Atlantic subtropical cell (STC) which carries subducted water equatorward but is normally blocked from getting into the tropics by the northward AMOC return flow (Fratantoni et al., 2000; Hazeleger and Drijfhout, et al., 2006) (Figure 4.10a) forms an important component of the WBC in trMOM3-BFE experiment, allowing the maximum salinity water access to the equatorial zone along the western boundary. This change in the oceanic pathway results in an increase in equatorial thermocline salinity, which eventually manifests itself as a surface salinity increase in the tropical Atlantic due to equatorial and coastal upwelling (Figure 4.9b). This is the same mechanism responsible for the surface warming over the equatorial south Atlantic ocean proposed by Chang et al. (2008). However, unlike the SST change, this increase in surface salinity is offset by the increase in the precipitation over the south tropical Atlantic ocean (Figure 4.9d).

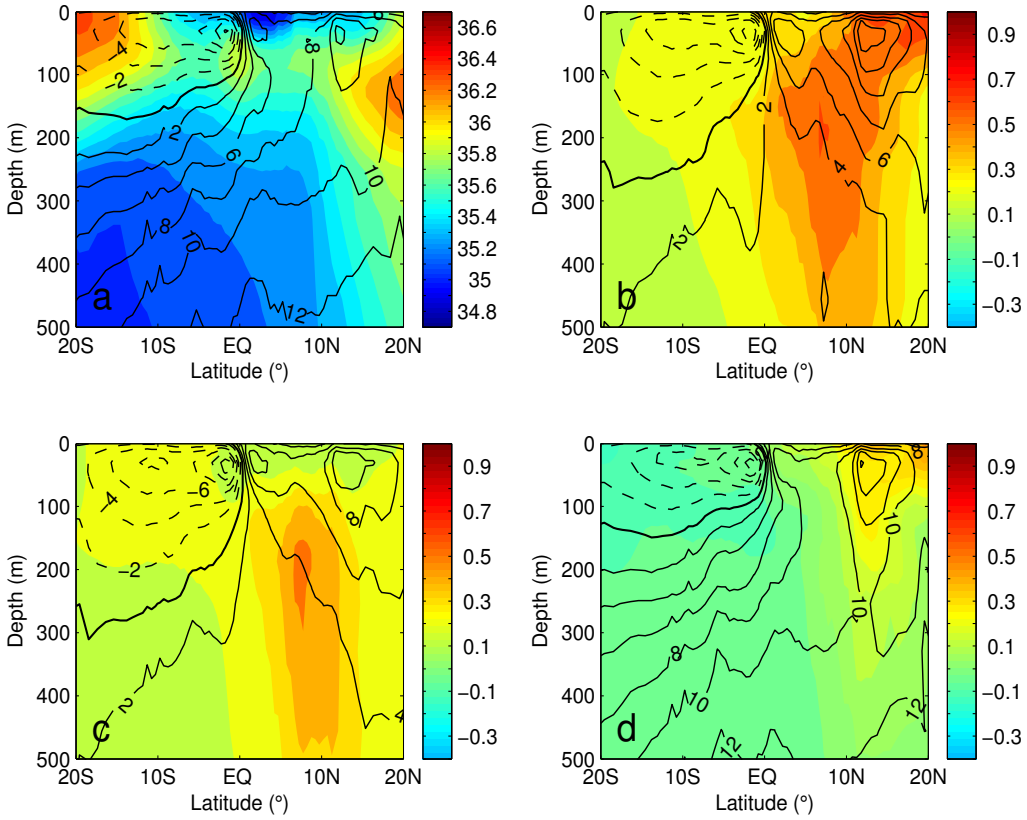

Figure 4.10 Upper Atlantic Ocean meridional overturning circulation streamfunction (contour) in trMOM3-CE (a), trMOM3-CFE-NA (b), trMOM3-BFE (c) and trMOM3-SFE-NA (d), superimposed on zonally averaged salinity (color) in trMOM3-CE (a), zonally averaged salinity difference (color) between trMOM3-CFE and trMOM3-CE-NA (b), trMOM3-BFE and trMOM3-CE (c), trMOM3-SFE-NA and trMOM3-CE (d), respectively. The color bars indicate the salinity (a) and the salinity changes (b, c, and d) and the streamfunction contour interval is 2Sv, where 1Sv = $10^6 m^3 s^{-1}$.

In contrast, if we only permit North Atlantic surface cooling to occur without changing ocean circulation, as in trMOM3-SFE-NA, then surface salinity changes resemble the result of trMOM3-CFE-NA in the north tropical Atlantic and EEP (Figure 4.9a and 4.9c), indicating that atmospheric processes dominate in these regions. In the equatorial south Atlantic, however, atmospheric processes cause a decrease in salinity (Figure 4.9d), contrary to the results of our trMOM3-CFE-NA experiment (Figure 4.9a) and with paleo-SSS reconstructions (Figure 4.2). Therefore, we conclude that ocean circulation changes associated with AMOC variability play a critical role in driving salinity changes in the equatorial South Atlantic.

Additionally, coupled ocean-atmosphere feedbacks make a contribution to the SSS change. In both trMOM3-CFE-NA and trMOM3-SFE-NA, there is a wide-spreading surface cooling over the North Atlantic that causes a southward shift of the Atlantic ITCZ and enhances trade wind strength. The strengthened trades increase the wind-driven STC, for example, from 12 Sv in trMOM3-CE to 14 Sv in trMOM3-SFE-NA (Figure 4.10a and 4.10d). This has two effects on SSS: 1) the enhanced STC amplifies the subsurface salinity anomaly by advecting more salinity maximum water into the equatorial south Atlantic (comparison between Figure 4.10b and 4.10c) and 2) the intensified northeasterly trades cause more evaporation (Figure 4.11) and produces more saline water in the subduction zone (Figure 4.10d). In the absence of a substantially weakened AMOC cell, as in trMOM3-SFE-NA, the saline water product, which is partly due to the enhanced evaporation in response to trade wind increase (Figure 4.11), is confined within the subtropical gyre by the northward flowing WBC and has little effect on the salinity budget south of 10°N. This feature is clearly demonstrated in Figure 4.10d. When the AMOC is substantially weakened as in trMOM3-CFE-NA, these wind-induced salinity increases get advected into the equatorial Atlantic and can therefore contribute to the basin-wide SSS increase shown in Figure 4.9a.

Finally, we would like to comment on the SSS response in the EEP region. As discussed in Benway et al. (2006), proxy-SSS records in both the EEP and the Caribbean indicate increased SSS during periods of reduced AMOC, such as during the Younger Dryas. The model simulations, on the other hand, show an opposite SSS response at these two regions, suggesting that the SSS change in the EEP in the model may be dominated by the vapor transport from the Atlantic to the Pacific in maintaining the modern inter-ocean salinity contrast, but not by cross-basin ITCZ shift. The lack of such a shift may be related to the fact that the imposed surface cooling is only confined to the North Atlantic and the Pacific ITCZ does not respond strongly to the cooling in the North Atlantic. To investigate this possibility, we conducted an additional experiment by imposing a surface cooling in the North Pacific north of 20ºN (trMOM3-SFE-NP experiment). Figure 4.12 shows the SSS difference between this experiment and trMOM3-CE. Evidently, the North Pacific cooling results in a southward shift of the Pacific ITCZ and produces an increase in SSS over EEP region that is consistent with paleo-salinity records. Interesting, the North Pacific cooling does not exert a significant impact on SSS changes in the Atlantic Ocean. This leads us to hypothesize that the surface cooling in the North Pacific and North Atlantic have opposing influences on SSS changes over the EEP region and a significant surface cooling exists in the North Pacific during times of reduced AMOC that is responsible for the SSS increase in the EEP region.

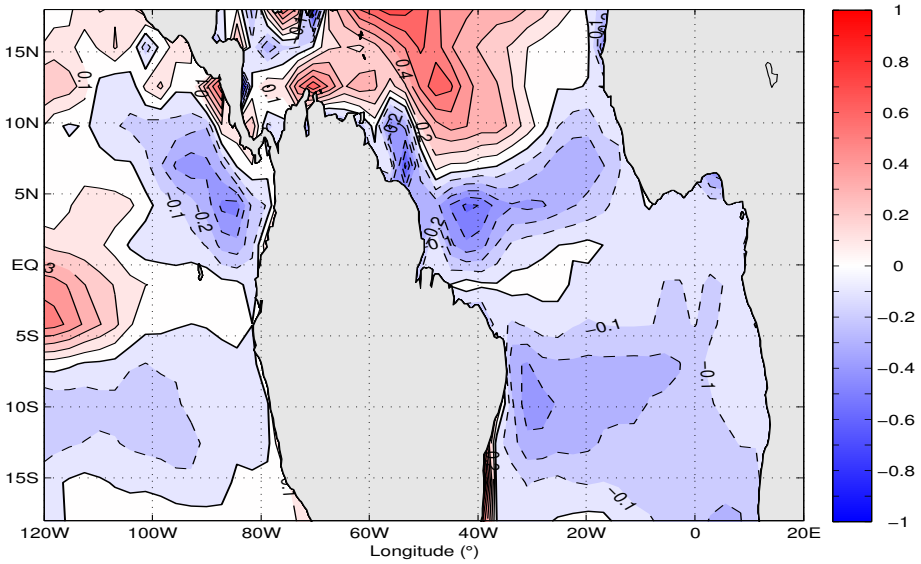

Figure 4.11 CCM3-trMOM3 simulated tropical evaporation difference between trMOM3-SFE-NA and trMOM3-CE. The interval of contour line is 0.1 mm/day for evaporation. Red (blue) color means positive (negative) values and dry (wet) for evaporation.

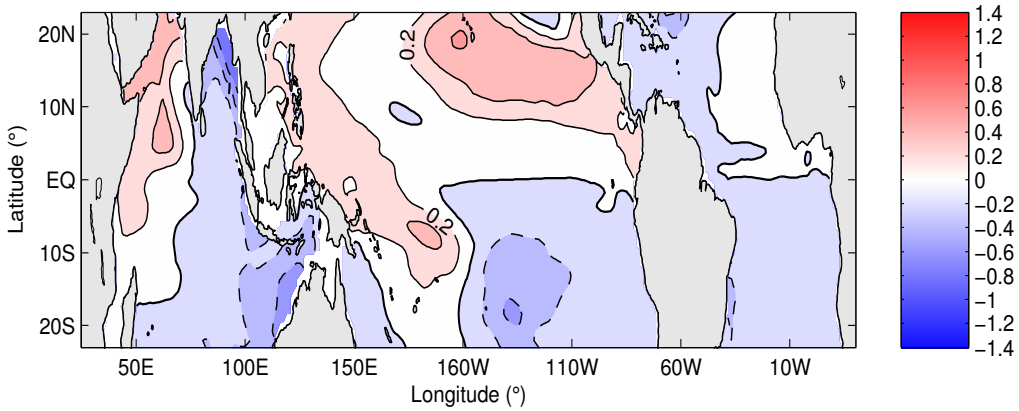

Figure 4.12 CCM3-trMOM3 simulated tropical surface salinity difference between the trMOM3-SFE-NP and trMOM3-CE. The interval of contour line for salinity is 0.2.

C. Impact of AMOC Changes on Tropical Climate Variability

Although previous studies put forward a number of potential teleconnection mechanisms between changes in the high latitude and tropical Atlantic in response to AMOC changes, such as the ocean wave mechanism by Yang (1999) and Timmermann et al. (1998), oceanic pathway change mechanism by Chang et al. (2008) and the atmospheric teleconnection mechanism by Chiang and Bitz (2005), their relative importance in affecting tropical climate is not well understood. In this section, we will shed some light on this issue through comparison among various CCM3-trMOM3 experiments discussed in Chapter II.

First, we examine changes in tropical Atlantic variability which is dominated by a zonal mode with a strong zonal gradient in the eastern equatorial Atlantic region and a meridional mode with a cross-equatorial gradient. These two modes of variability are shown by the first two leading EOFs of the simulated SST anomalies, in various CCM3-trMOM3 experiments as shown in Figure 4.13. A comparison of the EOFs from different experiments reveals only subtle differences among these EOFs, suggesting that TAV in the model is insensitive to AMOC changes. The standard deviation of ATL3 index, defined as an average of SST anomalies over the region between 3ºN-3ºS and 20ºW-0ºW, differs by less than 5% in these runs. The insensitivity of the model's TAV response to AMOC changes contradicts the previous modeling studies (Haarsma et al., 2008; Chang et al., 2008; Wen et al., 2008) which show a significant weakening in the zonal mode variability. Physical reasons for this difference are not clear at this point, but are likely to be related to the diffused thermocline in the model, as discussed in Chapter II. Further investigations are needed to resolve this issue.

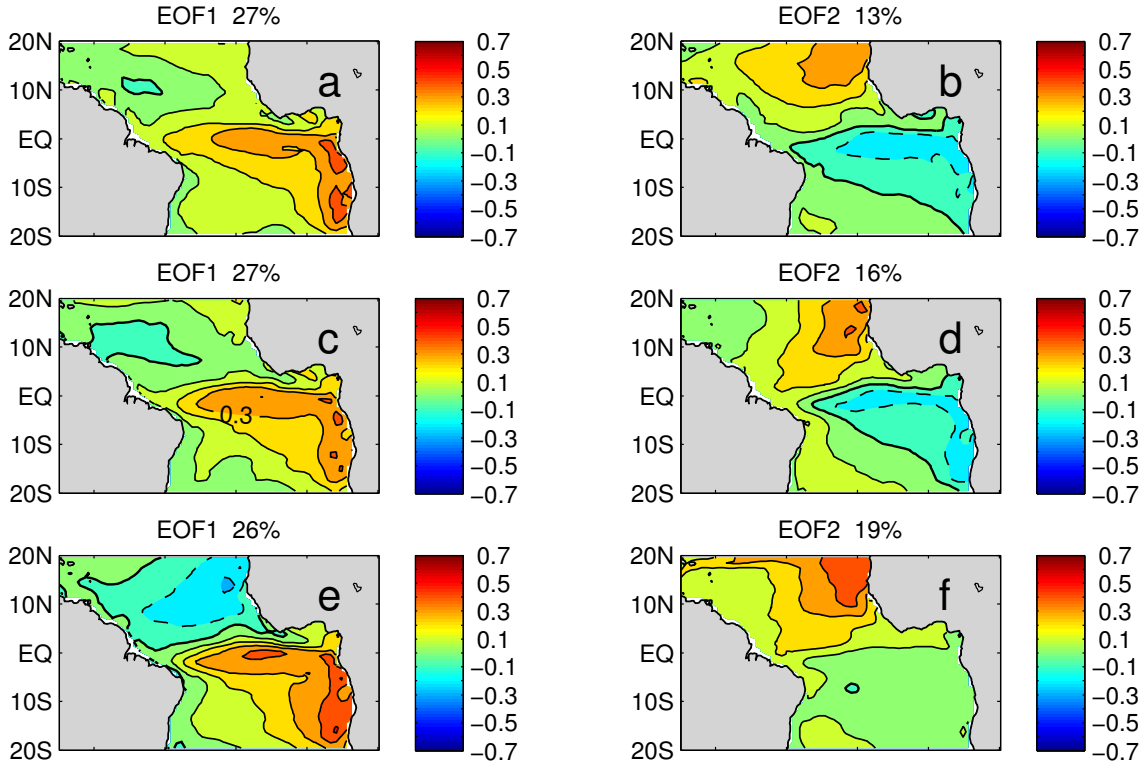

Figure 4.13 Tropical Atlantic variability of (a, b) trMOM3-CE, (c, d) trMOM3-CFE-NH (e, f) trMOM3-CFE-NA runs.

We next focus on the investigation of tropical Pacific variability in our runs and try to address questions such as: How do AMOC changes affect the tropical Pacific variability, in particular ENSO variability? What is the relative importance of atmospheric and oceanic processes in ENSO variability? The NINO3.4 index, defined as an average of SST anomalies over the region between 5ºN-5ºS and 170ºW-120ºW, is often used to characterize temporal variability of ENSO. The time series of the NINO3.4 index from different CCM3-trMOM3 model simulations are shown in Figure 4.14. The corresponding time series from observations for the period of 1889-2008 is shown in

Figure 4.15 (Smith and Reynolds, 2003, 2004; Smith et al., 2008). The amplitudes of the warm and cold events from the model experiments have a peak-to-peak value of -2.0ºC to 2.0ºC, which is weaker than the observed value that ranges from -2.0ºC to 3.0ºC. The standard deviation of the time series is 0.70 for the control run and 0.82 for the observations.

To better illustrate the effect of AMOC changes on the strength of ENSO, we computed the ratio between the standard deviation of the simulated NINO3.4 SSTA index in various sensitivity experiments and the standard deviation of the simulated NINO3.4 SSTA index in the control simulation. The results are shown in Figure 4.16. Compared to the control run, trMOM3-CE, all the sensitivity experiments except trMOM3-CFE-NH, show an increase in ENSO variance in excess of at least 10%. In contrast, the standard deviation of monthly NINO3.4 SST index in trMOM3-CFE-NH experiment where all boundary forcings are combined shows a 16% decrease, suggesting that some of the physical processes counteract among themselves. This result contradicts the finding by Dong and Sutton (2007) that shows an enhanced ENSO variability in a fully coupled GCM hosing experiment with a 1.0 Sv hosing freshwater input. This inconsistency could be due to the differences in model physics and numerics. It could also be a reflection of complex interactions among different physical processes that are represented differently in different models.

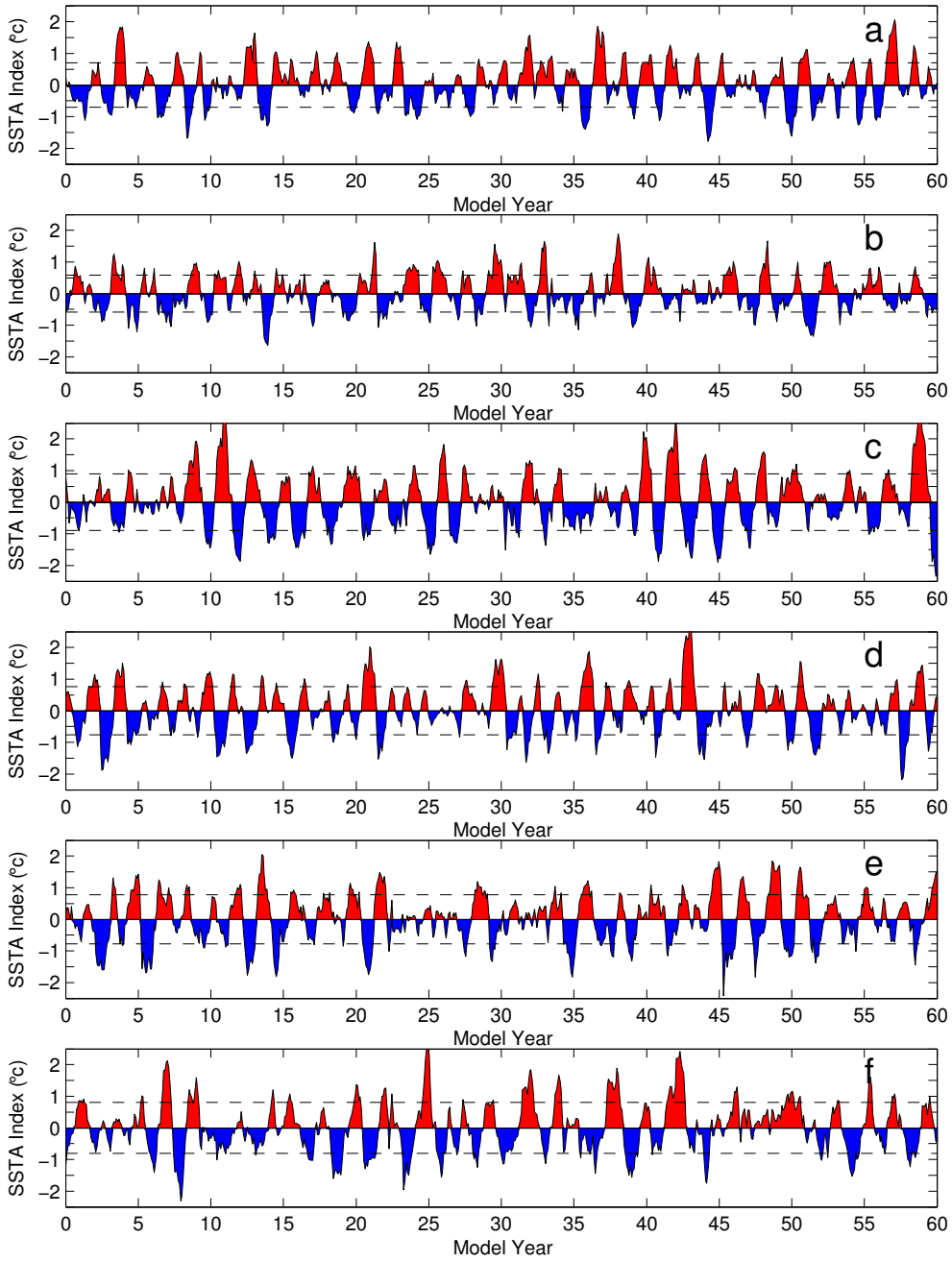

Figure 4.14 Monthly mean anomalous SST over Pacific NINO3.4 region (170ºW-120ºW, 5ºS-5ºN). a) trMOM3-CE, b) trMOM3-CFE-NH, c) trMOM3-CFE-NA, d) trMOM3-BFE, e) trMOM3-SFE-NP, f) trMOM3-SFE-NA. The dashed lines are the corresponding standard deviations of the indexes.

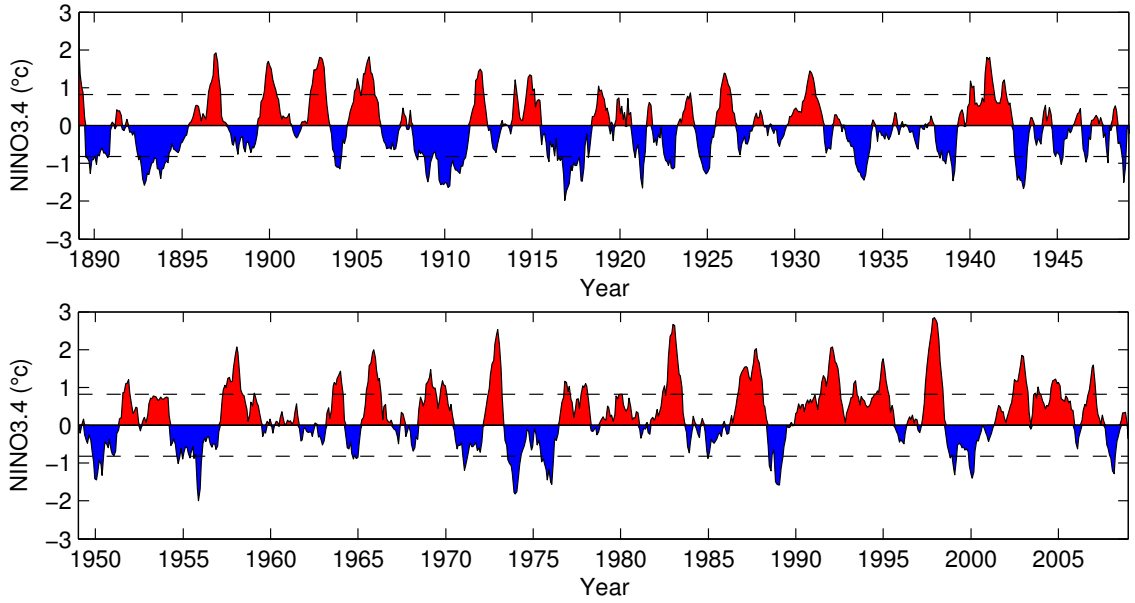

Figure 4.15 Time series of the monthly NINO3.4 SST anomalies from observations 1889-2008 of NOAA Extended Reconstructed SST V3.

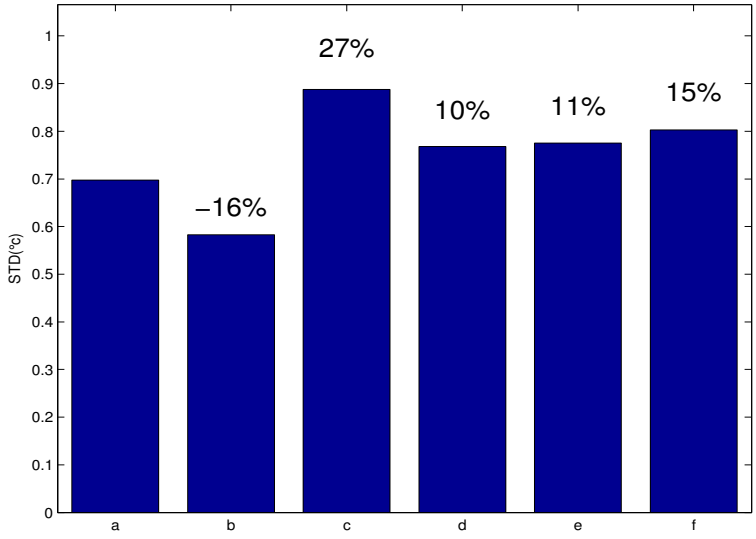

Figure 4.16 Standard deviation of monthly mean anomalous SST over Pacific NINO3.4 region (170ºW-120ºW, 5ºS-5ºN). a) trMOM3-CE, b) trMOM3-CFE-NH, c) trMOM3-CFE-NA, d) trMOM3-BFE, e) trMOM3-SFE-NP, f) trMOM3-SFE-NA

The changes of ENSO in different runs are also manifested in other characteristics. Figure 4.17 shows a wavelet power spectrum of NINO3.4 SST anomaly. The control experiment shows a dominant peak near 2 years. This period is considerably shorter than the observed ENSO period, which has a broad peak between 3 and 7 years with a maximum around 4 years. For all the experiments that are forced with the surface cooling in the Northern Hemisphere, power spectra show an increase in ENSO periodicity with enhanced power except for the trMOM3-CFE-NH experiment. This result is consistent with the variance analysis shown in Figure 4.16, hinting again that the effect of the North Pacific cooling and North Atlantic cooling on ENSO may have the opposite influence on ENSO. The leading EOFs of the simulated SST anomalies from these simulations are also consistent with this result, as shown in Figure 4.18. It clearly shows that ENSO in trMOM3-CFE-NH run weakens, while it strengthens in the other experiments, particularly the ones with the effect of the North Pacific cooling or North Atlantic cooling. These analyses, however, do not provide any information about changes in nonlinear characteristics of ENSO, such as skewness of SST anomaly.

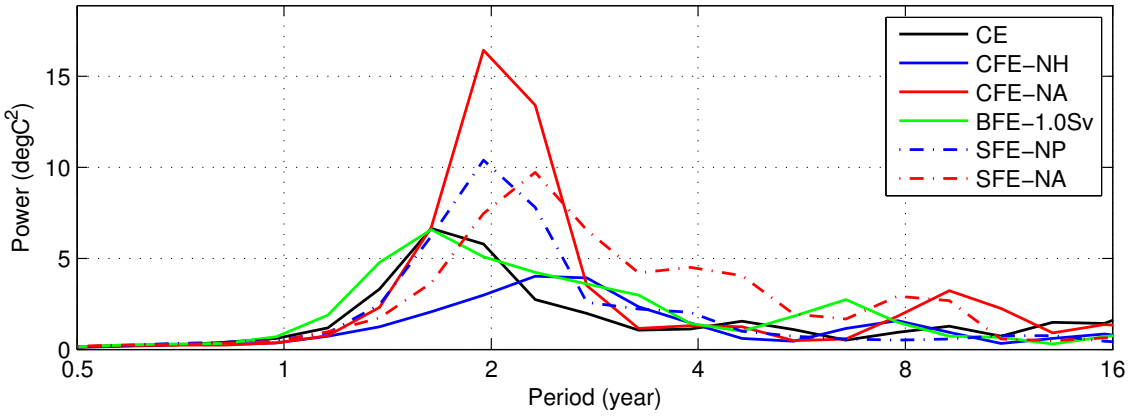

Figure 4.17 Wavelet power spectrums of NINO3.4 index anomalies for the six experiments of CCM3-trMOM3

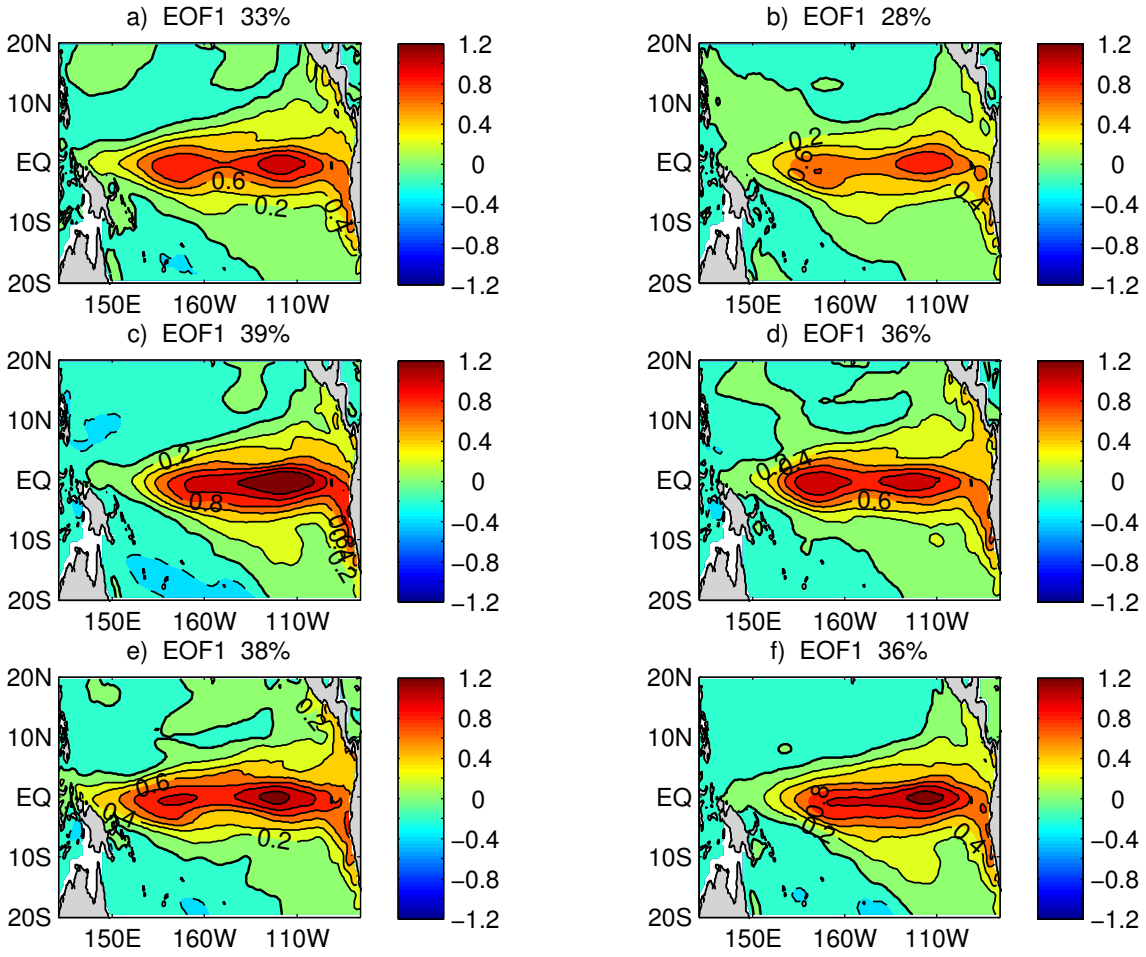

Figure 4.18 The first EOF of SST anomaly over tropical Pacific Ocean from a) trMOM3-CE, b) trMOM3-CFE-NH, c) trMOM3-CFE-NA, d) trMOM3-BFE, e) trMOM3-SFE-NP, f) trMOM3-SFE-NA.

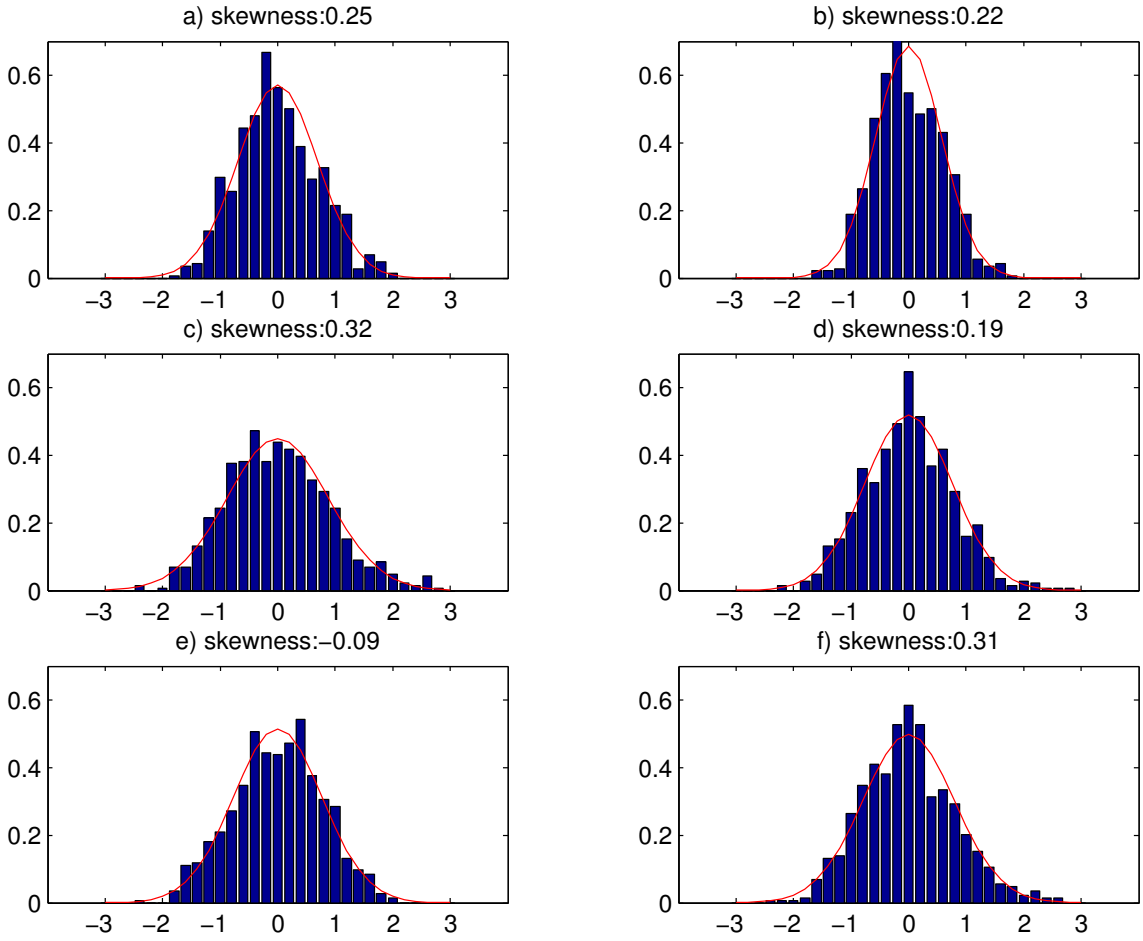

Figure 4.19 The PDF of the NINO3.4 SSTA index for model simulation a) trMOM3-CE, b) trMOM3-CFE-NH, c) trMOM3-CFE-NA, d) trMOM3-BFE, e) trMOM3-SFE-NP, f) trMOM3-SFE-NA. The red lines are the corresponding fitted normal distributions.

It is well known that the observed ENSO cycle has an asymmetry between El Niño and La Niña, with stronger warm events than cold events, as visually evident in Figure 4.15. A more quantitative measure of the asymmetry can be obtained by computing the skewness of the SST anomaly which shows a value of 0.32 for the observed NINO3.4

SSTA index. In the control simulation (Figure 4.14a), the skewness of the NINO3.4 SSTA index is 0.25, suggesting a weaker-than-observed asymmetry about its mean of the simulated ENSO. Interestingly, with the surface cooling in the North Atlantic, both the trMOM3-CFE-NA and trMOM3-SFE-NA show an increase in skewness to 0.32 and 0.31, respectively. On the other hand, with the North Pacific surface cooling, the trMOM3-SFE-NP shows drastically a decrease in skewness of the NINO3.4 SSTA index to a negative value of -0.09, suggesting that La Niña events become more dominant and stronger than El Niño events. The Probability Distribution Function (PDF) of simulated NINO3.4 SSTA indexes (Figure 4.19) is consistent with the skewness analysis. The PDF of trMOM3-CFE-NA does show obvious asymmetry between warm and cold events and is clearly skewed towards positive SST anomalies (Figure 4.19c), that is, there are stronger El Niños than La Niñas. The change in skewness suggests that the effect of AMOC changes on ENSO is achieved through a set of complex mechanisms involving different physical processes.

To look for possible causes of the ENSO changes, we examined the 20ºC isotherm depth, a proxy for the equatorial thermocline depth (Figure 4.20) and the temperature change along the equatorial Pacific section (Figure 4.21). As can be seen from Figure 4.20, for all the experiments, the thermocline depth increases in the North Pacific due to the enhanced wind stress curl as discussion in the previous chapter. This result is consistent with the previous ocean-only experiments and the others coupled GCM experiments (e.g., Zhang and Delworth, 2005). In the south tropical Pacific, the thermocline becomes shallower except for the trMOM3-BFE. However, there are major differences in the equatorial thermocline depth change among these experiments. In the trMOM3-CFE-NA experiment, the equatorial thermocline depth decreases in the western Pacific and increases in the eastern Pacific (Figure 4.20b). In fact, the whole upper ocean in the eastern Pacific warms (Figure 4.21b). This could be a consequence of

the increase in El Niño events in the trMOM3-CFE-NA experiment. In the trMOM3-SFE-NP experiment, the equatorial thermocline depth increases (decreases) in the western (eastern) Pacific (Figure 4.20d) and the whole upper equatorial ocean cools, reflecting the increase in La Niña events. In contrast, the upper ocean temperature in the trMOM3-CFE-NH experiment shows a cooling in upper 200 m and a warming below 200 m (Figure 4.21a), suggesting a decrease in vertical temperature gradient. This reduction in the vertical temperature gradient seems to be consistent with the reduced ENSO activity in the trMOM3-CFE-NH experiment. However, these changes in the upper ocean mean temperature do not necessarily explain the changes in ENSO characteristics, particularly the ENSO skewness change, in response to AMOC changes. For example, the thermocline change in the trMOM3-CFE-NA experiment suggests a weakening of the Bjerknes feedback, which would result in a weakened, but not a strengthened ENSO. Therefore, the changes in the ENSO cycle may be caused by other physical mechanisms.

One possible mechanism that relates changes in ENSO to extratropical influence is the seasonal footprinting mechanism (SFM) (Vimont et al., 2003; Alexander et al., 2009) or the Pacific Meridional Mode mechanism (PMM) (Chiang and Vimont, 2004; Chang et al., 2007). It is conceivable that the surface cooling in the North Atlantic and North Pacific can alter internal atmospheric variability in the extratropics, which in turn can have an influence on ENSO variability. To examine whether the evolution of the simulated ENSO in CCM3-trMOM3 is consistent with the SFM/PMM mechanism, we performed a composite analysis for the model simulated El Niño events in trMOM3-CE and trMOM3-CFE-NH (Figure 4.22) and in trMOM3-CFE-NA and trMOM3-SFE-NP (Figure 4.23). In both figures, the sequences of maps reveal the evolutions of El Niño event, which is a very important aspect of the ENSO cycle. Starting at the composite -6 month, positive SST anomalies can be seen, in all of the model simulations, in the

northern tropical Pacific just north of the ITCZ; while there are negative SST anomalies south of the ITCZ. This pattern is reminiscent of the SFM/PMM shown in Vimont et al. (2003) and Chang et al. (2007). Compared the SFM/PMM patterns in Figure 4.23 with that in control run of Figure 4.22, one can find that the pattern of trMOM3-CFE-NA is stronger and the pattern of trMOM3-SFE-NP is weaker, which may imply that the North Atlantic surface cooling and the North Pacific surface cooling have different effect on this critical pattern for the evolution of ENSO. Therefore, the changes in the ENSO cycle can be achieved through this possible mechanism.

The result that the North Atlantic surface cooling tends to strengthen El Niño, making ENSO related SST anomaly skew more positively is consistent with the modeling results by Dong and Sutton (2007), suggesting that this process may be dominating in their hosing simulation. There are also observational suggestions that the asymmetry between El Niño and La Niña has become stronger over the past few decades with the ENSO gaining strength (Jin et al., 2003; An and Jin, 2004). Dong et al., (2006) suggest that this change in ENSO may be induced by the AMO which was in its cold phase from early 1960s to mid 1990s (Dong et al., 2006). However, this assertion is not supported by more recent observations that show a positive AMO phase since mid 1990s with little change in ENSO behavior. Furthermore, North Pacific influence may further complicate AMOC's effect on ENSO. The modeling results presented here suggest that the surface cooling in the North Pacific has an opposite effect on ENSO, causing stronger La Niña than El Niño events. This effect may cancel the effect from the Atlantic, making the observations difficult to interpret. Therefore, further studies of the physical processes involved in these changes are required.

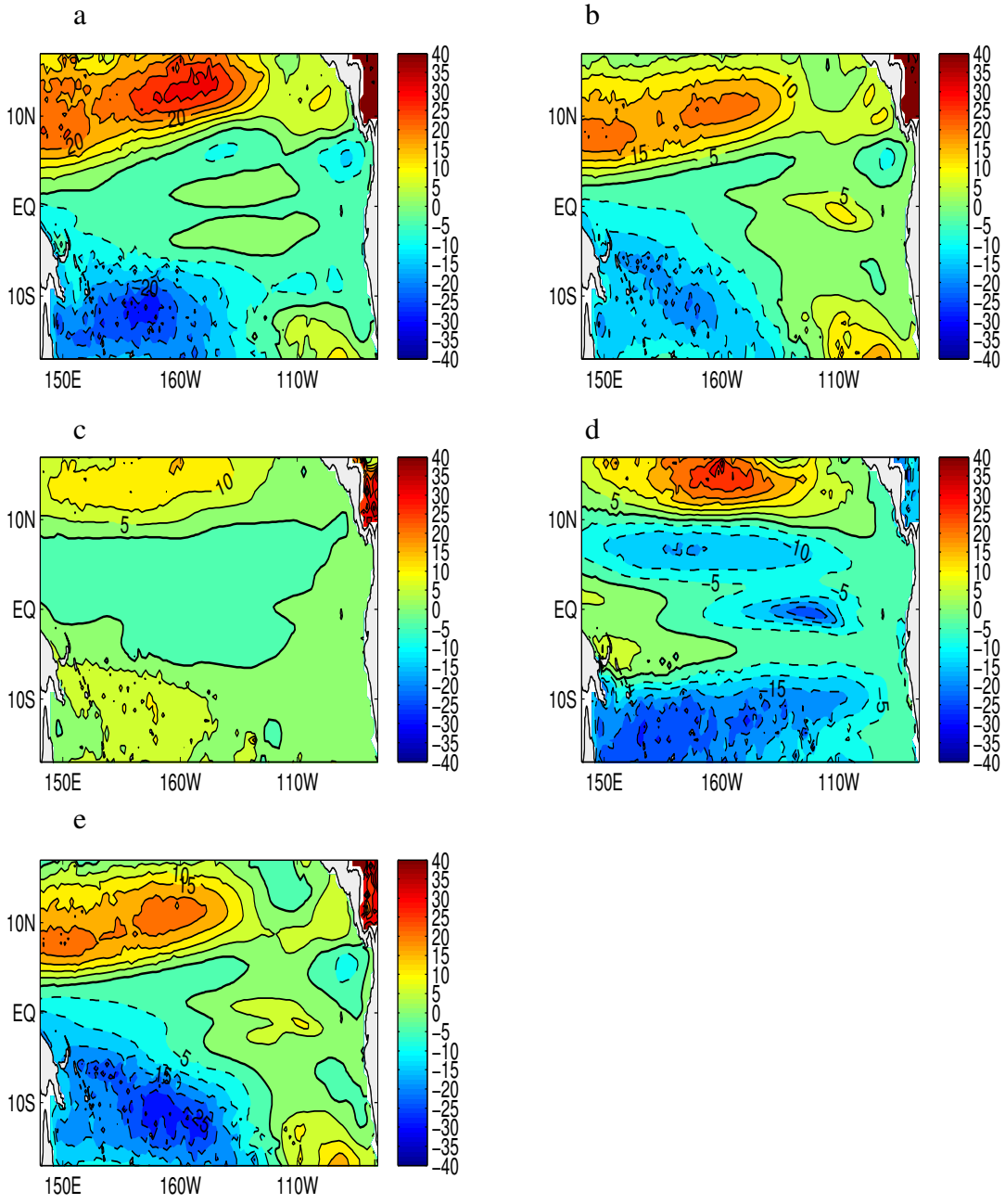

Figure 4.20 The difference of the 20ºC isotherm depth over Pacific region between a) trMOM3-CFE-NH, b) trMOM3-CFE-NA, c) trMOM3-BFE, d) trMOM3-SFE-NP, e) trMOM3-SFE-NA and trMOM3-CE. The depth is in meter.

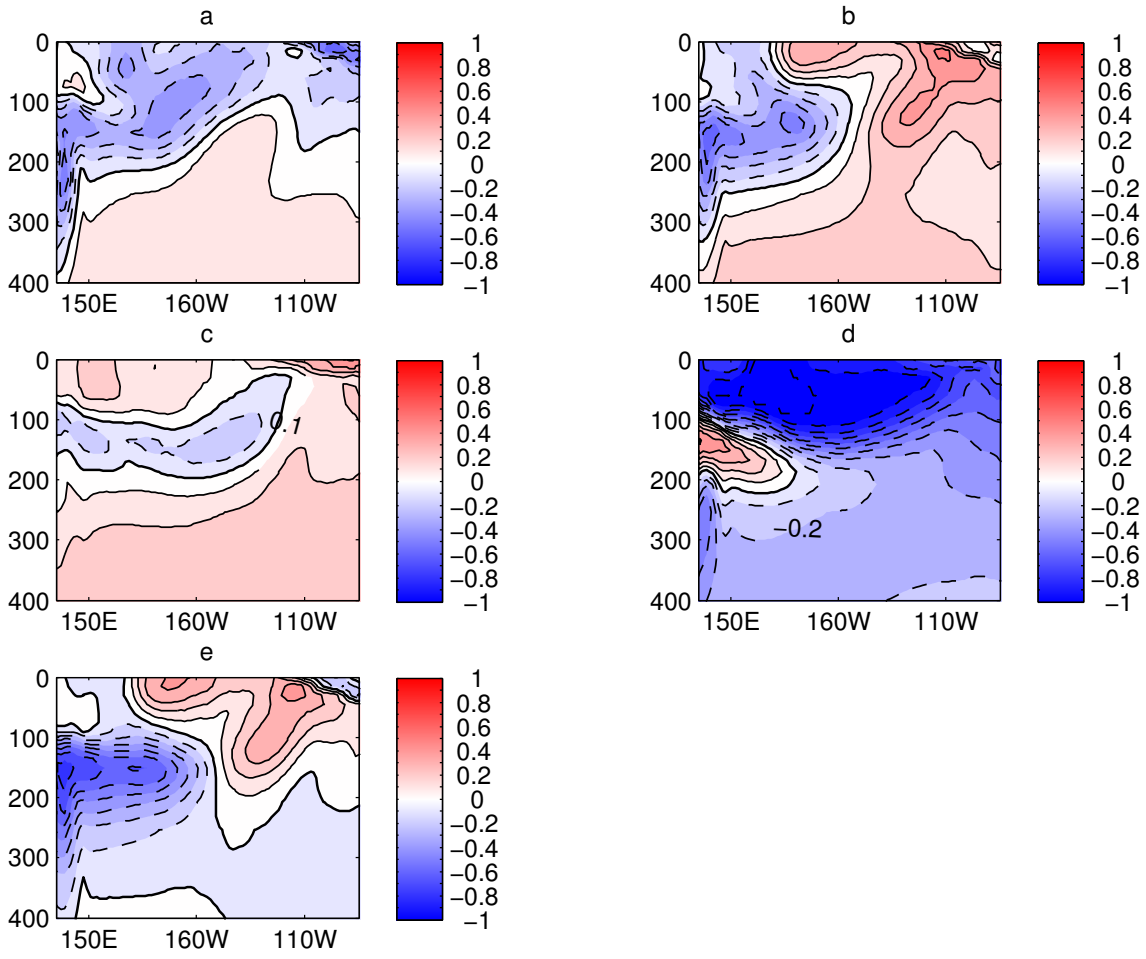

Figure 4.21 Temperature difference along the Equator section between a) trMOM3-CFE-NH, b) trMOM3-CFE-NA, c) trMOM3-BFE, d) trMOM3-SFE-NP, e) trMOM3-SFE-NA and trMOM3-CE. The depth is in meter and the contour interval is 0.1 ℃.

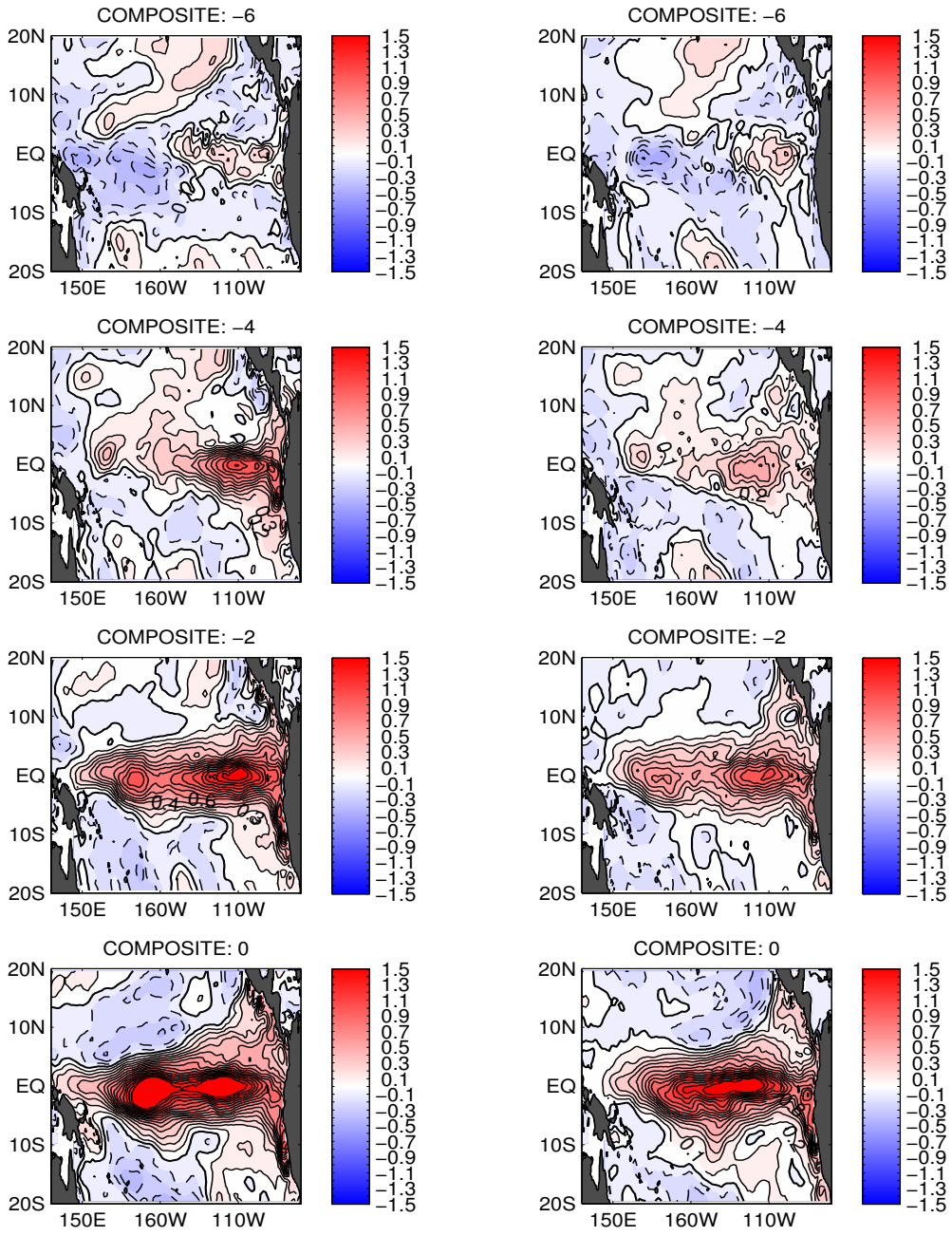

Figure 4.22 Composites of the El Niño event for trMOM3-CE (left-hand column) and trMOM3-CFE-NH (right-hand column).

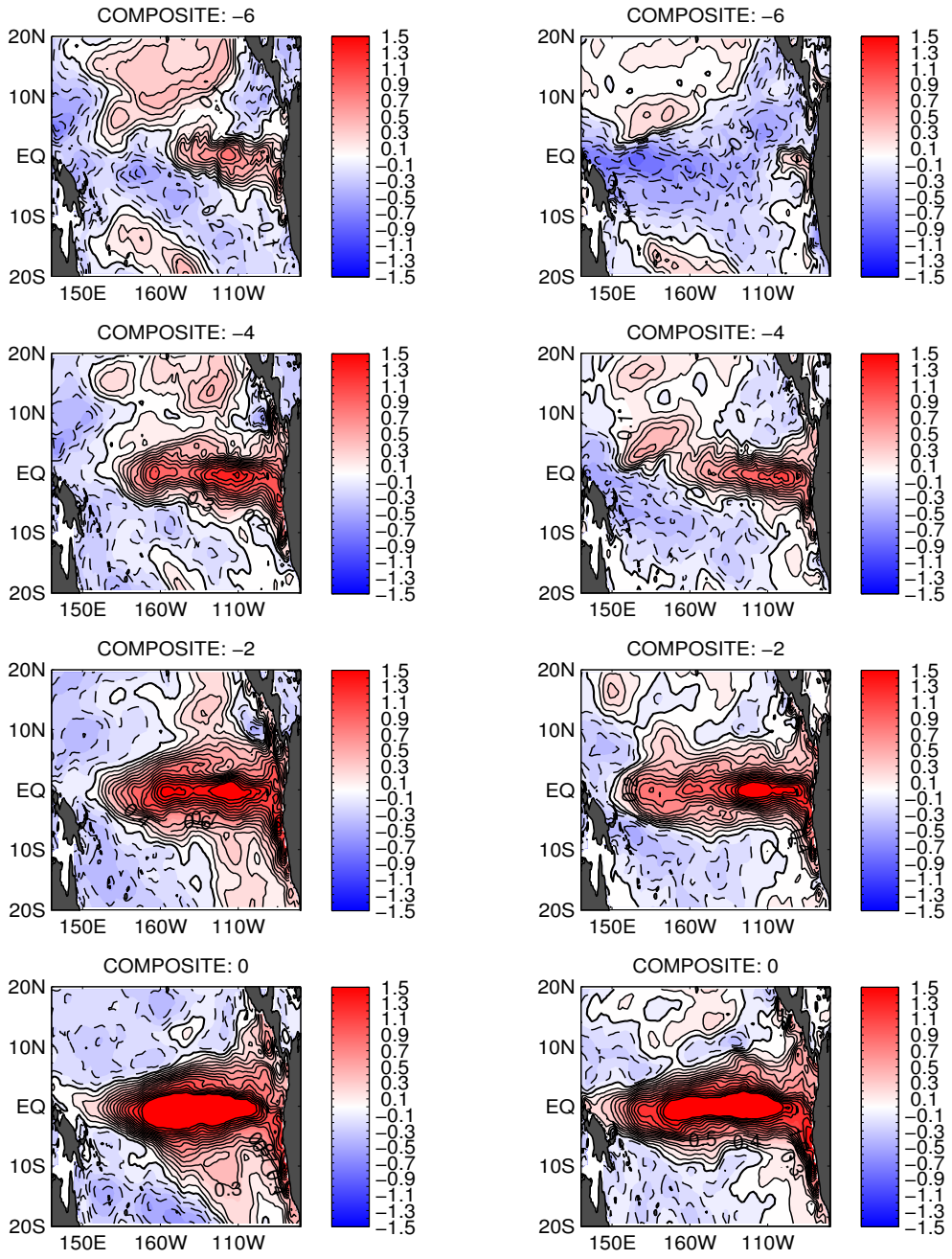

Figure 4.23 Composites of the El Niño event for trMOM3-CFE-NA (left-hand column) and trMOM3-SFE-NP (right-hand column).

D. Discussion

The modeling results presented here suggest that a substantially weakened AMOC can have significant impacts on both the mean climate conditions and also the climate variability over the tropical Atlantic and Pacific sectors. These impacts are achieved through a set of competing atmospheric and oceanic processes that tend to cancel out each other and thus giving rise to a tenuous and complex spatial formation of surface temperature response in the tropics. We argue that these modeling results can help us in interpreting the paleo proxy records during abrupt climate events, such as the Younger Dryas. In particular, we provide a dynamical explanation for the inconsistencies of surface temperature paleo reconstructions in the Southern Caribbean region. Our results suggest it is possible that the surface temperature change may have different signs within short spatial scales, as the published paleo records suggest. In general, a substantially weakened AMOC should produce surface cooling through atmospheric processes in much of the open ocean of the North Atlantic, except along the coast of northern South America and along the equatorial wave guide where surface warming may prevail due to the combined effects of subsurface ocean temperature change and upwelling. Faunal studies from the Colombian Basin (Kameo et al., 2004) and the Tobago Basin (Hüls and Zahn, 2000) do indeed suggest that a shallower thermocline existed in the southwestern Caribbean during glacial times due to increased coastal upwelling in this region. Therefore, whether a proxy reconstruction records a warming or a cooling response depends critically on whether the temperature change at the site is dominated by surface atmospheric processes or subsurface oceanic processes. Unfortunately, a direct comparison of the simulated and reconstructed temperature change would not be meaningful at this stage because 1) the current model resolutions are inadequate to fully resolve the complexity of bottom topography and coastline geometry in the Caribbean

region, and 2) past climatic boundary conditions should be used in order to fully simulate changes in past climatic events. Based on previous modeling studies (e.g., Chiang et al. 2003), we speculate that if Younger Dyras or glacial boundary conditions were used, the ice sheet build-up over the Northern Hemisphere would enhance surface cooling in the North Atlantic via atmospheric processes, acting to weaken the ocean-induced warming over the Caribbean.

The Mg/Ca-SST record from Lea et al. (2003) indicates a strong cooling in the Cariaco Basin of about 2-3°C at a time when the trMOM3-CFE-NA minus trMOM3-CE results indicate a strong subsurface warming at 10°N in the western tropical Atlantic (Figure 4.6b). Although this may appear as a discrepancy between the proxy data and our model results, the contradictory temperature trends can be explained by local dynamical responses within the Cariaco Basin. Today, the deepest sill in the Cariaco Basin is <146 m, restricting the horizontal flow of waters between the open Caribbean and the Basin. During the Younger Dryas, sea level was about 60 m lower, restricting mixing between the Cariaco Basin and the open Caribbean even further. The trMOM3-CFE-NA minus trMOM3-CE results clearly show that the subsurface warming is below 100 m at 10°N, with a maximum warming at about 300 m water depth (Figure 4.6b). Therefore, it is unlikely the subsurface warming in the Caribbean mixed into the isolated Cariaco Basin during the Younger Dryas. Although upwelling in the Cariaco Basin was enhanced during the Younger Dryas (Peterson et al., 2000; Haug et al., 2001), the source of the upwelled waters must have remained cold relative to the open Caribbean, resulting in the 2-3°C of cooling recorded in the Mg/Ca-SSTs (Lea et al., 2003).

Nevertheless, these modeling results suggest that a strong temperature gradient developed between the subtropical gyre and the western boundary current off the Venezuela and Guyana coast in response to reduced AMOC (Figure 4.5a). This region may be of particular importance in terms of understanding the temperature response of

the tropical Atlantic to AMOC changes, as much of the tropical Atlantic surface warming appears to originate in this region. The Caribbean SST change may be complicated by the competing physical processes and may vary from model to model as the relative strength of these processes may differ among models. For example, the water hosing experiments conducted with the GFDL CM2.1 model (Zhang, 2007) do not show the narrow strip of warm SST anomaly off the northern coast of South America, presumably because the simulated surface cooling is more dominant than the subsurface warming. The subsurface temperature warming along the gyre boundary, on the other hand, appears to be a common feature of many climate model water-hosing simulations (Stouffer et al, 2006). Zhang (2007) recently present observational evidence of an anti-correlated multidecadal variation of surface and subsurface temperature in the tropical North Atlantic that is consistent with AMOC-induced temperature changes in the coupled climate models.

Given the robust and unambiguous subsurface temperature change simulated by the models, it may be desirable to extend the paleo proxy reconstruction of temperature change to include the subsurface in this region. The only regional subsurface temperature record was generated by Rühlemann et al. (2004) using stable oxygen isotope values in benthic foraminiferal. These researchers estimated a rapid, 1-3^{o}C temperature increase at ~1300 m water depth in the Tobago Basin during the Younger Dryas, suggesting the magnitude of subsurface warming may have exceed that of the surface by as much as 2^{o}C at this location (Rühlemann et al., 1999). Clearly, an expanded proxy data base in this region can help address the importance of oceanic processes in abrupt climate change in the tropical Atlantic sector. Furthermore, climate models need to enhance spatial resolutions in simulations of past abrupt climate change events to fully resolve regional-scale circulation features and ocean-atmosphere interactions in the Caribbean and Western Tropical Atlantic.

We further propose that the similar set of competing oceanic and atmospheric processes can be applied to explain paleo-salinity reconstruction during the Youger Dryas. Our numerical experiments show that in North Tropical Atlantic, the oceanic advection tends to freshen the ocean surface by advecting fresh water input in the high latitude North Atlantic to the tropics. Meanwhile, the strengthening of the trades and the southward shift of the ITCZ tend to increase the surface salinity by enhancing the evaporation and reducing the precipitation in the region. We argue that it is the E-P change that dominates the surface salinity change in this region and is responsible for the SSS increase in paleo-salinity reconstruction.

The opposite occurs in the South Tropical Atlantic where the enhanced rainfall associated with the southward immigration of the ITCZ decreases the SSS, while the oceanic pathway change induced by the AMOC change acts to increase the SSS. The latter process operates in a manner similar to how surface warming occurs in the south equatorial Atlantic. The oceanic pathway change allows salty subtropical gyre water to enter the equatorial south Atlantic region, causing SSS increase in the region through upwelling. Our model experiments show that the oceanic process is more dominant and thus is responsible for the SSS increase in the South Tropical Atlantic. Together, these atmospheric and oceanic teleconnection processes explain the mono-pole like SSS response in the tropical Atlantic. The modeling results further suggest that the surface salinity change over the EEP region around Central America during the Younger Dryas can be attributed to two competing atmospheric processes. On one hand, the southward shift of the Atlantic ITCZ in response to the surface cooling in the North Atlantic tends to increase moisture transport across the Central America (Zaucker et al., 1994; Xie et al., 2008), resulting in an increase in precipitation in the region and thus an decrease in SSS. On the other hand, the surface cooling in the North Pacific tends to move the Pacific ITCZ southward, resulting in a decrease in the precipitation and increase in the SSS. The

net SSS change depends on the relative importance of these atmospheric processes.

Finally, we investigated the impact of the AMOC on tropical climate variability. The modeling results suggest that ENSO characteristics, including its amplitude, frequency and skewness, are significantly affected by AMOC-induced changes and the physical processes responsible for these changes are highly complex. For example, the surface cooling in the North Atlantic has a tendency to excite more El Niño events, enhancing positive skewness of ENSO. The surface cooling in the North Pacific has an opposite effect on ENSO, producing more La Niña events and moving the skewness towards negative direction. The combined effect of these surface coolings is to reduce ENSO variability, as the enhanced El Niño events in one case may cancel the enhanced La Niña events in the other case. These results suggest that climate change in the North Atlantic and North Pacific can potentially affect ENSO and other tropical climate variability. Detailed physical mechanisms, however, remains elusive and is beyond the scope of this dissertation.

The fact that AMOC-induced changes can affect Pacific climate variability through competing atmospheric and oceanic processes suggests that the results may be model dependent. Indeed, in an inter-model comparison study of coupled GCM hosing experiments (Stouffer et al. 2006), the impact of AMOC changes on Pacific climate varies considerably from model to model, despite the fact that the Atlantic response is consistent for most of the models. Therefore, it remains a challenge to pin down the effect of AMOC changes on ENSO event in climate model simulations. Observationally the challenge is even greater given the short observational records and difficulties in separating the influence of one ocean basin from another.

CHAPTER V
SUMMARY AND DISCUSSION

The overall goal of this dissertation is to shed light on the effect of the AMOC changes on tropical ocean-atmosphere coupled system and the physical processes that govern the influences, including the oceanic processes associated with AMOC changes and the atmospheric processes in response to the surface cooling in the North Atlantic and North Pacific. Two main numerical models are used: a global OGCM, MOM3, and a newly developed tropical regional coupled GCM, trMOM3-CCM3. In this section we summarize our findings and discuss some open issues that require further investigations in future studies.

A. Major Conclusions

Firstly, using the ocean-only global ocean model MOM3, an attempt was made to separate the total influence of various AMOC change scenarios into an oceanic-induced component and an atmospheric-induced component. Previous coupled climate model simulations suggest a dipole-like SST change with surface cooling over the North Atlantic and warming over the South Tropical Atlantic in response to a slow-down of the AMOC. This study, along with previous studies, shows that the cooling and warming of the Atlantic are governed by atmospheric and oceanic teleconnection mechanisms. The South Tropical Atlantic warming is mainly attributed to a set of oceanic mechanisms, including the Kelvin/Rossby wave adjustment mechanism and the oceanic gateway change mechanism proposed by Chang et al. (2008). A set of sensitivity experiments shows that the Kelvin/Rossby wave adjustment mechanism dominates the warming when the freshwater forcing is weak. The oceanic gateway change mechanism operates

in the regime where the freshwater forcing is strong, exceeding 0.3Sv. Strong AMOC change is required for the gateway mechanism to work because only when the AMOC is sufficiently weak, the North Brazil Undercurrent can flow equatorward, carrying warm and salty north Atlantic subtropical gyre water into the equatorial zone. This threshold is likely to be model-dependent. In contrast to coupled climate model water hosing simulations (Stouffer et al., 2006), the ocean-only model simulations presented here show no prominent SST changes in the Pacific Ocean and a surface warming, rather than surface cooling, in the tropical North Atlantic. It suggests that the surface SST changes in these regions are primarily attributed to atmospheric processes and the oceanic teleconnection mechanism dominates the SST change in the equatorial south Atlantic.

Second, a multidecadal AMOC oscillation is detected somewhat by surprise in the sensitivity experiments where the freshwater forcing strength is varied systematically. We found that the SST and SSS changes associated with north-south shifts of the Gulf Stream near its exit region appear to drive an AMOC oscillation when the freshwater forcing reaches a critical value of around 0.4Sv. In contrast to the multidecadal oscillation documented in previous CGCM studies (Delworth et al., 1993; Dong and Sutton, 2005; Dai et al., 2005), the AMOC oscillation in our simulations does not show a strong connection to temperature and salinity changes in the DWF regions that have been identified to be a key driving mechanism for the AMOC oscillations in the fully coupled models (e.g., Delworth et al., 1993). Instead, the AMOC oscillation in our ocean-only simulation appears to be associated with changes in the North Atlantic subtropical gyre circulation. Although a more detailed analysis of this oceanic mode of oscillation is required to further understand its physical mechanism and its relevance to reality, the possibility of the existence of a multi-decadal AMOC oscillation purely driven by oceanic processes is intriguing.

Third, a new regional coupled modeling tool consisting of an AGCM (CCM3) and a

tropical-channel OGCM (trMOM3) is developed to include the effects of atmospheric processes and ocean-atmosphere interactions in response to a weakening of the AMOC. Coupled model experiments reveal a competing role of atmospheric and oceanic teleconnection processes in the Atlantic sector. We propose that this competition between the atmospheric and oceanic influence can be applied to explain certain features of the reconstructed paleo-SST and paleo-SSS in the tropical Atlantic during the Younger Dryas. As paleo-records suggest, the SST changes over the southern Caribbean and the western Tropical Atlantic region during the Younger Dryas are complex. Despite the proximity of core locations, some proxy reconstructions record a surface cooling, while others indicate a warming. We suggest that this seemingly paradoxical finding may, at least partially, be attributed to the competing oceanic and atmospheric processes that result in opposing signs of temperature change in the region in response to a substantially weakened AMOC. Our coupled ocean-atmosphere model experiments indicate that the temperature response over the southern Caribbean and Western Tropical Atlantic regions can vary considerably in small spatial scales, depending on the nature of physical processes that dominate. The warming originated from the subtropical and tropical gyre boundary off northern South America can dominate the SST signal along the coastal zone, while away from the coastal zone the atmospheric process may be more dominant, giving rise to a broad surface cooling in much of the North Atlantic. Therefore, depending on the core locations, some of the cores may record coastal warming while others may record surface cooling in the ocean interior.

A similar argument can be applied to explain the reconstructed paleo-SSS changes during the Younger Dryas. In contrast to the SST dipole, the SSS change is characterized by a basin-wide increase of surface salinity in the tropical Atlantic. This response pattern could not be simply explained by the E-P change associated with a southward shift of the ITCZ, as it would give rise to a dipole-like SSS anomaly with a high SSS in the North

Tropical Atlantic and a low SSS in the South Tropical Atlantic. Our modeling results suggest that the monopole SSS response is attributed to the combined influence of the atmospheric and oceanic processes. In the North Tropical Atlantic, the E-P change generated by the atmospheric circulation change in response to the surface cooling in the North Atlantic dominates the SSS response. In the South Tropical Atlantic, the oceanic pathway change which allows the warm and salty subtropical gyre water to intrude the equatorial Atlantic thermocline layer and then upwell to the surface is mainly responsible for the SSS increase. Furthermore, the modeling results suggest that the AMOC-induced atmospheric circulation change can also have a significant influence on the SSS change in the EEP region. On one hand, the Atlantic ITCZ change in response to the surface cooling in the North Atlantic can increase the moisture transport across Central America, enhancing local precipitation and decreasing the SSS in the EEP region, as suggested by Zaucker et al. (1994) and Xie et al. (2008), while on the other hand, the surface cooling in the North Pacific in response to a weakening in the AMOC can move the Pacific ITCZ southward, resulting in an increase in SSS. These competing mechanisms for controlling the SSS change will be helpful to interpret paleo proxy records in this region.

Finally, we show that oceanic and atmospheric circulation changes in response to substantial AMOC changes can alter ENSO characteristics, including its amplitude, frequency and skewness. Overall, the effect of atmospheric processes on ENSO outweighs the effect of oceanic processes. However, the former has competing elements that can counteract each other. For example, the surface cooling in the North Atlantic tends to enhance El Niño events and thus increase the positive skewness, while the surface cooling in the North Pacific tends to enhance La Niña events and thus move the skewness towards negative. Therefore, how ENSO responds to a weakening of the AMOC depends on the relative strength and importance of these competing dynamical

elements, which makes the understanding of the associated dynamics difficult. This result may also explain why there is such a wide range of different ENSO responses in different coupled climate model hosing simulations (Timmermann et al., 2005; Dong et al., 2006; Dong et al., 2007).

B. Discussion and Future Work

The results of this investigation present a consistent picture of the tropical responses to the Northern Hemisphere cooling associated with a weakening of the AMOC. The results are also consistent with most paleoclimate proxy recoreds in this region, even though they do not completely resolve or explain the paleoclimate data, which is as much due to poor data coverage as to the modeling limitations. The other concern is that the model is forced with modern climatic boundary conditions when compared with paleo-observations during the Younger Dryas period. This inconsistency can be addressed by repeating the simulations with glacial boundary conditions. Based on previous modeling studies (Chiang et al., 2003), we speculate that if Younger Dryas or glacial boundary conditions were used, the ice sheet build-up over the Northern Hemisphere would enhance surface cooling in the North Atlantic via atmospheric processes, acting to weaken the ocean-induced warming over the Caribbean region. Further work is also needed to improve the realism of melt water input in the models. As mentioned in the previous sections, the crude representation of the freshwater forcing in the existing hosing simulations is likely to result in significant errors in the estimates of SSS changes in the North Atlantic Ocean, making it difficult to compare with paleo proxy records.

In terms of understanding the role of the oceans in climate, one important issue that deserves further investigation concerns the relationship between SST changes and

meridional heat transport. The meridional heat transport has been widely considered as one of the most important physical factors relating AMOC changes to SST changes. It is often stated (e.g., Zhang and Delworth, 2005) that as the AMOC slows down, the northward meridional heat transport decreases, which causes cooling in the North Atlantic and warming in the South Atlantic. It implies that the reduction in the meridional heat transport alone should produce a dipole-like SST response in the tropical Atlantic, causing a southward shift of the ITCZ. The modeling results presented in this study contradict this argument. By forcing the coupled model with AMOC changes along the open boundaries, the model responds with a basin wide warming without changes in cross-equatorial SST gradient. Figure 5.1 shows the meridional heat transport in the model run of trMOM3-CE and trMOM3-BFE. Clearly, the net heat transport is decreased by as much as 0.5 PW, but the decrease occurs at every latitude within the tropical basin, resulting in little change in the heat transport divergence. Therefore, no significant temperature changes are produced by the change in the meridional heat transport. Instead, the basin wide warming is attributed to the Kelvin/Rossby wave adjustment and oceanic pathway change mechanisms as discussed in the previous section. The extent to which the meridional heat transport change can cause SST changes in reality needs to be carefully examined.

Finally, further studies are clearly needed to understand fully the effect of the AMOC on ENSO. While previous studies suggest that AMOC changes can influence ENSO either through its effect on the tropical annual cycle or on the mean climate of the tropical coupled system, this study suggests that its effect on ENSO appears to be felt through the changes in extratropical atmospheric variability. We hypothesize that the AMOC-induced surface cooling in the extratropical North Atlantic and North Pacific affects the internal atmospheric variability, which exerts an influence on ENSO via the Pacific meridional mode as proposed by Chiang and Vimont (2004), Chang et al. (2007),

Zhang et al. (2009) and Alexander et al. (2009). More in-depth analysis is needed to test the validity of this hypothesis.

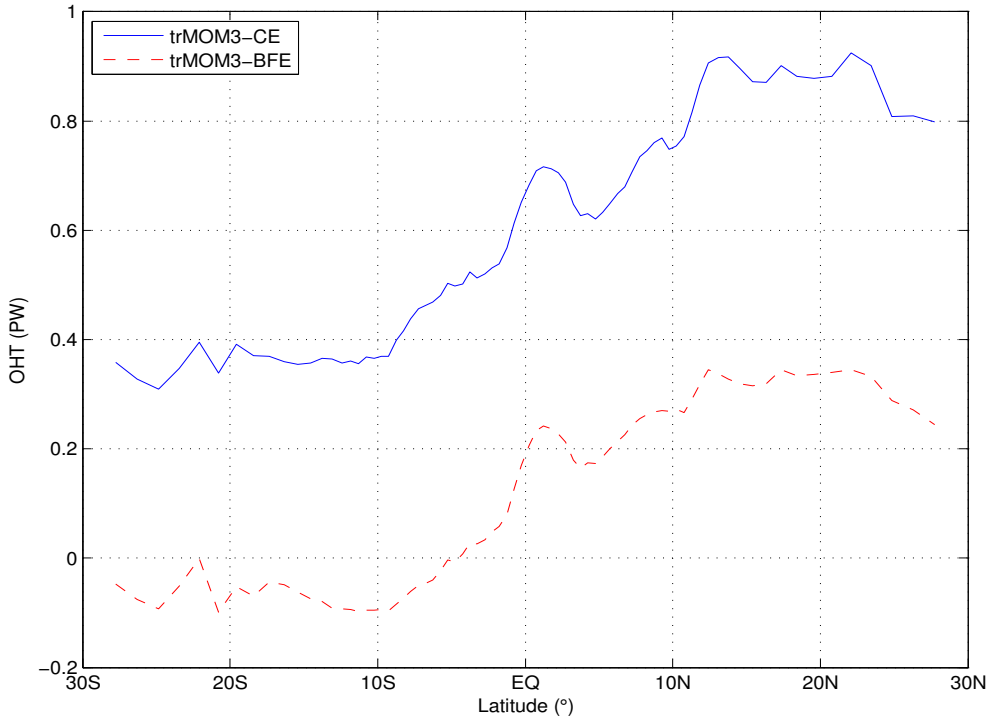

Figure 5.1 Annual mean Atlantic meridional ocean heat transport in the model runs of trMOM3-CE and trMOM3-BFE. Here, 1 PW = 10^{15} W.

REFERENCES

Alexander, M. A., D. J. Vimont, P. Chang and J. D. Scott, 2009: The impact of extratropical atmospheric variability on ENSO: Testing the seasonal footprinting mechanism using coupled model experiments. *J. Climate,* Submitted.

Altabet, M. A., M. J. Higginson, and D. W. Murray, 2002: The effect of millennial-scale changes in Arabian Sea denitrification on atmospheric CO_2. *Nature*, **415,** 159-162.

Ammann B., U. Eicher, M.J. Gaiullard, W. Haeberli, G. Lister, A.F. Lotter, M. Maisch, F. Niessen, C.H., Schluchter, and B. Wolfarth, 1994: The Wurmian late-glacial in lowland Switzerland. *J. Quaternary Sci.*, **9,** 119-127.

An, S.-I., and F.-F. Jin, 2004: Nonlinearity and asymmetry of ENSO. *J. Climate*, **17,** 2399-2412.

Arz H.W., J. Pätzold, and G. Wefer, 1999: The deglacial history of the western tropical Atlantic as inferred from high resolution stable isotope records off northeastern Brazil. *Earth Planet. Sci. Lett.,* **167,** 105–117.

Bard E., F. Rostek, J.-L. Turon, and S. Gendreau, 2000: Hydrological impact of Heinrich events in the subtropical northeast Atlantic. *Science*, **289,** 1321-1324.

Barreiro, M., A. Fedorov, R. Pacanowski, and S.G. Philander, 2008: Abrupt climate changes: how freshening of the northern Atlantic affects the thermohaline and wind-driven oceanic circulations. *Annu. Rev. Earth Planet. Sci*., **36,** 33-58.

Belkin, I. M., S. Levitus, J. Antonov, and S.-A. Malmberg, 1998: "Great salinity anomalies" in the North Atlantic. *Prog. Oceanogr.*, **41**, 1–68.

Benway, H. M., A. C. Mix, B. A. Haley, and G. P. Klinkhammer, 2006: Eastern Pacific Warm Pool paleosalinity and climate variability: 0-30 kyr. *Paleoceanography*, **21,** doi:10.1029/2005PA001208.

Boccaletti, G., R. Ferrari, A. Adcroft, D. Ferreira, and J. Marshall, 2005: The vertical

structure of ocean heat transport. *Geophys. Res. Lett.,* **32,** L10603, doi:10.1029/2005GL022474.

Boyle E. A., 2000: Is ocean thermohaline circulation linked to abrupt stadial/interstadial transitions? *Quat. Sci. Rev*., **19,** 255-272.

Brix, H., and R. Gerdes, 2003: North Atlantic deep water and Antarctic bottom water: Their interaction and influence on the variability of the global ocean circulation. *J. Geophys. Res.*, **108(C2),** 3022, doi:10.1029/2002JC001335.

Bryden, H.L., H. R. Longworth, and S. A. Cunningham, 2005: Slowing of the Atlantic meridional overturning circulation at 25°N. *Nature*, **438,** 655-657.

Capotondi, A., and W. R. Holland, 1997: Decadal variability in an idealized ocean model and its sensitivity to surface boundary conditions. *J. Phys. Oceanogr*., **27,** 1072-1093.

Carlson, A. E., D. W. Oppo, R. E. Came, A. N. Legrande, L. D. Keigwin, and W. B. Curry, 2008: Subtropical Atlantic salinity variability and Atlantic meridional circulation during the last deglaciation. *Geology*, **36,** 991-994, doi:10.1130/G25080A.1.

Cessi, P., K. Bryan, and R. Zhang, 2004: Global seiching of thermocline waters between the Atlantic and the Indian-Pacific Ocean basins. *Geophys. Res. Lett.,* **31,** L04302, doi:10.1029/2003GL019091.

Chang, P., and Coauthors, 2006: Climate fluctuations of tropical coupled system – The role of ocean dynamics. *J. Climate*, **19,** 5122-5174.

Chang, P., L. Ji, and H. Li, 1997: A decadal climate variation in the tropical Atlantic Ocean from thermodynamic air-sea interactions. *Nature*, **385,** 516-518.

Chang, P., R. Zhang, W. Hazeleger, C. Wen, X. Wan, L. Ji, R. J. Haarsma, W.-P. Breugem, and H. Seidel, 2008: Oceanic link between abrupt changes in the North Atlantic Ocean and the African monsoon. *Nature Geosci.*, **1,** 444-448,

doi:10.1038/ngeo218.

Chang, P., L. Zhang, R. Saravanan, D. J. Vimont, J. C. H. Chiang, L. Ji, H. Seidel, and M. K. Tippett, 2007: Pacific meridional mode and El Niño—Southern Oscillation, *Geophys. Res. Lett*., **34,** L16608, doi:10.1029/2007GL030302.

Cheng, W., R. Bleck, and C. Rooth, 2004: Multi-decadal thermohaline variability in an ocean-atmosphere general circulation model. *Climate Dyn.*, **22,** 573-590.

Chiang, J.C.H., M. Biasutti and D. S. Battisti, 2003: Sensitivity of the Atlantic ITCZ to Last Glacial Maximum boundary conditions. *Paleoceanograaphy*, **18,** doi:10.1029/2003PA000916.

Chiang, J.C.H., and C. Bitz, 2005: Influence of high latitude ice cover on the marine intertropical convergence zone. *Climate Dyn.,* **25,** 477-496.

Chiang, J.C.H., W. Cheng, and C. M. Bitz, 2008: Teleconnection mechanism to the tropical Atlantic sector from Atlantic thermohaline adjustment. *Geophys. Res. Lett.*, **35,** L07704.

Chiang, J.C.H., and D. J. Vimont, 2004: Analogous Pacific and Atlantic meridional modes of tropical atmosphere-ocean variability, *J. Climate*, **17,** 4143–4158.

Church, J. A., 2007: A change in circulation? *Science*, **317,** 908-909.

Clark, P. U., A. M. McCabe, A. C. Mix, and A. J. Weaver, 2004: Rapid rise of sea level 19,000 years ago and its global implications. *Science*, **304,** 1141-1144.

Clark, P. U., N. G. Pisias, T. F. Stocker, and A. J. Weaver, 2002: The role of the thermohaline circulation in abrupt climate change, *Nature*, **415,** 863-869.

Colin de Verdiere, A., and T. Huck, 1999: Baroclinic instability: An oceanic wavemaker for interdecadal variability. *J. Phys. Oceanogr.,* **29,** 893-910.

Collins, M., S. F. B. Tett, and C. Cooper, 2001: The internal climate variability of HadCM3, a version of the Hadley Centre coupled model without flux adjustments. *Climate Dyn*., **17,** 61-81.

Cunningham, S.A., and Coauthors, 2007: Temporal variability of the Atlantic meridional overturning circulation at 26.5°N. *Science*, **317,** 935-938.

Curry, R., B. Dickson, and I. Yashayaev, 2003: A change in the freshwater balance of the Atlantic Ocean over the past four decades. *Nature*, **426,** 826–829.

Curry, R. and C. Mauritzen, 2005: Dilution of the northern North Atlantic ocean in recent decades. *Science*, **308,** 1772-1774.

Dahl, K. A., A. J. Broccoli, and R. J. Stouffer, 2005: Assessing the role of North Atlantic freshwater forcing in millennial scale climate variability: A tropical Atlantic perspective. *Climate Dyn.*, **24,** 325-346.

Dai, A., A. Hu, G. A. Meehl, W. M. Washington and W. G. Strand, 2005: Atlantic thermohaline circulation in a coupled general circulation model: Unforced variations versus forced changes. *J. Climate*, **18,** 3270-3293.

Danabasoglu, G, 2008: On multi-decadal variability of the Atlantic meridional overturning circulation in the community climate system model version 3 (CCSM3). *J. Climate*, DOI:10.1175/2008JCLI2019.1.

deBeaulieu J-L., V. Andrieu, J. J. Lowe, P. Ponel, and M. Reille, 1994: The Weichselian late-glacial in southwestern Europe Iberian Peninsula, Pyrenees, Massif Central, Northern Appenines. *J. Quaternary Sci.*, **9,** 101-108.

Delworth, T. L., and R. J. Greatbatch, 2000: Multidecadal thermohaline circulation variability in the Northern Hemisphere. *Climate Dyn.*, **16,** 661-676.

Delworth, T. L., S. Manabe, and R. J. Stouffer, 1993: Interdecadal variations of the thermohaline circulation in a coupled ocean-atmosphere model. *J. Climate*, **6,** 1993-2011.

Delworth, T. L., S. Manabe, and R. J. Stouffer, 1997: Multidecadal climate variability in the Greenland Sea and surrounding regions: A coupled model simulation. *Geophys. Res. Lett*., **24,** 257-260.

Delworth, T. L., and M. Mann, 2000: Observed and simulated multidecadal variability in the Northern Hemisphere. *Climate Dyn.,* **16,** 661-676.

Dickson, B., I. Yashayaev, J. Meincke, B. Turrell, S. Dye, and J. Holfort, 2002: Rapid freshening of the deep North Atlantic ocean over the past four decades. *Nature*, **416,** 832-837.

Dickson, R. R., J. Meincke, S. A. Malmberg, and A. J. Lee, 1988: The "great salinity anomaly" in the northern North Atlantic 1968-1982. *Prog. Oceanogr.,* **20,** 103-151.

Dong, B.-W., R. T. Sutton, and A. A. Scaife, 2006: Multidecadal modulation of El Niño-Southern Oscillation (ENSO) variance by Atlantic Ocean sea surface temperature. *Geophys. Res. Lett.*, **33,** L08705, doi: 10.1029/2006GL025766.

Dong, B.-W., and R. T. Sutton, 2002: Adjustment of the coupled ocean-atmosphere system to a sudden change in the thermohaline circulation. *Geophys. Res. Lett.*, **29(15),** 1728, doi:10.1029/2002GL0l5229.

Dong, B.-W., and R. T. Sutton, 2007: Enhancement of ENSO variability by a weakened Atlantic thermohaline circulation in a coupled GCM. *J. Climate*, **20,** 4920-4939.

Enfield, D. B., A. M. Mestas-Nuñez, and P. J. Trimble (2001), The Atlantic multidecadal oscillation and its relation to rainfall and river flows in the ontinental U.S., *Geophys. Res. Lett.*, **28,** 2077 – 2080.

Fratantoni, D. M., W. E. Johns, T. L. Townsend, and H. E. Hurlburt, 2000: Low-latitude circulation and mass transport pathways in a model of the tropical Atlantic Ocean. *J. Phys. Oceanogr.*, **30,** 1944-1966.

Fukumori, I., T. Lee, B. Cheng, and D. Menemnlis, 2004: The origin, pathway, and destination of Niño-3 water estimated by a simulated passive tracer and its adjoint. *J. Phys. Oceanogr.*, **34,** 582-604.

Gent, P. R., and J. C. McWilliams, 1990: Isopycnal mixing in ocean circulation models. *J. Phys. Oceanogr.*, **20,** 150-155.

Greatbatch, R. J., and S. Zhang, 1995: An interdecadal oscillation in an idealized ocean basin forced by constant heat flux. *J. Climate*, **8,** 81-91.

Gu, D., and S.G.H. Philander, 1995: Secular changes of annual and interanuual variability in the Tropics during the past century. *J. Climate*, **8,** 864-876.

Gu, D., and S.G.H. Philander, 1997: Interdecadal climate flunctuations that depend on exchanges between the tropics and extratropics. *Science*, **275,** 805-807.

Guilderson T. P., R. G. Fairbanks, and J. L. Rubenstone, 2001: Tropical Atlantic coral oxygen isotopes: Glacial-interglacial sea surface temperatures and climate change. *Marine Geology*, **172,** 75-89.

Guilyardi, E., 2006: El Niño-mean state-seasonal cycle interactions in a multi-model ensemble. *Climate Dyn*., **29,** 329-348.

Haarsma, R, E. Campos, W. Hazeleger, and C. Severijns, 2008: Influence of the meridional overturning circulation on tropical Atlantic climate and variability. *J. Climate*, **21,** 1403-1416.

Häkkinen, S., and P. B. Rhines, 2004: Decline of subpolar North Atlantic circulation during the 1990s. *Science*, **304,** 555–559.

Hansen, B., W. R. Turrell, and S. Osterhus, 2001: Decreasing overflow from the Nordic seas into the Atlantic Ocean through the Faroe Bank channel since 1950. *Nature*, **411,** 927–930.

Harper, S., 2000: Thermocline ventilation and pathways of tropical-subtropical water mass exchange. *Tellus*, **52A,** 330-345.

Haug, G. H., and Coauthors, 2001: Southward migration of the Intertropical Convergence Zone through the Holocene. *Science*, **293,** 304-1308.

Hazeleger, W. and S. Drijfhout, 2006: Subtropical cells and meridional overturning circulation pathways in the tropical Atlantic. *J. Geophys. Res*., **111,** 3013–3025.

Herbert, T. D., and J. D. Schuffert, 2000: Alkenone unsaturation estimates of sea-surface

temperatures at ODP Site 1002 over a full glacial cycle [online], *Proc. Ocean Drill. Program Sci. Results* (edited by R.M. Leckie et al.), **165,** 239-247. (Available at http://www-odp.tamu.edu/publications/165_SR/chap_16/ chap_16.htm).

Huang, B., and Z. Liu, 1999: Pacific subtropical-tropical thermocline water exchange in the National Centers for Environmental Prediction ocean model. *J. Geophys. Res.*, **104,** 11065-11076.

Hubeny, J. B., J. W. King and A. Santos, 2006: Subdecadal to multidecadal cycles of Late Holocene North Atlantic climate variability preserved by estuarine fossil pigments. *Geology*, **34,** 569-572.

Hughen, K., and Coauthors, 2004: ^{14}C activity and global carbon cycle changes over the past 50000 years. *Science*, **303,** 202-207.

Hüls M. and Zahn R., 2000: Millennial-scale sea surface temperature variability in the western tropical North Atlantic from planktonic foraminiferal census counts. *Paleoceanography*, **15,** 659-678.

Jaeschke, A., C. Rühlemann, H. Arz, G. Heil, and G. Lohmann, 2007: Coupling of millennial-scale changes in sea surface temperature and precipitation off northeastern Brazil with high-latitude climate shifts during the last glacial period, *Paleoceanography*, **22,** PA4206, doi:10.1029/2006PA001391.

Jin F.-F., S.-I. An, A. Timmermann, and J. Zhao, 2003: Strong El Niño events and nonlinear dynamical heating. *Geophys. Res. Lett*., **30,** 1120, doi:10.1029/ 2002GL016356.

Johnson, G. C., and M. J. McPhaden, 1999: Interior pycnocline flow from the subtropical to the equatorial Pacific Ocean. *J. Phys. Oceanogr.*, **32,** 1121-1132.

Johnson, H. L., and D. P. Marshall, 2002: A theory for the surface Atlantic response to thermohaline variability. *J. Phys. Oceanogr.,* **32,** 1121-1132.

Jungclaus, J. H., H. Haak, M. Latif, and U. Mikolajewicz, 2005: Arctic-North Atlantic

interactions and multidecadal variability of the meridional overturning circulation. *J. Climate*, **18,** 4013-4031.

Kameo K., M. C. Shearer, A. W. Droxler, I. Mita, R. Watanabe and T. Sato, 2004: Glacial-interglacial surface water variations in the Caribbean Sea during the last 300 ky based on calcareous nannofossil analysis. *Palaeogeog., Palaeoclimatol., Palaeoecol.*, **212,** 65–76.

Kanzow, T., and Coauthors, 2007: Observed flow compensation associated with the MOC at 26.5°N in the Atlantic. *Science*, **317,** 938-941.

Kerr, R. A., 2000: A North Atlantic climate pacemaker for the centuries. *Science*, **288,** 1984–1985.

Kiehl, J. T., J. J. Hack, G. Bonan, B. A. Boville, D. Williamson, and P. Rasch, 1998: The National Center for Atmospheric Research Community Climate Model: CCM3. *J. Climate*, **11,** 1131-1149.

Kirtman, B. P., Y. Fan, and E. K. Schneider, 2002: The COLA global coupled and anomaly coupled ocean-atmosphere GCM, *J. Climate*, **15,** 2301-2320.

Kitoh, A., and S. Murakami, 2002: Tropical Pacific climate at the mid-Holocene and the Last Glacial Maximum simulated by a coupled ocean-atmosphere general circulation model, *Paleoceaograhy*, **17,** 1047, doi:10.1029/2001PA000724.

Kleeman, R., J. P. McCreary, Jr., and B. A. Klinger, 1999: A mechanism for generating ENSO decadal variability. *Geophys. Res. Lett.*, **26,** 1743-1746.

Knight, J. R., R. J. Allan, C. K. Folland, and M. Vellinga, 2003: Quasi-periodic natural variations in the thermohaline circulation and climate in a 1400 year coupled model calculation. Preprints, *14th Symp. on Global Change and Climate Variations*, Long Beach, CA, Amer. Meteor. Soc., CD-ROM, P13.11.

Knutti, R., J. Fluckiger, T. F. Stocker, and A. Timmermann, 2004: Strong hemispheric coupling of glacial climate through freshwater discharge and ocean circulation.

Nature, **430,** 851-856.

Koutavas, A., J. Lynch-Stieglitz, T. M. Marchitto Jr., and J. P. Sachs, 2002: El Niño-like pattern in ice age tropical Pacific sea surface temperature. *Science*, **297,** 226-230.

Kroon D., W. E. N. Austin, M. R. Chapman, and G. M. Ganssen, 1997: Deglacial surface circulation changes in the northeastern Atlantic: temperature and salinity records off NW Scotland on a century scale. *Paleoceanography*, **12(6),** 755-763.

Kushnir, Y., 1994: Interdecadal variations in North Atlantic sea surface temperature and associated atmospheric conditions. *J. Phys. Oceanogr.,* **7,** 141-157.

Large, W. G., J. C. McWilliams, and S. C. Doney, 1994: Oceanic vertical mixing: A review and a model with a nonlocal boundary layer parameterization. *Rev. Geophys.*, **32,** 363-403.

Latif, M., and Coauthors, 2006: Is the thermohaline circulation changing? *J. Climate*, **19,** 4631-4637.

Lea D. W., D. K. Pak, L. C. Peterson, K. A. Hughen, 2003: Synchroneity of tropical and high-latitude Atlantic temperatures over the last glacial termination. *Science*, **301,** 1361-1364.

Leduc, G., L. Vidal, K. Tachikawa, F. Rostek, C. Sonzogni, L. Beaufort, and E. Bard, 2007: Mositure transport across Central America as a positive feedback on abrupt climatic changes. *Nature*, **445,** 908-911.

Liu, Z., S.G.H. Philander, and P. C. Pacanowski, 1994: A GCM study of tropical-subtropical upper-ocean water exchange. *J. Phys. Oceanogr*., **24,** 2606-2623.

Lu, P., J. P. McCreary, and B. A. Klinger, 1998: Meridional circulation cells and the source waters of the Pacific equatorial undercurrent. *J. Phys. Oceanogr.*, **28,** 62-84.

Luyten, J.R., J. Pedlosky, and H. Stommel, 1983: The ventilated thermocline. *J. Phys. Oceanogr.*, **13,** 292-309.

Malanotte-Rizzoli, P., K. Hedstrom, H. Arango, and D. B. Haidvogel, 2000: Water mass

pathways between the subtropical and tropical ocean in a climatological simulation of the North Atlantic Ocean circulation. *Dyn. Atmos. Ocean.*, **32,** 331-371.

Manabe, S., R. J. Stouffer, M. J. Spelman, and K. Bryan, 1991: Transient response of a coupled ocean-atmosphere model to gradual changes of atmospheric CO2. Part I: Annual mean response. *J. Climate*, **4,** 785-818.

Marsh, R., 2000: Recent variability of the North Atlantic thermohaline circulation inferred from surface heat and freshwater fluxes. *J. Climate*, **13,** 3239–3260.

Matei, D., N. Keenlyside, M. Latiff, and J. Jungclaus, 2008: Subtropical forcing of tropical Pacific climate and Decadal ENSO modulation. *J. Climate*, **21,** 4691-4709.

McCreary, J. P., Jr., and P. Lu, 1994: Interaction between the subtropical and equatorial ocean circulations: The subtropical cell. *J. Phys. Oceanogr.*, **24,** 466-497.

McManus, J. F., R. Francois, J.-M. Gherardl, L. D. Keigwin and S. Brown-leger, 2004: Collapse and rapid resumption of Atlantic meridional circulation linked to deglacial climate changes. *Nature*, **428,** 834-837.

McPhaden, M. J., and D. Zhang, 2002: Slowdown of the meridional overturning circulation in the upper Pacific Ocean. *Nature*, **415,** 603-608.

Moron V., R. Vautard and M. Ghil, 1998: Trends, interdecadal and interannual oscillations in global sea-surface temperature. *Climate Dyn.*, **14,** 545-569.

Mulitza S., and C. Rühlemann, 2000: African monsoonal precipitation modulated by interhemispheric temperature gradients. *Quaternary Res*. **53,** 270–274.

Neelin, J. D., and W. Weng, 1999: Analytical prototypes for ocean-atmosphere interaction at midlatitudes. Part I: Coupled feedbacks as a sea surface temperature dependent stochastic process. *J. Climate,* **12,** 697-721.

Oppo, D. W., G. A. Schmidt, and A. N. LeGrande, 2007: Seawater isotape constraints on tropical hydrology during the Holocene. *Geophys. Res. Lett*., **34,** L13701, doi:10.1029/2007GL030017.

Pacanowski, R.C., and S. M. Griffies, 1999: MOM 3.0 manual. NOAA/Geophysical Fluid Dynamics Laboratory, Princeton, NJ., pp668.

Pedlosky, J., 1987: An inertial theory of the equatorial undercurrent. *J. Phy. Oceanogr.*, **17,** 1978-1985.

Peterson, L.C., G. H. Haug, K. A. Hughen and U. Röhl, 2000: Rapid changes in the hydrological cycle of the tropical Atlantic during the last glacial. *Science*, **290,** 1947-1951.

Piotrowski, A. M., S.L. Goldstein, S.R. Hemming and R.G. Fairbanks, 2005: Temporal relationships of carbon cycling and ocean circulation at glacial boundaries. *Science,* **307,** 1933-1938.

Redi, M. H., 1982: Oceanic isopycnal mixing by coordinate rotation. *J. Phys. Oceanogr.*, **12,** 1155-1158.

Rothstein, L. M., R.-H. Zhang, A. J. Busalacchi, and D. Chen, 1998: A numerical simulation of the mean water pathways in the subtropical and tropical Pacific Ocean. *J. Phys. Oceanogr.*, **28,** 322-342.

Roulston, M. S., and J. D. Neelin, 2000: The response of an ENSO model to climate noise, weather noise and intraseasonal forcing. *Geophys. Res. Lett.,* **27,** 3723-3726.

Rühlemann, C, S. Mulitza, G. Lohmann, A. Paul, M. Prange, and G. Wefer, 2004: Intermediate-depth warming in the tropical Atlantic related to weakened thermohaline circulation: combining paleoclimate and modeling data for the last deglaciation. *Paleoceanography*, **19,** Doi:1029/2003PA0000948.

Rühlemann, C., S. Mulitza, P. J. Muller, G. Wefer, and R. Zahn, 1999: Warming of the tropical Atlantic Ocean and slowdown of the thermohaline circulation during the last deglaciation. *Nature*, **402,** 511-514.

Saravanan, R., and J. C. McWilliams, 1997: Stochasticity and spatial resonance in inter-decadal climate fluctuations. *J. Climate*, **10,** 2299-2320.

Saravanan, R., G. Danabasoglu, S. C. Doney, and J. C. McWilliams, 2000: Decadal variability and predictability in the midlatitude ocean-atmosphere system. *J. Climate*, **13,** 1073-1097.

Schmidt, M. W., H. J. Spero and D. W. Lea, 2004: Links between salinity variation in the Caribbean and north Atlantic thermohaline circulation. *Nature*, **428,** 160-163.

Schneider, E. K., and Coauthors, 1997: Annual cycle and ENSO in a coupled ocean-atmosphere general circulation model. *Mon. Wea. Rev*., **125,** 680-702.

Smagorinsky, J., 1963: General circulation experiments with the primitive equations. I. The basic experiment. *Mon. Wea. Rev.*, **91,** 99-164.

Smith, T. M., and R. W. Reynolds, 2003: Extended reconstruction of global sea surface temperatures based on COADS Data (1854-1997). *J. Climate*, **16,** 1495-1510.

Smith, T. M., and R. W. Reynolds, 2004: Improved extended reconstruction of SST (1854-1997). *J. Climate,* **17,** 2466-2477.

Smith, T. M., R. W. Reynolds, T. C. Peterson, and J. Lawrimore, 2008: Improvements to NOAA's historical merged land-ocean surface temperature analysis (1880-2006). *J. Climate,* **21,** 2283-2296.

Stott, L., C. Poulsen, S. Lund and R. Thunell, 2002: Super ENSO and global climate oscillations at millennial time scales. *Science*, **297,** 222-226.

Stouffer, R. J., and Coauthors, 2006: Investigating the causes of the response of the thermohaline circulation to past and future climate change. *J. Climate*, **19,** 1365-1387.

Sun, D. Z., T. Zhang, and S.-Z. Shin, 2004: The effect of subtropical cooling on the amplitude of ENSO: A numerical study. *J. Climate*, **17,** 3786-3798.

Te Raa, L. A., and H. A. Dijkstra, 2002: Instability of the thermohaline ocean circulation on interdecadal timescales. *J. Phys. Oceanogr.*, **32,** 138-160.

Tedesco, K., and R. Thunell, 2003: High resolution tropical climate record for the last

6,000 years. *Geophys. Res. Lett.,* **30(17),** 1891, doi:10.1029/2003GL017959.

Thompson, L. G., E. Mosley-Thompson, M. E. Davis, P.-N. Lin, K. A. Henderson, J. Cole-Dai, J. F. Bolzan, K. B. Liu, 1995: Late glacial stage and Holocene tropical ice core records from Huascarán, Peru. *Science*, **269,** 46-50.

Timmermann, A., 2003: Decadal ENSO amplitude modulations: A nonlinear paradigm. *Global Planet. Change*, **37,** 135-156.

Timmermann, A., S.-I. An, U. Krebs, and H. Goosse, 2005: ENSO suppression due to weakening of the North Atlantic thermohaline circulation. *J. Climate*, **18,** 3122-3139.

Timmermann, A., M. Latif, R. Voss, and A. Grotzner, 1998: Northern Hemispheric interdecadal variability: A coupled air-sea mode. *J. Climate*, **11,** 1906-1931.

Tourre, Y. M., Rajagopalan and Kushnir Y., 1999: Dominant patterns of climate variability in the Atlantic Ocean during the last 136 years. *J. Climate*, **12,** 2285-2299.

Toggweiler, J. R., and B. Samuels, 1995: Effects of Drake Passage on the global thermohaline circulation. *Deep-Sea Res.*, **42(4),** 477-500.

Tziperman, E., M. A. Cane, S. E. Zebiak, Y. Xue, and B. Blumenthal, 1998: Locking of El Niño's peak time to the end of the calendar year in the delayed oscillator picture of ENSO. *J. Climate*, **11,** 2191-2199.

Vellinga, M. and R. A. Wood, 2002: Global climatic impacts of a collapse of the Atlantic thermohaline circulation, *Climate Change*, **54,** 251-267.

Vimont, D. J., J. M. Wallace, and D. S. Battisti, 2003: The seasonal footprinting mechanism in the Pacific: Implications for ENSO. *J. Climate*, **16,** 2668-2675.

Walker, M.J.C., S.J.P Bohncke, G. R. Coope, M. O'Connell, H. Usinger, and C. Verbruggen, 1994: The devensian/Weichselian late-glacial in northwest Europe (Ireland, Britain, north Belgium, the Netherlands, northwest Germany). *J.*

Quaternary Sci., **9,** 109-118.

Wang, Y. J., H. Cheng, R. L. Edwards, Z. S. An, J. Y. Wu, C.-C. Shen, and J. A. Dorale, 2001: A high-resolution absolute-dated late Pleistocene monsoon record from Hulu cave, China. *Science*, **294,** 2345-2348.

Weaver, A. J., and E. S. Sarachik, 1991: Evidence for decadal variability in an ocean general circulation model: An advective mechanism. *Atmosphere-Ocean*, **29,** 197-231.

Weijers J.W.H, E. Schefuß, S. Schouten, and J.S.S. Damsté, 2007: Coupled thermal and hydrological evolution of tropical Africa over the last deglaciation. *Science*, **315,** 1701-1704.

Wen, C., P. Chang, and R. Saravanan, 2009: Effect of Atlantic meridional overturning circulation changes on tropical Atlantic sea-surface temperature variability: A 2-1/2 layer reduced gravity ocean model study. *J. Climate,* submitted.

Weldeab S., R. R. Schneider and M. Köllinga, 2006: Deglacial sea surface temperature and salinity increase in the western tropical Atlantic in synchrony with high latitude climate instabilities. *Earth Planet. Sci. Lett.*, **241,** 699-706.

Wu, L., F. He, Z. Liu, and C. Li, 2007: Atmospheric teleconnections of tropical Atlantic variability: Interhemispheric, tropical-extratropical, and cross-basin interactions. *J. Climate*, **20,** 856-870.

Wu, L., Z. Liu, R. Gallimore, R. Jacob, O. Lee, and Y. Zhang, 2003: Pacific decadal variability: The tropical Pacific mode and the north Pacific mode. *J. Climate*, **16,** 1101-1119.

Xie, S.-P., and S. G. H. Philander, 1994: A coupled ocean-atmosphere model of relevance to the ITCZ in the eastern Pacific. *Tellus*, **46A,** 340-350.

Xie, S.-P., Y. Okumura, T. Miyama, and A. Timmermann, 2008: Influence of Atlantic climate change on the tropical Pacific via the Central American Isthmus. *J. Climate*,

21, 3914-3928.

Yang, J., 1999: A linkage for decadal climate variations in the Labrador Sea and the tropical Atlantic Ocean. *Geophys. Res. Lett.*, **30,** 1070-1073.

Yeh, S. W., J. G. Jhun, I. S. Kang, and B. P. Kirtman, 2004: The decadal ENSO variability in a hybrid coupled model. *J. Climate*, **17,** 1225-1238.

Zaucker, F., T. F. Stocker, and W. S. Broecker, 1994: Atmospheric freshwater fluxes and their effect on the global thermohaline circulation. *J. Geophys. Res.,* **99,** 12443-2457.

Zhang, L., P. Chang, and M. K. Tippett, 2009: Linking the Pacific Meridional Mode to ENSO: Utilization of a noise filter, *J. Climate,* **22(4),** 905.

Zhang, R., 2007: Anticorrelated multidecadal variations between surface and subsurface tropical North Atlantic. *Geophys. Res. Lett.*, **34,** L12713, doi:10.1029/ 2007GL030225

Zhang, R., and T. L. Delworth, 2005: Simulated tropical response to a substantial weakening of the Atlantic Thermocline Circulation. *J. Climate*, **18,** 1853-1860.

Zhang, R., and T. L. Delworth, 2006: Impact of Atlantic multidecadal oscillations on India/Sahel rainfall and Atlantic hurricanes, *Geophys. Res. Lett*., **33,** L17712, doi:10.1029/2006GL026267.

Zhao, M., N.A.S. Beveridge, N. J. Shackleton, M. Sarnthein, and G. Eglinton, 1995: Molecular startigraphy of cores off northwest Africa: Sea-surface temperature history over the last 80 ka. *Paleoceanograpy*, **10,** 661-675.

Zheng, Y., 2007: Ocean heat transport in SODA: Structure, mechanisms, and impacts on climate, *dissertation of Texas A&M University, College Station,* P94.

APPENDIX

ABBREVIATIONS USED IN THIS DISSERTATION

AGCM Atmospheric GCM

AMO Atlantic Multidecadal Oscillation

AMOC Atlantic Meridional Overturning Circulation

BFE Boundary-Forcing Experiment

BP Before Present

CCM3 Community Climate Model version 3.6.6

CCM3-trMOM3 CCM3 coupled with trMOM3

CE Control Experiment

CFE Combined-Forcing Experiment

CGCM Coupled GCM

CM2.1 Climate Model version 2.1 of GFDL

DWF Deep Water Formation

ECMWF European Center for Medium-Range Weather Forecasts

EEP Eastern Equatorial Pacific

ENSO El Niño / Southern Oscillation

EOF Empirical Orthogonal Function

EUC Equatorial Undercurrent

GCM General Circulation Model

GFDL Geophysical Fluid Dynamics Laboratory

gMOM3 global version of MOM3

IOD Indian Ocean Dipole

ITCZ Intertropical Convergence Zone

JGR Journal of Geophysical Research

KPP K-profile parameterization

MOC Meridional Overturning Circulation

MOM3 Modular Ocean Model version 3.0

NA Northern Atlantic

NADW North Atlantic Deep Water

NAO North Atlantic Oscillation

NBC North Brazil Current

NCAR National Center for Atmosphere Research

NH Northern Hemisphere

NP Northern Pacific

NSTC Northern STC

ODA Ocean Data Assimilation

ODP Ocean Drilling Program

OGCM Oceanic GCM

PDF Probability Distribution Function

PMM Pacific Meridional Mode

RAPID Rapid Climate Change

SFE Surface-Forcing Experiment

SFM Seasonal Footprinting Mechaniam

SSS Sea Surface Salinity

SST Sea Surface Temperature

STC Subtropical Cell

Sv Sverdrup (1 Sv = 10^6 m^3/s)

TAV Tropical Atlantic Variability

trMOM3 tropical channel version of MOM3

WES Wind-Evaporation-SST

VITA

Xiuquan Wan received his B.S. degree in oceanography in 2000, and his M.S. degree in physical oceanography in 2003, both from Ocean University of China. He entered the Department of Oceanography at Texas A&M University in January 2004 to pursue a Ph.D. degree in oceanography with special interest in climate studies and received his Ph.D. degree in August 2009.

He may be reached at: MS3146, Department of Oceanography, Texas A&M University, College Station, TX, 77843. His email is xiuquanwan@gmail.com.